Distribution Agreement

In presenting this thesis or dissertation as a partial fulfillment of the requirements for an advanced degree from Emory University, I hereby grant to Emory University and its agents the non-exclusive license to archive, make accessible, and display my thesis or dissertation in whole or in part in all forms of media, now or hereafter known, including display on the world wide web. I understand that I may select some access restrictions as part of the online submission of this thesis or dissertation. I retain all ownership rights to the copyright of the thesis or dissertation. I also retain the right to use in future works (such as articles or books) all or part of this thesis or dissertation.

Signature:

_____ _____

PamelaSara Elbaz Head Date

Sirtuin 2 is a Human Tumor Suppressor and a Novel Regulator of the Non-Homologous End Joining Repair Pathway

By
PamelaSara Elbaz Head
Doctor of Philosophy
Graduate Division of Biological and Biomedical Sciences
Genetics and Molecular Biology

_____

David S. Yu
Advisor

_____

Paul W. Doetsch
Committee Member

_____

Anita H. Corbett
Committee Member

_____

Paula M. Vertino
Committee Member

_____

William Dynan
Committee Member
Accepted:

_____

Lisa A. Tedesco, Ph.D.
Dean of the James T. Laney School of Graduate Studies

_____

Date

Sirtuin 2 is a Human Tumor Suppressor and a Novel Regulator of the Non-Homologous End Joining Repair Pathway

By

PamelaSara Elbaz Head

B.S., Georgia Institute of Technology, 2013

Advisor: David S. Yu, M.D., Ph.D.

An abstract of

A dissertation submitted to the Faculty of the

James T. Laney School of Graduate Studies of Emory University

in partial fulfillment of the requirements for the degree of

Doctor of Philosophy

in Genetics and Molecular Biology

2018

Abstract

Sirtuin 2 is a Human Tumor Suppressor and a Novel Regulator of the Non-Homologous End Joining Repair Pathway

By PamelaSara Elbaz Head

Sirtuin 2 (SIRT2) is a class III NAD^+ dependent histone deacetylase implicated in maintaining genomic stability and tumor suppression in that genetic loss of *Sirt2* results in both genomic instability and specific murine breast and liver tumors. *SIRT2* deficiency in human cells results in hypersensitivity to DNA damage, impaired recovery from replication arrest, and a defect in the G2/M checkpoint in response to ionizing radiation (IR). Here we confirm SIRT2 as a tumor suppressor in humans by mutational analysis and demonstrated a novel role for SIRT2 in non-homologous end joining (NHEJ). Using structural insight combined with bioinformatics and functional analyses, we show that naturally occurring cancer-associated *SIRT2* mutations at evolutionarily conserved sites disrupt its deacetylation of DNA-damage response proteins by impairing SIRT2 catalytic activity or protein levels but not its localization or binding with substrate. We observed that these SIRT2 mutant proteins fail to restore the replication stress sensitivity, impairment in recovery from replication stress, and impairment in ATR-interacting protein (ATRIP) focus accumulation of *SIRT2* deficiency. Moreover, the SIRT2 mutant proteins failed to rescue the spontaneous induction of DNA damage and micronuclei of *SIRT2* deficiency in cancer cells. Additionally, preliminary data demonstrates *SIRT2* deficiency results increased sensitivity to IR and Camptothecin (CPT) treatment and reduced NHEJ efficiency. Mass spectrometry analysis indicates an interaction between SIRT2 and NHEJ kinase DNA-PKcs which we confirmed in human cell lines. Furthermore, we establish SIRT2 deacetylates DNA-PKcs, in response to DNA damage and that this deacetylation is important for proper DNA-PKcs localization to sites of DNA damage and therefore its interaction with Ku at DSBs. SIRT2 deacetylation of DNA-PKcs also is important for the regulation of DNA-PKcs kinase activity on itself and downstream NHEJ substrates Artemis and XRCC4 following DNA damage. Overall, our work provides a mechanistic basis for understanding the biological and clinical significance of *SIRT2* mutations in genome maintenance and tumor suppression.

Sirtuin 2 is a Human Tumor Suppressor and a Novel Regulator of the Non-Homologous End Joining Repair Pathway

By

PamelaSara Elbaz Head

B.S., Georgia Institute of Technology, 2013

Advisor: David S. Yu, M.D., Ph.D.

A dissertation submitted to the Faculty of the

James T. Laney School of Graduate Studies of Emory University

In partial fulfillment of the requirements for the degree of

Doctor of Philosophy

in Genetics and Molecular Biology

2018

Acknowledgments

I wish to thank the members of the Yu lab both past and present especially Sasha Petrova who served as my mentor during my rotation, Hui Zhang who served as a mentor for my thesis project, and my PI David Yu. I am elated that I will be able to say that I am the first graduate student to finish a PhD dissertation in the Yu lab at Emory University. I also want to thank all my committee members: Paula, Anita, Paul, and Bill. It goes without saying that your advice and expertise were paramount to my transition from student to independent scientist, however, it was also your encouragement that I feel made an enormous difference. Thank you to the Genetics and Molecular Biology Program, GDBBS, and LGS for not only accepting me 5 years ago but for the LGS fellowship. Lastly, I want to thank my family and all the friends I've made in my time at Emory. You helped me through the rough times and I cannot fathom making it this far without you behind me at every step of the way.

Table of Contents

List of Figures

Chapter 1: Introduction

1.1 The DNA Damage Response

Our cells amass thousands of lesions in their DNA on a daily basis as a result of exogenous and endogenous sources of damage such as ionizing radiation (IR), chemical exposures, ultra violet (UV) light, errors in replication, and byproducts of cellular metabolism [1]. These lesions activate the DNA Damage Response (DDR). The DDR is composed of pathways for cell-cycle arrest, DNA repair, recovery, and apoptosis, all of which are critical for maintaining genome integrity and preventing disease, such as premature aging and cancer [1-4]. DDR mechanisms repair multiple forms of DNA damage or replication blocks, such as DNA crosslinks, mismatches, insertions, deletions, and strand breaks, before DNA replication and cell division occur [3, 5, 6]. If the damage is too severe for repair, prolonged activation of the DDR will induce apoptotic pathways (Figure 1.1) [7].

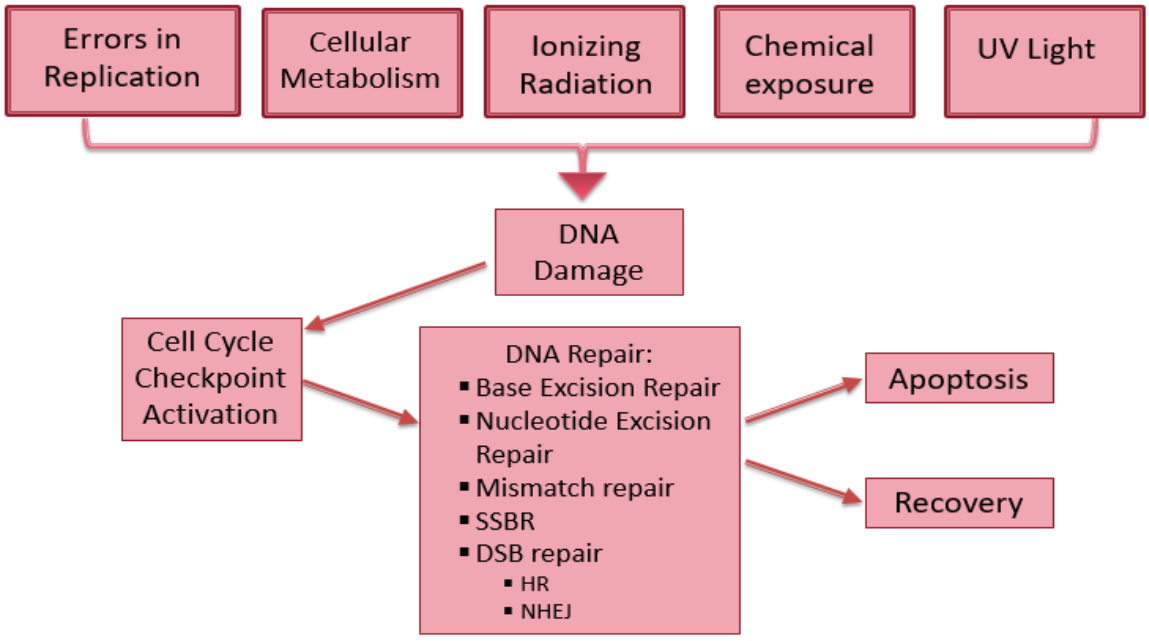

Figure 1.1 Flow Through Representation of the DNA Damage Response

1.1.1 The DNA Damage Response: Cell Cycle Checkpoint Pathways

When DNA damage occurs, the cell cycle must come to a halt to prevent the incorporation of mutations or chromosomal abnormalities into the genome while simultaneously providing the cell time to repair the damage [7, 8]. This is accomplished through the activation of cell cycle checkpoint pathways. There are three main checkpoint pathways named for the phase in the cell cycle in which they are activated: the G1/S checkpoint, the intra-S phase checkpoint, and the G2/M checkpoint [7, 8]. The G1/S checkpoint stalls the cell in G1 thereby preventing initiation of replication before repair, the intra-S phase checkpoint stalls the cell cycle after replication initiation but before G2 in response to DNA damage or a shortage of nucleotides, and the G2/M checkpoint stalls the cell in G2 to prevent segregation of damaged DNA or chromosomes during mitosis [8]. In each of these pathways, the checkpoint is activated through kinase cascades. Sensor proteins localize to the sites of damage or stalled replication forks and activate signal transducer proteins that provide the activation signal to effector proteins. Effector proteins slow or halt the cell cycle [7, 8].

In both the G1/S and G2/M checkpoint pathways, the major DNA damage sensory proteins are the kinases Ataxia Telangiectasia-Mutated (ATM) and ATM-Rad3-Related (ATR) [7, 8]. ATM is activated by double strand breaks (DSBs) and phosphorylates the signal transducer serine/threonine-protein kinase checkpoint protein 2 (CHK2) [7]. ATR is activated by recruitment to ssDNA formed from replication fork stalling or processing of DSBs and phosphorylates the signal transducer serine/threonine-protein kinase

checkpoint protein 1 (CHK1) [7]. CHK2 or CHK1 phosphorylate Cell Division Cycle 25 homolog A, B, or C (CDC25A, -B, or -C) depending on the checkpoint in order to down regulate phosphatase activity of these CDC25 proteins[7]. Phosphorylated CDC25 proteins are then exported from the nucleus and degraded in the cytoplasm [7]. Normally, CDC25 proteins dephosphorylate cyclin dependent kinase 2 (CDK2) in order to upregulate its kinase activity on downstream cell cycle dependent targets needed for replication or mitotic initiation [7].

Once arrested, ATM/ATR phosphorylates p53, which maintains G1 cell cycle arrest [7]. Phosphorylation of p53 prevents its nuclear export and degradation and thus increases its nuclear concentration [7]. During the G1/S cell cycle checkpoint, p53 activates p21 which binds to and inhibits the activities of the CyclinE-CDK2 complex [7]. The CyclinE-CDK2 complex normally upregulates S phase initiation [7]. Alternatively in G2 cell cycle arrest, Wee1 is upregulated in order to suppress CyclinB-CDK2 complex activity to prevent progression into mitosis [7]. In addition, DNA damage during G2 leads to the activation of the anaphase promoting complex/cyclosome (APC/C) through activation of its subunit protein cadherin 1 (CDH1) [9]. Activated APC/C prevents G2 arrest recovery by ubiquitinating recovery proteins such as Polo-like Kinase 1 (PLK1), Cyclin A, and Cyclin B1 [9]. Ubiquitination targets these proteins for proteasomal degradation [9].

The intra-S checkpoint (also known as the replication stress response or RSR), unlike the G1/S and G2/M checkpoints, does not occur at a cell cycle phase transition point [7, 8].

Rather, when activated by stalled replication forks, the intra-S checkpoint represses late replication origin firing [7, 8]. Replication forks become stalled due to a lack of nucleotides needed for DNA synthesis or to DNA lesions encountered by replication forks [8]. At these stalled forks, DNA helicase uncouples from DNA polymerase and continues to unwind the DNA leading to the production of single stranded DNA (ssDNA) which is then bound by Replication Protein A (RPA) [8]. In response, sensory proteins are recruited RPA coated ssDNA [8].

The RAD9A-RAD1-HUS1 (9-1-1) sensory complex is loaded onto the RPA coated ssDNA followed by recruitment of ATR Interacting Protein (ATRIP) [8]. ATRIP recruits ATR localization to stalled replication forks where ATR kinase activity is stimulated by further recruitment of DNA Topoisomerase 2-Binding Protein 1 (TopBP1) [8]. The 9-1-1 complex then recruits Claspin (CLSPN) which together with ATR is necessary for the activation of the signal transducer protein CHK1 [7, 8]. CHK1 in turn phosphorylates and deactivates CDC25A [7, 8]. Without active CDC25A, CDK2 remains in an inactive phosphorylated form leading to the inhibition of late origin firing [7, 8]. The binding of sensory and adaptor proteins to the fork is not only necessary for activation of the checkpoint cascade, but also for the stabilization of the replication fork itself to prevent collapse [7, 8].

DSBs during S-phase are sensed by ATM, which potentiates downstream signaling kinase cascades [7, 8]. Either ATM phosphorylates CHK2 in order to ultimately inhibit CDK2, or it phosphorylates Nibrin (NBS1 or NBN), Breast Cancer Type 1 (BRCA1),

Structural Maintenance of Chromosome 1 (SMC1), and Fanconi Anemia group D2 (FANCD2) [7]. Following cell cycle arrest, one or more DNA damage repair pathways are activated depending on the type of damage incurred.

1.1.2 The DNA Damage Response: DNA Damage Repair Pathways

The DDR consists of many types of DNA damage repair pathways, and the type of DNA lesion incurred dictates which repair pathway or pathways are activated [1]. DNA repair pathways include: Mismatch Repair (MMR), Nucleotide Excision Repair (NER), Base Excision Repair (BER), Single Strand Break Repair (SSBR), Homologous Recombination Repair (HRR), and Non-Homologous End Joining (NHEJ) (Table 1.1). MMR recognizes incorrect base incorporation and base damage [10].

Mismatched bases can arise from errors made by DNA polymerase during DNA replication, from insertions or deletions caused by polymerase slippage in a highly repetitive DNA region, from recombination errors, and/or from exogenous damaging agents [10, 11]. MMR, therefore, is heavily tied to replication [10, 11]. In this pathway, MutL Homologue 6 (MLH6) forms a dimer with MutS Homologue 2 (MSH2) which binds to the DNA at the site of mismatch [12]. Once bound, MLH6/MSH2 undergoes an ATP dependent conformational change that allows the dimer to slide along the DNA like a clamp [12]. This conformational change is required for recruitment of the MutL Homologue 1 (MLH1) and Post Meiotic Segregation Increased 2 (PMS2) dimer [12]. MLH1/PMS2 nicks the nascent DNA strand 5' of the mismatch error in an ATP dependent manner [12]. Exonuclease 1 (Exo1) then generates a single strand gap in the 5'

to 3’ direction over and beyond the site of mismatch [12]. The ssDNA generated is coated in RPA until DNA Polymerase δ fills the gap and DNA ligase I ligates the end to the nascent strand [12]. Other forms of base damage are recognized by NER or BER.

UV radiation can create DNA helix-distorting bulky DNA adducts such as thymine dimers, which are repaired by the NER pathway [13]. NER can be divided into two sub-pathways: Global Genomic Repair (GGR) and Transcription-Coupled Repair (TCR) [13]. In both pathways, dual incisions are made in the DNA strand on either side of the adduct to remove the damaged nucleotide(s) [13]. The resulting gap is filled using the non-damaged strand as a template by DNA polymerase followed by ligation [13]. In TCR, RNA polymerase II (RNAPII) senses the lesion during transcription and arrests [13]. In GGR the bulky adduct is recognized by Xeroderma Pigmentosum, Complementation group C (XPC) in complex with hRAD23B and Centrin 2 (CETN2) and by the heterodimer composed of DNA damage binding protein 1 (DDB1) and DNA damage binding protein 2 (DDB2) [13].

In TCR, RNAPII along with other TCR factors opens up the DNA around the lesion, but in GGR the XPC-hRAD23B-CETN2 complex performs this task [13]. At this point, the pathways converge with the recruitment of Transcription Factor II H (TFIIH) [13]. Xeroderma Pigmentosum type B (XPB) and Xeroderma Pigmentosum type D (XPD) unwind the DNA around the lesion site [13]. RPA coats the 30 nt ssDNA on the non-damaged strand and excisions are made by Xeroderma Pigmentosum complementation group G (XPG) and DNA Excision Repair protein (ERCC1) [13]. The gap is then filled

by DNA polymerase and ligated by Ligase I or III [13]. NER is responsible for repairing bulky lesions that distort the DNA helix, but smaller non-distorting lesions are repaired by BER [14].

Reactive oxidative species (ROS), ionizing radiation, and chemical agents can lead to deamination, oxidation, or methylation of DNA bases which activate the BER pathway [14]. In this repair pathway, a DNA glycosylase (11 exist in mammals) recognizes and removes the damaged base to produce an abasic (AP) site [14]. The AP site is cleaved by an AP endonuclease such as AP Endonuclease 1 (APE1) and is repaired by short-patch or long patch BER [14]. Short-patch BER generates a single nucleotide gap whereas long patch BER produces a 2-10 nucleotide gap [14]. The gaps have a hydroxyl group on the DNA 3' end and a phosphate group on the DNA 5' end [14]. This alteration is produced by polynucleotide kinase-phosphatase (PNKP) and is necessary for downstream polymerase and ligase function [14]. Gaps are filled by DNA polymerase β or δ/ε, depending on the type of BER pathway used, followed by ligation with DNA ligase I or III [14]. Additionally, both Poly(ADP-ribose) Polymerase I (PARP1) and XRCC1 have been shown to play a role in short-patch BER[14]. BER base lesions are small and are often the result of ROS, however ROS can also result in more devastating forms of DNA damage such as single strand breaks [15].

The most common form of DNA damage is the single strand break (SSB) [15]. SSBs can result from replication stress (stalled or collapsed replication forks), IR, ROS, abortive topoisomerase I (TOPI) activity, and crosslinking agents [15]. Breaks are sensed by

PARP1 which binds to the DNA, stimulating self poly(ADP-ribosylation) or PARylation [15]. This is likely necessary for regulating chromatin structure, for recruitment of other repair proteins such as X-Ray repair cross-complementing protein 1 (XRCC1), for DNA ligase adenylation, for inhibiting recombination, and for transcriptional regulation [15]. After PARP1 SSB detection, the ends of the broken DNA strand are cleaned to form 3' hydroxyl and 5' phosphate moieties by APE1 and PNKP followed by DNA Polymerase β gap filling and ligation by Ligase I or III [15].

Although SSB are the most common type of DNA damage, the most detrimental form of DNA lesions are DSBs which are predominantly repaired via two pathways: HRR and NHEJ [16-18]. DSBs can result from collapsed replication forks, IR, UV radiation, ROS, and DNA crosslinking agents. HRR is an error-free repair pathway because it involves the use of a repair template from a sister chromatid. It therefore only occurs during S and G2 [16-18]. In this pathway, Breast Cancer Type 1 (BRCA1) suppresses TP53-binding protein 1 (53BP1) upregulation of NHEJ repair so that the MRN complex can localize to the site of damage [19]. The MRN complex recruits and activates the ATM kinase necessary for downstream HRR signaling [19]. MRN, facilitated by CtBP-Interacting Protein (CtIP), also resects DNA at the break in a 5' to 3' fashion [19]. BRCA1 may be involved in the regulation of CtIP in this step [19]. Exo1 and/or DNA2 provide more extensive end resection facilitated by the Bloom syndrome protein (BLM) helicase [19]. Then, ssDNA is coated with RPA which is necessary for ATR activation [19]. Next, RPA is replaced by RAD51 with the help of Breast Cancer Type 2 (BRCA2) and BRCA1 [19]. This step is necessary for proper homology sequence searching and strand invasion

followed by DNA synthesis and Holliday junction resolution [19]. When a repair template is not available, the NHEJ pathway is used [16-18].

During NHEJ, X-Ray Repair Cross-Complementing protein 6 (XRCC6 or Ku70) and X-Ray Repair Cross-Complementing protein 5 (XRCC5 or Ku80) form heterodimers which slide onto the DNA on both sides of the DSB [17, 18]. The Ku heterodimer (Ku) proceeds to recruit the DNA-dependent protein kinase, catalytic subunit (DNA-PKcs) to form the stable DNA-PK complex on the DNA ends [17, 18, 20, 21]. DNA-PK formation is necessary for DNA-PKcs conformational change and kinase activation as well as for holding the DNA ends in proximity to each other [17, 18, 20, 21]. Interaction between the two DNA-PK complexes on either side of the break allows for the formation of the DNA-PK holoenzyme dimer [17, 18, 20, 21]. DNA-PKcs is one of the phosphatidylinositol-3 kinase-like (PIKK) family members [17, 18, 22, 23]. Other well-known members of this family include ATM, ATR, and mTOR, [22, 23]. PIKK family members recognize and phosphorylate SQ/TQ (serine or threonine followed by glutamine) motifs [17, 18, 22, 23].

DNA-PKcs is regulated in NHEJ by phosphorylation of its ABCDE and PQR clusters [17, 18, 24, 25]. Phosphorylation of the ABCDE cluster (sites between residues 2609 and 2647) by ATM or ATR promotes end resection by Artemis (an endonuclease recruited by Ku which resects the damaged ends to create blunt ends for ligation) [17, 18, 24, 25]. DNA-PKcs also phosphorylates a number of NHEJ substrates including Artemis, XRCC4, Ku, XLF, and DNA Ligase IV. However, these phosphorylation events do not appear to be necessary for proper NHEJ [17, 18, 25]. Next, DNA-PKcs

autophosphorylates its PQR cluster (sites between residues 2023 and 2056) to promote end ligation and the release of DNA [17, 18, 24, 25]. End ligation is accomplished by XRCC4-Like Factor (XLF), X-Ray Repair Cross-Complementing protein 4 (XRCC4), and DNA ligase IV [17, 18]. Another repair pathway similar to NHEJ is alternative NHEJ (alt-NHEJ) in which DSBs are repaired by utilizing microhomologies near the site of the DSB[26].

Knowledge of the proteins involved in the alt-NHEJ repair process is limited, but it is known that PARP1 likely recognizes the damage and recruits downstream repair proteins instead of Ku, that end processing is performed by the MRN instead of Artemis, and that ligation is dependent on XRCC1 and DNA ligase III instead of XRCC4 and DNA ligase III [26]. In addition, ligation is dependent on the annealing of microhomology regions at the DSB and repair results in either insertions or deletions at sites of repair [26]. Once repair processes are complete or if damage is too severe for proper repair, the DDR activates cell cycle recovery pathways to restart the cell cycle or apoptotic pathways to induce cell death respectively [7].

Repair Pathway	**MMR**	**NER**	**BER**	**SSBR**	**HRR**	**NHEJ**	**alt-NHEJ**
Major Damage Source	Errors in replication	UV	ROS, IR, Chemical exposure	IR, ROS, abortive TOPI, crosslinking agents	IR, UV, ROS, crosslinking agents		
Type of Damage	Mismatched Base Pairs	Bulky DNA Adducts	Non-Bulky DNA Adducts	SSBs	DSBs (S/G2 dependent)	DSBs	
Sensor Proteins	MLH6/MSH2	XPC, DDB2, CETN2, DDB1, RNAPII	DNA Glycosylases	PARP1	MRN	Ku70/ Ku80	PARP1
Major Repair Proteins	MLH1, PMS2, EXO1, DNA Pol δ, Ligase I	XPC, CENT2, hRAD23B, TFIIH, XPB, XPD, RPA, XPG, ERCC1, Ligase I or III	APE1, PNKP, DNA Pol β or δ/ε, PARP1, XRCC1	XRCC1, APE1, PNKP, DNA Pol β, Ligase I or III	MRN/CtIP, Exo1, BRCA1, BRCA2, RAD51, RPA, DNA2, BLM, PARP1, ATR	DNA-PKcs, Artemis, ATM, XLF, Ligase IV, XRCC4,	Ligase III, XRCC1, MRN

Table 1.1 Summary of DNA Damage Repair Pathways. The above table summarizes the various DNA damage repair pathways discussed above, the damage that activate them, and the proteins involved in each repair pathway. This table highlights protein crosstalk of various proteins across these pathways as well.

1.1.3 The DNA Damage Response: Recovery or Apoptosis

Recovery from cell cycle arrest involves the inactivation of cell cycle arrest and cell cycle arrest maintenance proteins and activation of CDKs [9]. Additionally, there is often increased proteasomal degradation of both cell cycle checkpoint proteins and DNA repair proteins [9]. Recovery from the G1/S checkpoint, for example, has been tied to the

dephosphorylation and activation of Transcription Intermediary Factor 1-Beta (TIF1-β) [27].

During the G1/S checkpoint, TIF1-β is phosphorylated by the ATM/CHK2 kinases leading to repression of its protein activity [27]. Dephosphorylation of TIF1-β activates its repression activity on the G1/S checkpoint maintenance protein p21 [27]. During recovery, downregulation of ATM/CHK2 as well as activation of Protein Phosphatase 4 Catalytic subunit (PP4C) leads to this dephosphorylation and activation of TIF1-β [27]. Overall this results in de-repression of necessary Cyclins and CDKs necessary for S phase initiation [27]. Whereas the G1/M checkpoint is maintained by upregulation of p21 transcription, the G2/M checkpoint is more reliant on p53 activation [27].

Proteins PLK1 and Protein Phosphatase 1D (PPM1D) have been identified as crucial G2/M checkpoint recovery pathway proteins [9]. PLK1 both upregulates Aurora and Bora (upstream activators of mitotic promoting complex Cyclin B1-CDK1) and targets CLSPN for degradation (represses CHK1 activation) [9]. PPM1D dephosphorylates p53 at serine 15 and CHK1 at serine 345 leading to inactivation of both proteins which are necessary for arrest maintenance and propagation respectively [9]. This ultimately leads to stabilization of CDC25B and other Cyclins and CDKs necessary for mitotic initiation [9]. Unlike the recovery pathways for G1/S and G2/M, recovery from the RSR (the intra-S phase checkpoint) requires not only inactivation of checkpoint signals but the restart of replication forks as well [9].

Recovery from the intra-S phase checkpoint exhibits many of the same mechanisms seen in the G1/S and G2/M checkpoint recovery pathways in that checkpoint signaling is inactivated (through protein degradation, PTM, and/or transcriptional regulation) and cycling proteins are upregulated (through stabilizing PTMs, and/or transcriptional regulation) [9]. For instance, PLK1 phosphorylates CLSPN to promote its degradation and downregulate CHK1 activation and signaling [9]. Following checkpoint signaling inactivation, cells must restart the replication forks to complete replication and move into G2.

Less is known about the mechanisms underlying proper replication fork restart but they likely involve formation of Holliday junctions, double strand break mediated restart, or reannealing of ssDNA generated by unwinding the template [28]. Recently RECQ helicases including BLM, REQ4, WRN, RECQ5, and RECQ1 have been implicated in these pathways [29]. They are important to the resolution of DNA structures formed at the fork, resolution of replication intermediates, and degradation of nascent DNA formed by reversed forks [29]. For example, BLM prevents excessive HR at stalled forks as well as upregulates efficient replication fork restart while suppressing dormant origin firing [29].

Restart of replication forks is the last step in the replication stress response/intra-S phase checkpoint recovery pathway and following restart the cell cycle proceeds normally. Failure to resolve DNA damage or to restart the cell cycle leads to prolonged cell cycle checkpoint activation, and stimulates the activation of apoptotic pathways [7]. Apoptotic

pathways are composed of cascades of cysteine aspartyl proteases known as caspases which upregulate programed cell death through the cleavage of specific substrates resulting in the dismantling of the cell [30]. For instance, upregulated p53 can stimulate (BCL-2 Associated X protein) BAX expression [31]. BAX forms a homodimer which releases cytochrome c from the cell's mitochondria [31]. This release leads to Caspase-9 activation and subsequent activation of the caspase cascade [31]. Just as cell cycle checkpoints and DNA repair pathways protect our genome from the incorporation of mutations and chromosomal abnormalities, apoptotic pathways protect against proliferation of damaged cells by eliminating these cells from population. Therefore, dysregulation of one or more of these pathways could lead to increased susceptibility to tumor development [1-4, 32].

1.1.4 The DNA Damage Response: Dysregulation, Genomic Instability, and Cancer

Dysregulation of DDR pathways leads to the genomic incorporation of mutations and chromosomal abnormalities which can cause increased genomic instability and increased susceptibility to tumorigenesis [1-4, 32]. Dysregulation of DDR pathways is often the result of proto-oncogene protein activation, and/or loss of tumor suppressor protein function [33]. Proto-oncogenes are genes that encode proteins that upregulate cell growth and/or proliferation or that downregulate apoptotic pathways [34]. When these genes are mutated with gain of function mutations or when they are expressed at abnormally high levels, proto-oncogenes have the potential to cause cancer and are reclassified as oncogenes [34].

For example, the proto-oncogene protein Myc is a transcription factor that normally upregulates the transcription of CDKs and Cyclins, such as CDC25A, to promote normal cell cycle progression in the absence of cellular stress or DNA damage [35]. Myc also represses cell cycle arrest proteins such as p21 through transcriptional repression or increased protein degradation to promote cell proliferation [35]. When mutated, Myc can promote cell proliferation while down regulating maintenance of cell cycle checkpoints even in the presence of cellular stress or DNA damage [35]. The result is increased mutagenesis in the genome. If necessary regulator proteins of apoptosis are concurrently mutated (loss of function), cancer can result. Therefore, mutations in Myc would serve as driver mutations in that it they would provide a selective growth advantage and would push the cell towards cancer [36].

Oncogene activation can lead to development of other oncogenic mutations, passenger mutations (mutations that are often by-products of the increased genomic instability caused by driver mutations but that do not alter fitness of the cell), and loss of function mutations in tumor suppressor genes [36]. Tumor Suppressor genes or antioncogenes are genes that encode proteins that work to decelerate cell proliferation and growth, that function in DNA damage repair pathways, or that upregulate apoptotic pathways in order to suppress oncogenic proliferative phenotypes [37]. Loss of function in these genes can also be driver mutations [36].

Unlike oncogenes which only require a gain of function mutation in one allele, tumor suppressor genes normally require loss of function mutations in both alleles [36].

However, loss of one tumor suppressor allele still leads to increased cancer susceptibility and, for certain genes, to tumor permissive phenotypes as a result of haploinsufficiency or a dominant-negative mutation [38]. For example, p53 is a well-established tumor suppressor gene involved in both cell cycle checkpoint maintenance and pro-apoptotic pathways that has exhibited haploinsufficiency phenotypes in certain cancers [38]. Overall, proto-oncogene activation and/or tumor suppressor loss of function results in dysregulation of one or more DDR pathways [1-4]. Dysregulation in turn leads to increased incidence of genomic incorporation of mutations and chromosomal abnormalities and ultimately genomic instability [1-4]. Current cancer treatments therefore employ sequencing technology to classify tumors based on biomarkers, choose the most effective targeted treatment agents on an individual patient basis, and increase the efficiency of general cancer treatment therapies through combination with specific protein inhibitors [39].

Identification of cancer biomarkers are important to predicting patient outcome and choosing the best treatment option [40]. For instance, if a patient's tumor is deficient in NHEJ due to loss of function or expression of Artemis, treatment with chemotherapies directed at DSB induction in S-phase such as Camptothecin (topoisomerase I inhibitor CPT) may prove effective. These cancer cells would be deficient in HRR and NHEJ and thus rely on error prone alt-NHEJ for repair of DSBs induced by CPT. Combination with radiotherapies could overwhelm the cancer cells capacity for repair and apoptotic pathways would be activated as a result. Another avenue of treatment lies in small molecule inhibitors and enhancers.

Use of small molecule inhibitors and enhancers against known oncogenes and tumor suppressors (biomarkers) could increase patient tumor sensitivity to current chemo and radiation based therapies and allow for greater effectiveness at lower doses [41]. For instance, the Human Epithelial Receptor 2 (HER-2) oncogene is transmembrane tyrosine kinase growth factor receptor commonly upregulated in certain breast cancers [39]. Inappropriate activation of HER-2 leads to activation of the anti-apoptotic RAS signaling cascade preventing cell death and upregulating cell growth [39]. Gefitinib is a small molecule inhibitor for Epidermal Growth Factor Receptors (EGFRs) including HER-2 that inhibits the tyrosine kinase domain and subsequent downstream signaling [39]. It inhibits cell growth and the anti-apoptotic RAS pathway for more effective cancer treatment [39]. Although personalized medicine approaches to cancer are promising, there are still limitations to their applications.

DDR pathways are highly complex and involve a great deal of crosstalk and we do not yet fully understand how these pathways are regulated or even what all proteins are involved in their regulation. In addition, patients can possess or acquire resistance to current targeted therapies [42]. Therefore, treatments based on biomarkers with specific chemotherapies and small molecules may not produce the expected outcomes of increased cancer cell death. In addition, current therapies are limited to pre-established protein targets. Overall there is an urgent need to enhance our understanding of DDR regulatory mechanisms so that we may continue to develop more effective cancer

diagnostics and treatments. One novel regulator and potential therapeutic target is Sirtuin 2 (SIRT2).

1.2 The Class III Histone Deacetylases Sirtuins: Cellular Functions

The first sirtuin protein was identified in yeast as Silent Information Regulator 2 (Sir2) and was determined to be an epigenetic regulator most closely related to the human SIRT1 [43-46]. Since then, seven members have been identified in the human sirtuin protein family, all of which have been classified as class III NAD^+ dependent Histone Deacetylases (HDACs) [43-47]. All members of this protein family contain a core deacetylase domain but vary in their N- and C-terminal domains and primary catalytic activities [43-47]. This variation allows for regulation of their diverse cellular compartment localizations [43-47].

SIRT1 has two Nuclear Import Signals (NLS) and two Nuclear Export Signals (NES) which allow it to shuttle between the nucleus and cytoplasm although it localizes primarily to the nucleus [45]. SIRT2 can also localize to both to the cytoplasm and nucleus; however, SIRT2 is only documented to have an NES (no recognizable NLS) and is primarily localized to the cytoplasm. [45]. SIRT6 is also localized to the nucleus and SIRT7 to the nucleolus, and both contain an NLS but not NES [43-47]. SIRT3, SIRT4, and SIRT5 are all mitochondrial and lack NLS and NES motifs [43-47]. They do, however, possess mitochondrial import signals [43-47]. Due to their assorted locations in the cell, it comes as no surprise that the sirtuins are extensively involved in a wide array

of cellular processes including aging, metabolism, and tumor suppression (Figure 1.2) [43-47].

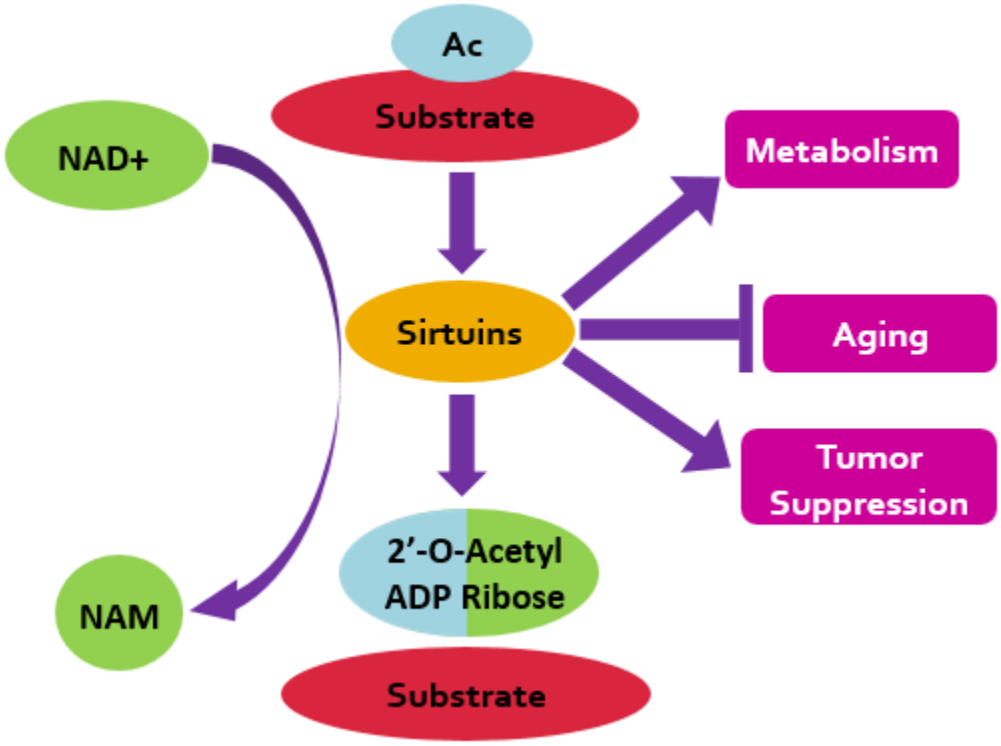

Figure 1.2 Sirtuin Deacetylase Activity and Cellular Function. Sirtuins are NAD^+ dependent class III HDACs that remove acetyl groups from substrate proteins in various pathways such as metabolism, aging, and tumor suppression to regulate substrate protein activity. Sirtuins transfer the acetyl groups from substrate onto the ADP-ribose moiety of NAD^+ resulting in 2'-O-Acetyl ADP-ribose, nicotinamide and deacetylated substrate.

1.2.1 Nuclear Sirtuins: SIRT1, SIRT6, and SIRT7

Sirtuin 1 (SIRT1)

SIRT1 functions as a deacetylase of histone and non-histone proteins in order to regulate metabolic pathways, cell proliferation pathways, aging pathways, and DDR pathways

through transcriptional repression or through target protein deacetylation [48]. SIRT1 is crucial to many metabolic pathways as it serves as cytosolic sensory protein for $NAD^+/NADP^+$ levels [49]. During caloric restriction, AMP-activated Protein Kinase (AMPK) senses cellular changes in cellular AMP/ATP ratios (decrease in ATP compared to AMP) and enhances cellular NAD^+ levels to activate SIRT1 [49]. SIRT1 then activates Peroxisome Proliferator-activated Receptor-γ Coactivator α (PGC-1α) and Hypoxia-Inducible Factor 1-α (HIF-1α) to upregulate mitochondrial biogenesis and ATP production [49]. In fact, SIRT1 levels are reported to increase in most tissues in mice living under caloric restriction [49, 50]. Transgenic mice with knocked in SIRT1 overexpression exhibit caloric restriction phenotypes such as lower levels of blood cholesterol, adipokines, insulin and fasted glucose [50]. Not only is mitochondrial biogenesis regulation important for metabolism but to aging as well.

Decreased mitochondrial biogenesis results in increased accumulation of oxidized lipids, proteins, and DNA as a consequence of lower mitochondrial turnover, which normally protects against aging and age-related diseases [51]. Also, when ATP levels do not meet minimal thresholds required for homeostasis due to reduced biogenesis, apoptotic pathways are activated which contributes to aging onset and progression [51]. Conversely, increased mitochondrial biogenesis allows for upregulation of cell proliferation [51]. During the natural aging process, both SIRT1 cellular levels and mitochondrial biogenesis decrease leading to decreased proliferation and increased apoptosis, but extended SIRT1 activation from caloric restriction leads to extended lifespan [51]. SIRT1 also provides protection against neurodegenerative effects that result

from aging [51]. In addition to regulating cell proliferation, cell metabolism, and aging, SIRT1 is also involved in DDR pathway regulation [51].

SIRT1 is known to regulate many DNA damage repair and apoptotic proteins including but not limited to NBS1, Werner syndrome ATP-dependent helicase (WRN), Forkhead Box O 3 protein (FOXO3), p53, and Ku70 [43-47]. In response to DNA damage, SIRT1 deacetylates NBS1 to increase its recruitment of ATM to sites of damage and activate downstream repair pathways [43-47]. SIRT1 deacetylation of WRN during the DDR increases its helicase and exonuclease activities necessary for its roles in HR and the replication stress response [52]. Deacetylation by SIRT1 also increases WRN localization to sites of DNA damage [52].

In response to oxidative stress SIRT1 deacetylates FOXO3a which leads to FOXO3a activation of cell cycle arrest while repressing FOXO3a mediated induction of apoptosis transcriptional activities. SIRT1 also reduces apoptosis through negative regulation of p53 and Ku70 [51]. Deacetylation of p53 by SIRT1 results in reduced transcription of proapoptotic genes while deacetylation of Ku70 leads to increased Ku70 sequestering of BAX preventing activation of apoptosis [51]. Overall, SIRT1 tends to promote DNA damage repair and cell proliferation pathways while repressing apoptosis indicating SIRT1 could serve as either a proto-oncogene or tumor suppressor. In fact, *Sirt1* knockout mice usually die within one month following birth and are smaller and weaker compared to control littermates [48]. In fact, *Sirt1* knockout mouse embryos exhibit

increased incidence of chromosomal aberrations and genomic instability indicating that SIRT1 is important to both viability and the maintenance of genomic stability [43-47].

Sirtuin 6 (SIRT6)

SIRT6, unlike SIRT1, has a weaker deacetylase activity and has demonstrated additional enzyme functions such as deacylation of fatty acyl groups and mono-ADP-ribosylation [43-47]. However, like SIRT1, SIRT6 regulates many cellular activities such as metabolism (glucose production/uptake and lipid metabolism), aging, and the DDR [53]. Whereas SIRT1 is involved in pathways for NAD^+ and ATP homeostasis, SIRT6 regulates glucose metabolism [53].

SIRT6 represses the expression of glucose metabolic genes such as pyruvate dehydrogenase kinase-1 (PDK1), lactate dehydrogenase (LDH), phosphofructokinase-1 (PFK1) and Glucose transporter-1 (GLUT1) [53]. Transcriptional repression of these genes is achieved by deacetylation and repression of their transcription factor HIF1-α as well as direct gene silencing through deacetylation of Histone 3 Lysine 9 (H3K9) at their promoters [53]. In addition, SIRT6 represses gluconeogenesis in the liver through indirect suppression peroxisome Proliferator-activated receptor-γ coactivator 1-α (PGC-1α) via direct deacetylation of General Control Non-repressed Protein 5 (GCN5) [53]. When SIRT6 is lost such as in SIRT6 knockout mice, there is increased glucose uptake by brown adipose tissue and muscle in conjunction with reduced glucose production leading to hypoglycemic phenotypes [53].

In addition to glucose metabolism, SIRT6 also regulates genes involved in lipid metabolism [53]. SIRT6 regulates triglyceride homeostasis, Low-Density Lipoprotein (LDL)-cholesterol homeostasis, and serum cholesterol levels through transcriptional repression of genes involved in triglyceride synthesis, of proprotein convertase subtilisin/kexin type 9 (PCSK9), and of sterol-regulatory element binding protein (SREBP) [53]. Transcriptional repression is achieved by SIRT6 deacetylation of H3K9 and H3K56 at gene promoters or by activating protein repressors of the pathways [53]. SIRT6 overexpression in mice can lead to decreased triglyceride accumulation in the liver, decreased LDL levels, and decreased serum cholesterol levels while SIRT6 loss causes and increase in these factors [53]. SIRT6 has established roles in aging as well.

SIRT6 potentially regulates lifespan through regulation of insulin-like growth factor 1 (IGF1) levels in white adipose tissue [53]. Furthermore, SIRT6 has been shown to regulate telomere maintenance pathways [53]. SIRT6 deacetylates H3K9 and H3K56 within telomeres during S phase to allow for proper recruitment of WRN, which is likely necessary for telomere capping and proper replication of telomeres [53]. SIRT6 deficiencies lead to premature telomere shortening during replication, accumulation of DNA damage in telomeres, and increased chromosomal telomere fusions [53].

SIRT6 functions in DNA damage repair pathways as well to maintain genomic stability of the cell. SIRT6 mono-ADP-ribosylates PARP1 and deacetylates CtIP to upregulate HRR. Activation of PARP1 also leads to upregulation of alternative-NHEJ (alt-NHEJ) repair, SSBR, and BER [54-57]. It has also been demonstrated that Sirt6 recruits

SWI/SNF-related matrix-associated actin-dependent regulator of chromatin subfamily A member 5 (SMCA5 or SNF2H) to sites of DNA damage to ensure a euchromatic state to ensure DNA repair proteins have access to the damaged site [54, 58]. Sirt6 was also found to bind Ku80 and aid in the recruitment of DNA-PKcs to chromatin in NHEJ to promote repair, but it did not exhibit enzymatic activity on these proteins [54]. *Sirt6* knockout mice, like *Sirt1* knockouts, often die within one month of life and exhibit accelerated aging phenotypes [54]. Moreover, SIRT6 loss would result in the dysregulation of multiple DNA damage repair pathways, dysregulation of telomere maintenance, and increased uptake of glucose and glycolysis thereby promoting tumor permissive phenotypes. In fact, *Sirt6* loss in mouse embryonic fibroblasts leads to tumor formation [53].

Sirtuin 7 (SIRT7)

SIRT7 contains both a NLS and nucleolar localization signal and has regulatory roles in cellular proliferation, stress resistance, aging, DDR pathways [59]. SIRT7 is primarily localized to the nucleoli where it upregulates tRNA transcription and RNA Polymerase I (PolI) dependent transcription of rRNA genes through deacetylation and activation of the PolI subunit polymerase-associated factor 53 (PAF53) [59]. Following transcription, SIRT7 is essential to ribosomal pre-rRNA processing to rRNA and thus is necessary for ribosome biosynthesis [59]. Ribosomal biosynthesis is needed for cell cycle progression and cell growth and proliferation [59].

SIRT7 has been shown to increase cellular resistance to stress and thus maintain metabolic homeostasis through regulation of ribosomal biosynthesis, protein synthesis, and HIF-1α/β transcriptional target synthesis [60]. When there is an accumulation of unfolded or misfolded proteins in the Endoplasmic Reticulum (ER), ER stress results and can lead to the activation of apoptotic pathways [60]. To prevent this, Myc recruits SIRT7 to promoters of ribosomal subunits for suppression to reduce the amount of protein being made and transported to the ER for folding [60]. During genomic stress, SIRT7 relocates from the nucleoli to the nucleus which leads to increased acetylation of PAF53 and inhibited rRNA transcription and reduced ribosome biosynthesis [60]. During hypoxic stress, SIRT7 represses HIF1-α/β and their transcriptional targets in a similar fashion to SIRT6 to promote stress resistance [60]. SIRT7 also likely plays a role in aging regulation in that SIRT7 knockout mice display premature aging phenotypes like those seen in SIRT6 knockout mice but the mechanisms behind this is not yet clear [60].

Novel roles are also becoming apparent for SIRT7 in genomic stability maintenance through regulation of DNA damage repair. SIRT7 deacetylates H3K18 which is necessary for 53BP1 recruitment in DSB repair [61, 62]. SIRT7 has also recently been demonstrated to possess desuccinylation activity that may impact DSB repair [59]. Following DSB induction, SIRT7 is recruited to sites of damage in a PARP1-dependent manner where it desuccinylates H3K122 to promote chromatin condensation and DSB repair [59]. Moreover, *Sirt7* depletion in mice leads to impairment of DSB repair, increased replication stress, and genomic instability [61, 62]. Overall, dysregulation of

SIRT7 could lead to increased ribosome biosynthesis and cell proliferation while suppressing apoptosis.

1.2.2 Mitochondrial Sirtuins: SIRT3, SIRT4, and SIRT5

Sirtuin 3 (SIRT3)

SIRT3 is a mitochondrial sirtuin that contains deacetylase, deactylase and ADP-ribosyl transferase enzymatic activities [63, 64]. As a mitochondrial protein, SIRT3 is involved in metabolism (energy production from fatty acids), ROS detoxification, aging, and the DDR. In general, SIRT3 upregulates processes involved in respiration (energy production) while reducing the production of ROS [63, 64]. During caloric restriction or metabolic stress, SIRT3 deacetylates Acetyl-Coenzyme A Synthetase (ACS), long-chain acyl-coenzyme A (acyl-CoA) dehydrogenase (LCAD), and 3-hydroxy-3-methylglutaryl CoA synthase 2 (HMGCS2) to upregulate their enzymatic activities [65]. These proteins convert fatty acids from triglycerides into usable forms of energy through lipid oxidation [65].

Furthermore, caloric restriction also stimulates SIRT3 to deacetylate and activate superoxide dismutase 2 (SOD2) and isocitrate dehydrogenase 2 (IDH2) to reduce ROS produced by oxidation of metabolic substrates [65]. Reduction of ROS leads to decreased activity of HIF-1α which works to slow cell proliferation through decreased glucose uptake and lysis [63, 64]. Through regulation of metabolic homeostasis and ROS levels, SIRT3 provides protection against age-related disease [63, 64].

The exact mechanisms in which SIRT3 is involved in aging is unclear but evidence suggests that SIRT3 repression of ROS production and regulation AMPK/PGC1α axis likely protects against aging related diseases [63, 64]. In fact, *Sirt3* knockout mice exhibit accelerated aging associated diseases. For instance, these mice exhibit age related hearing loss, cardiac hypertrophy, and cancer [63, 64].

Sirt3 knockout mouse embryonic fibroblasts (MEFs) transformed into cancer cells upon the addition of an oncogene indicating the potential for SIRT3 to works as a tumor suppressor protein [63, 64]. *Sirt3* knockout mice also began to develop mammary tumor at the age of 2 [63, 64]. These phenotypes are likely the result of increased ROS generation and therefore DNA damage (genomic instability) and HIF-1α activation [63, 64].

Sirtuin 4 (SIRT4)

SIRT4 is a less well characterized sirtuin that possess both deacetylase and ADP-ribosyl transferase activities and is involved in insulin secretion pathways, gliogenesis, lipid metabolism, and tumor suppression [66]. SIRT4 ADP-ribosylates Glutamate Dehydrogenase (GDH) and downregulates its activity which results in decreased insulin secretion. SIRT4 represses GDH to promote gliogenesis in the brain, providing a neuroprotective effect for glial cells and astrocytes [66]. SIRT4 also represses fatty acid oxidation, but promotes lipid anabolism under nutrient abundant conditions through deacetylation of malonyl CoA decarboxylase (MCD) [66]. Like SIRT3, SIRT4 may also

play a regulatory role in the AMPK/PGC1α axis and potentially provides protective effects against type 2 diabetes [66].

Despite our limited knowledge of SIRT4 and its potential substrates, it is still considered to be a potential tumor suppressor alongside many of the other Sirtuins in that loss of SIRT4 would lead to dysregulation of glutamine metabolism allowing the cell to promote cell growth and proliferation phenotypes [66]. Indeed, *SIRT4* knockout mice are more prone to developing lung tumors [66].

Sirtuin 5 (SIRT5)

SIRT5 is a lysine demalonylase, desuccinylase, and deglutarylase capable of removing malonyl, succinyl and glutaryl groups from protein substrates respectfully [66]. Less is known about SIRT5 function other that its role in regulating the urea cycle and in ROS reduction [66]. SIRT5 desuccinylates and deglutarylates Carbamoyl Phosphate Synthetase 1 (CPS1) which is the major regulator of the urea cycle [66]. SIRT5 modification of CPS1 upregulates its activity leading to ammonia detoxification and reduced ammonia levels [66].

Additionally, SIRT5 desuccinylates SOD1 leading to SOD1 activation and ultimately reduced ROS [66]. *Sirt5* knockout mice do not demonstrate abnormal metabolic phenotypes or spontaneous tumor formation [66]. At this time, there is little evidence to suggest SIRT5 could play a major role in tumor development [66].

1.2.3 Cytoplasmic Sirtuin: SIRT2

SIRT2 is the only sirtuin primarily localized to the cytoplasm and is the only sirtuin capable of nuclear localization without a recognizable NLS [45]. Currently, SIRT2 has established functions in a wide array of protein pathways including cell cycle control, microtubule dynamics, aging, metabolism, and the DDR [45, 67-74]. SIRT2 is essential to cell cycle regulation through histone modification and potentially centriole and spindle fiber modification (Figure 1.3) [67, 69, 74, 75].

Beginning in late S phase and proceeding through the G2/M transition SIRT2 moves from the cytoplasm into the nucleus where it localizes to chromatin [69, 74, 75]. SIRT2 deacetylates H4K16 to promote the formation of condensed chromatin [75]. Deacetylation of H4K16 also allows for deposition of H4K20 methylation (H4K20me2/3) by N-lysine methyltransferase KMT5A (PR-Set7) for further chromatin compaction [74]. SIRT2 may directly help stabilize PR-Set7 at chromatin through deacetylation at lysine 90 [74]. This condensation is necessary for proper cell division and mitotic exit [74]. Additionally, SIRT2 may regulate microtubule networks [67, 69].

Microtubules are formed from polymerization of α- and β- tubulin heterodimers and they regulate cell structure, movement, intercellular transport, and cell division [67]. SIRT2 deacetylates α-tubulin at lysine 40 in the cytoplasm of cells, but the functional significance of this deacetylation event is not well understood [67]. SIRT2 also colocalizes with the mitotic regulatory kinase Aurora A at centrosomes and along spindle fibers during prophase and metaphase of mitosis [69]. During cytokinesis, SIRT2

colocalizes with Aurora B at midbody structures indicating SIRT2 likely has a role in regulating microtubules during mitosis [69]. In fact, SIRT2 overexpression lead to an increase in multinucleation following mitosis, suggesting over activation of SIRT2 may have an inhibitory role for cell division [69].

SIRT2 is also thought to have an inhibitory role in cell adhesion and migration through regulation of microtubules [76]. For example, SIRT2 overexpression inhibits neurite outgrowth in and upregulates growth cone collapse in mouse hippocampal neurons [76]. Like other Sirtuins, SIRT2 is also involved in aging and metabolism [68, 77].

SIRT2 has been established to regulate the mitotic checkpoint kinase BubR1 in mice which is important to repression of aging and the development of age related disease [68]. BubR1 overexpression in mice leads to prolonged longevity while BubR1 hypomorphic mice exhibit reduced lifespan and accelerated aging [68]. BubR1 levels decline naturally with age, and this decline correlates to a decline in cellular NAD^+ levels [68]. SIRT2 overexpression in BubR1 hypomorphic mice partially rescues longevity [68]. It was determined that acetylation of BubR1 at lysine 668 by CBP leads to increased ubiquitination and degradation of BubR1 while SIRT2 deacetylates BubR1 at lysine 668, stabilizing the protein [68]. Stable BubR1 suppresses aging and age-related disease [68]. During caloric restriction, NAD^+ levels increase leading to increased SIRT2 activation and BubR1 deacetylation and stabilization further demonstrating how SIRT2 can contribute to longevity [68]. Increased NAD^+ levels in response to cellular stress results

in the upregulation of other SIRT2 functions that help maintain metabolic homeostasis [77].

SIRT2 is upregulated in response to caloric restriction and oxidative stress where it binds and deacetylates FOXO3a similar to SIRT1 [77]. FOXO3a deacetylation leads to increased FOXO3a DNA binding and upregulation of FOXO3a target genes including p27, Manganese Superoxide Dismutase (SOD2), and Bcl-2-like protein 11 (BIM) [77]. These proteins function in pathways that reduce cellular ROS levels [77]. In addition, BIM activation can upregulate apoptotic pathways and SIRT2 promotes cell death under severe stress conditions through BIM upregulation [77]. Reducing cellular ROS levels is important to genome maintenance (reduced ROS induced DNA damage) and preventing metabolic dysfunction which is important to tumor suppression [63, 64]. However, SIRT2 has additional, more direct, roles in genomic stability maintenance through its regulation of DDR pathways [78].

As discussed previously, the RSR is a subset of the DDR which is activated in response to stalled replication forks [7, 8]. Replication forks stall when they encounter DNA lesions, in response to DNA damage during S phase, or in response to nucleotide depletion [7, 8]. Extended replication fork stalling can result in fork collapse into strand breaks and/or activation of apoptotic pathways [73]. SIRT2 functions as a replication checkpoint protein through the positive regulation of CDK9 and ATRIP via deacetylation in the RSR [71, 73].

In vitro and in cells, SIRT2 deacetylates Cyclin Dependent Kinase 9 (CDK9) at lysine 48 leading to increased kinase activity [73]. Activated CDK9 is recruited to stalled forks to promote fork stabilization (preventing fork collapse) and replication stress recovery (replication fork restart) [73]. SIRT2 also deacetylates ATRIP at lysine 32 during the ATR checkpoint pathway in response to replication stress [71]. SIRT2 deacetylation of ATRIP promotes ATRIP binding and accumulation at stalled replication fork RPA-coated ssDNA [71]. This accumulation potentiates the ATR checkpoint, promotes ATR phosphorylation, stabilizes the stalled replication fork, and drives the signaling necessary for DNA replication fork restart and replication stress recovery [71]. Other functions for SIRT2 in DDR pathways regulations were found through the generation of a *Sirt2* knockout mouse model.

SIRT2 was further implicated in DDR pathway regulation in mice where it was established to maintain genomic stability through positive regulation of APC/C activity. SIRT2 deacetylates CDH1 and cell division cycle protein 20 (CDC20) [78]. CDC20 activates APC/C in the early phases of mitosis through anaphase and then CDH1 activates APC/C activity in late mitosis and G1 to regulate multiple proteins involved in mitotic progression [78]. CDH1 activation of APC/C activity is also necessary for the activation of the G2/M cell cycle checkpoint and may be regulated in G2 by SIRT2 [9]. Active APC/C ubiquitinates a multitude of mitotic regulator proteins including PLK1, Never in Mitosis A-related Kinase 2 (Nek2A), Aurora-A, Aurora-B, Cyclin-A, Cyclin-B, Survivin, and Securin to upregulate their proteasomal degradation and promote mitotic progression [78]. Additionally, SIRT2 acts as a mitotic checkpoint protein in that it

inhibits chromatin condensation in early phases of mitosis in response to elevated mitotic stress induced by mitotic poisons [79]

Sirt2 knockout mice exhibit impaired mitotic function, centrosome amplification, and increased levels of mitotic regulators all of which can lead to mitotic catastrophe, aneuploidy (chromosomal abnormalities), and genomic instability [78]. Furthermore, *Sirt2* knockout mice exhibit increased sex specific tumor formation in that male mice develop liver tumors and female mice develop breast tumors demonstrating that SIRT2 functions as a murine tumor suppressor [78].

1.3 Establishing SIRT2 as a Human Tumor Suppressor

Sirt2 is a murine tumor suppressor and exhibits several features that are common to established human tumor suppressors. SIRT2 contributes to the suppression of cell adhesion and cell movement (functions upregulated in metastasis), the upregulation of apoptotic pathways in response to severe cellular stress, and the regulation of cell cycle checkpoints and cell division (Figure 1.3) [45, 67-74]. Moreover, *SIRT2* depletion in human cell lines leads to genomic instability phenotypes and increased sensitivity to DNA damaging agents [73, 74].

Decreased *SIRT2* expression has also been found in many human cancers including breast, liver, glioma, renal, prostate, lung, uterine, and basal cell carcinomas [78, 80-85]. Additionally, *SIRT2* has been found to be mutated or deleted in multiple cancers such as ovarian, adenoid cystic, cervical, uterine, lung, pancreatic, gastric, esophageal, colorectal,

liver, melanoma, testicular germ cell, and thyroid cancers [73, 86]. In addition, *SIRT2* depletion in human cell lines and mouse embryo fibroblasts (MEFs) results in hypersensitivity to replication stress, delayed S-phase progression, spontaneous accumulation of RPA foci, and G2/M checkpoint deficits in response to IR [73, 74]. Furthermore, *SIRT2* depletion in chicken DT40 cells results in increased sensitivity to cisplatin [87].

Identification of human cancers that exhibit large scale deletions in SIRT2 allows for the establishment of SIRT2 as a candidate tumor suppressor, but whether or not SIRT2 is a true human tumor suppressor that could be used as a future cancer biomarker and therapeutic target has yet to be fully demonstrated [88]. One method used in the confirmation of a candidate gene as tumor suppressor is to demonstrate its biological relevance to the development of cancer [88]. Additional confirmation is provided by the identification of missense mutations which affect normal cellular function of its encoded protein in primary tumors and cell lines [88]. Furthermore, according to Robertson et al, "The ultimate validation is reintroduction of the putative cancer suppressor gene into cancer derived cell lines lacking expression and observing a reversion to a less tumorigenic, more "normal" phenotype" [88].

In the following chapters, I provide evidence that suggests SIRT2 is a human tumor suppressor by demonstrating cancer associated point mutations in *SIRT2* result in loss of SIRT2 function and by rescuing tumorigenic phenotypes in cell lines deficient for *SIRT2* with reintroduction of *SIRT2* wildtype but not *SIRT2* containing cancer associated point

mutations. Moreover, in addition to regulatory functions in suppression of cell motility, regulation of metabolism, upregulation of apoptosis in response to extreme stress conditions, and regulation of cell cycling and division I demonstrate a novel role for SIRT2 in DNA damage repair through the regulation of DNA-PKcs.

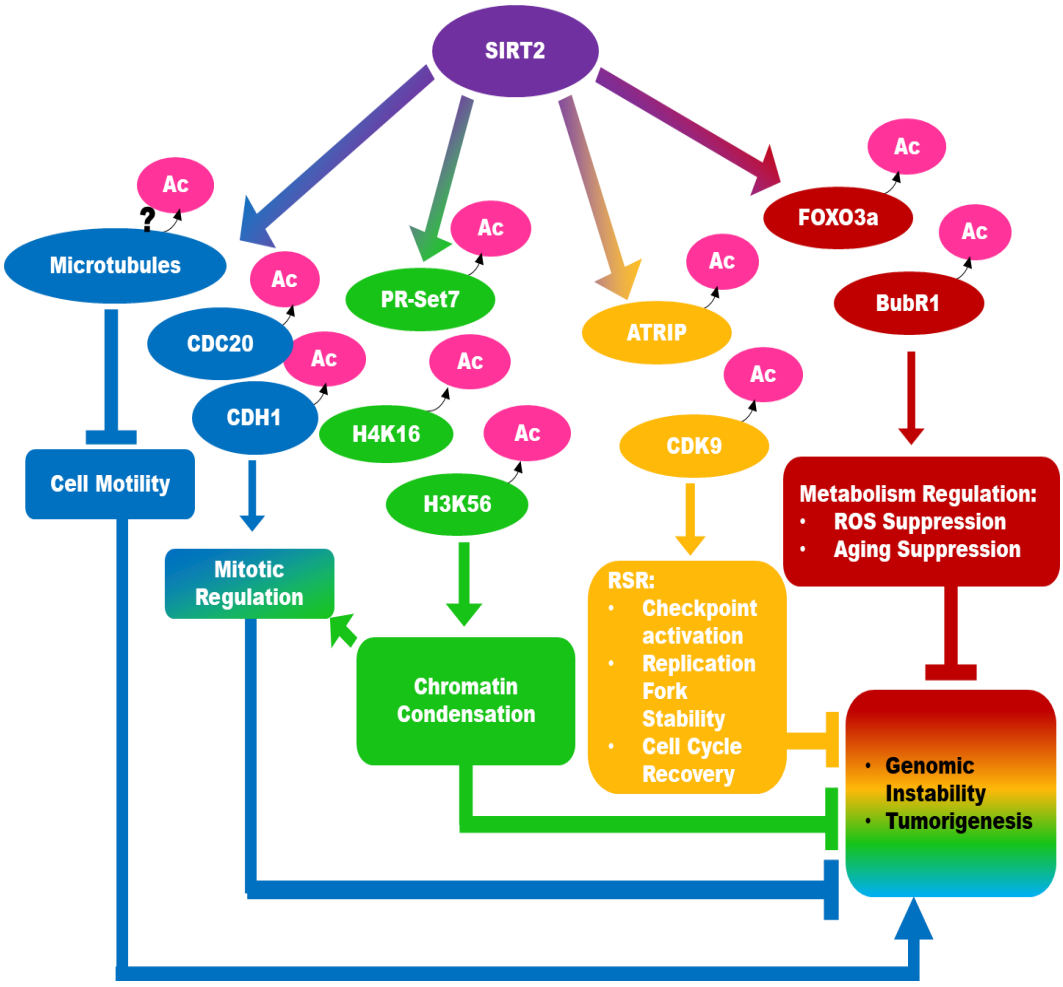

Figure 1.3. SIRT2 Pathway Regulation Schematic SIRT2 regulates a network of proteins over multiple cellular pathways to regulate cell motility, chromatin condensation and mitosis, the RSR, metabolism and tumor suppression.

Chapter 2: Sirtuin 2 mutations in human cancers impair its function in genome maintenance

Published by the Journal of Biological Chemistry, May 2017.

2.1 Author's Contribution and Acknowledgement of Reproduction

PamelaSara Head and David Yu conceived and coordinated the study, designed experiments, and wrote the paper. PamelaSara Head performed and analyzed the experiments shown in **Figure**s 2, 3, 4, 5, and 6. Hui Zhang assisted in conception of and experimental design, and experiments for **Figure**s regarding GFP-ATRIP foci. Amanda Bastien designed, performed and analyzed the experiments shown in **Figure** 1. Allyson Koyen also contributed to the design of **Figure** 6C-D. Allison Withers contributed to the design of **Figure** 2A. Waaqo Daddacha provided assistance in generation of the *SIRT2* knockout lines by CRISPR CAS9. Xiaodong Cheng assisted in conception and production of **Figure** 3. All authors reviewed the results and approved the final version of the manuscript.

2.2 Abstract

Sirtuin 2 (SIRT2) is a sirtuin family deacetylase, which maintains genome integrity and prevents tumorigenesis. Although *Sirt2* deficiency in mice leads to tumorigenesis, the functional significance of somatic *SIRT2* mutations in human tumors is unclear. Using structural insight combined with bioinformatics and functional analyses, we show that naturally occurring cancer-associated *SIRT2* mutations at evolutionarily conserved sites disrupt its deacetylation of DNA-damage response proteins by impairing SIRT2 catalytic activity or protein levels but not its localization or binding with substrate. We observed that these SIRT2 mutant proteins fail to restore the replication stress sensitivity, impairment in recovery from replication stress, and impairment in ATR-interacting protein (ATRIP) focus accumulation of *SIRT2* deficiency. Moreover, the SIRT2 mutant proteins failed to rescue the spontaneous induction of DNA damage and micronuclei of *SIRT2* deficiency in cancer cells. Our findings support a model for SIRT2's tumor-suppressive function in which somatic mutations in *SIRT2* contribute to genomic instability by impairing its deacetylase activity or diminishing its protein levels in the DNA-damage response. In conclusion, our work provides a mechanistic basis for understanding the biological and clinical significance of *SIRT2* mutations in genome maintenance and tumor suppression.

2.3 Introduction

Sirtuin 2 (SIRT2) is a class III NAD^+-dependent deacetylase, which regulates a broad range of biological functions, including aging, metabolism, differentiation, genome maintenance, and tumor suppression [44, 46, 47, 72, 89, 90]. SIRT2 over-expression prolongs longevity in mice hypomorphic for BubR1 [68], and mice deficient in *Sirt2* develop breast, liver, and other cancers [74, 78, 91], suggesting that SIRT2 functions in both aging and tumor suppression. Indeed *SIRT2* expression is decreased in a number of cancers, including human breast, liver, glioma, renal, prostate, lung, uterine, and basal cell carcinomas [71, 78, 80, 81, 83-85], and moreover *SIRT2* is mutated or deleted in ovarian, adenoid cystic, cervical, uterine, lung, pancreatic, gastric, esophageal, colorectal, liver, melanoma, testicular germ cell, thyroid, and breast cancers [73, 86]. Genetic loss of *Sirt2* in mice results in genomic instability [74, 78], suggesting that SIRT2 prevents tumorigenesis at least in part by protecting cells against DNA damage and thereby promoting the DNA-damage response (DDR). *SIRT2* depletion in cells results in hypersensitivity to replication stress, spontaneous induction of DNA damage, delayed S phase progression following replication stress, and an impaired G_2/M checkpoint [71, 73, 74, 87]. SIRT2 deacetylates ATR-interacting protein (ATRIP) at lysine (Lys) 32 to drive the ATR checkpoint by facilitating binding to replication protein A-coated single-stranded DNA [71] and deacetylates cyclin-dependent kinase 9 (CDK9) at Lys-48 to promote its activity in facilitating recovery from replication stress [73]. SIRT2 also promotes the mitotic checkpoint through deacetylation of α-tubulin at Lys-40 [67, 79], anaphase-promoting complex/cyclosome co-activators CDH1 and CDC20 [92], histone H4 at Lys-16 and PR-Set7 at Lys-90 [74], and BubR1 at Lys-250 [93]. Thus, SIRT2 is a

critical regulator of the DDR in maintaining genome integrity. Although *Sirt2* deficiency in mice leads to genomic instability and tumorigenesis, and SIRT2 is often dysregulated in human cancers, the functional significance of somatic *SIRT2* mutations in cancer is not known. Here, we show that naturally occurring cancer-associated *SIRT2* mutations contribute to genomic instability of cancer cells by impairing its deacetylase activity or protein level in the DDR.

2.4 Materials and Methods

Transfections

SiRNA were obtained from Thermo Scientific or Qiagen. Transfections were performed using Lipofectamine 2000 (Invitrogen) or RNAi Max (Invitrogen) following the manufacturer's instructions. Individual siRNAs sequences include:

1. siSIRT2-10 UTR: (TGGGCAGAAGACATTGCTTAT);
2. siSIRT2-5: (GGAGAAAGCTGGCCAGTCG);
3. siATR: (CCTCCGTGATGTTGCTTGA);
4. Nontargeting siRNA: (ATGAACGTGAATTGCTCAATT)

Cell Cycle Recovery

HCT116 cells were transfected with ATR, NS, or SIRT2 siRNA, and 24 hours later with SIRT2-FLAG WT (Addgene 13813) [67] or mutants, treated with or without 3mM HU 72 hours post-knockdown for 20 hours (arrested) [94], and released into 0.5 μg/mL nocodazole (Fisher Scientific) for 10 hours. Cells were harvested and fixed in ice-cold 70% ethanol and DNA was stained with 25 μg/mL propidium iodide (Sigma-Aldrich) with 100 μg/mL RNase A (Qiagen). DNA content was measured by flow cytometry using a BD FACS Canto II flow cytometer and then analyzed by FlowJo software gating analysis tool (Tree Star).

Immunofluorescence

For SIRT2 localization experiments, U2OS cells were transfected with SIRT2-FLAG WT or mutants, treated 72 hours post transfection with 5 nM Leptomycin B (Sigma) for 4

hours, fixed in 4% PFA for 10 minutes, and permeabilized in 0.5% triton X-100 for 10 minutes. Cells were blocked in 5% BSA and immunostained with anti-FLAG (Cell Signaling: 2368P) and Alexa Fluor 555 anti-rabbit secondary antibody (Invitrogen) followed by DAPI stain (Southern Biotech). For GFP-ATRIP experiments, a stably transfected GFP-ATRIP U2OS cell line was used. Cells were transfected with nontargeting siRNA (siNS) or siSIRT2-5 followed by transfection with pcDNA3.1 empty vector (EV) or SIRT2-FLAG WT or mutants. SIRT2-FLAG constructs contained wobble mutations to protect exogenous expression from knockdown. Cells were treated with 3mM HU for 24 hours prior to fixation and were fixed and blocked as described above. Cells were immunostained with anti-FLAG (Cell Signaling: 2368P) followed by Alexa Fluor 555 secondary antibody (red), and DAPI Stain. GFP-ATRIP did not require antibody (green). SIRT2-FLAG positive cells were used for quantitation of these experiments with an exception for EV transfected conditions. For spontaneous γH2AX foci experiments, we utilized SIRT2 WT or KO U2OS cells transfected with or without SIRT2-FLAG WT or mutants [95]. Cells were fixed and blocked as described above, immunostained with anti-FLAG (Cell Signaling: 2368P) and anti-γH2AX (Millipore 05-636) followed by Alexa Fluor 488/555 secondary antibodies and DAPI stain. SIRT2-FLAG positive cells were used for quantitation of these experiments with an exception for non-SIRT2 transfected conditions. Percentage of cells positive for GFP-ATRIP or γH2AX foci was counted from three replicas of 100 cells each. Micronuclei experiments were fixed and processed as described above. Only SIRT2-FLAG positive cells were used in quantitation analysis. The percentage of cells positive for micronuclei was

counted from three replicas with 100 cells each. All Images were captured on a Zeiss Observer Z1 microscope equipped with Axio vision Rel 4.8 software.

Immunoblot

Harvested cells were lysed for 30 minutes on ice in Nonidet P-40 buffer (200 mM NaCl, 1% Nonidet P-40, 50 mM Tris·HCl pH 8.0) freshly supplemented with protease inhibitors. Protein samples were resolved by SDS/PAGE and probed with indicated antibodies: SIRT2 (Santa Cruz sc-20966), GAPDH (Santa Cruz sc-25778 or sc-47724), Flag (Sigma F4042), CDK9 (Santa Cruz sc-13130), GFP (Abcam; Ab6556), HA (Sigma; H9658), Ac-CDK9 Lys-48 (custom generated through Epitomics), Ac-tubulin Lys-40 (Sigma; T7451), tubulin (Sigma; T6074), Ac-ATRIP Lys-32 (custom generated through Epitomics) and ATR (Santa Cruz; sc-1887). Detection was performed with the Odyssey system. All western blots were performed at least 4 times.

Immunoprecipitation

Harvested cells were lysed for 40 minutes on ice in IP lysis buffer (0.75% CHAPS, 10% (vol/vol) glycerol, 150 mM NaCl, 50 mM Tris pH 7.5) freshly supplemented with protease inhibitors. Supernatants were diluted to adjust the CHAPS concentration to 0.375%. Target proteins from 3 mg of lysate were captured with anti-GFP antibody (Abcam; Ab6556) and protein A agarose beads (Invitrogen) or with HA preconjugated beads (Sigma A2095). Complexes were washed four times with IP washing buffer (0.375% CHAPS, 10% glycerol, 150 mM NaCl, 50 mM Tris pH 7.5) supplemented with protease inhibitors. Immunoprecipitation experiments were performed at least 4 times.

Generation of CRISPR/Cas9 SIRT2 Knockout Cells

U2OS/HCT116 cells were transfected with plasmid containing guide RNAs (sgRNA), targeting an early *SIRT2* exon or a nontargeting control, and Cas9-GFP construct (Sigma). 72 hours after transfection, cells were harvested and sorted by FACs into 96 well plates with one cell per well based on high level of GFP expression. Single cells that survived and gave rise to cell lines were tested for *SIRT2* knockout by western blot analysis.

In vitro or Cellular Deacetylation Experiments

For *in vitro* deacetylation analysis of CDK9 and ATRIP, 293T cells were transiently transfected with CDK9-GFP or HA-ATRIP and histone acetyltransferase (p300/CBP/pCAF) or SIRT2-FLAG WT or mutants, and treated with 0.5 μM TSA and 20 mM nicotinamide for 12 h. Cells were lysed with IP buffer (20 mM Hepes pH 7.4, 180 mM KCl, 0.2 mM EGTA, 1.5 mM MgCl2, 20% glycerol, 1.0% Nonidet P-40) supplemented with 1 μM TSA and fresh protease inhibitors. Acetyl-CDK9 or acetyl-ATRIP were immunoprecipitated using anti-GFP (Abcam; Ab6556) and protein A agarose beads (Invitrogen) or anti-HA preconjugated beads (Sigma), washed with IP buffer containing 1μM TSA to remove nicotinamide, and washed an additional 2 times with deacetylation buffer (50 mM Tris pH 7.5, 150mM NaCl, and 1mM MgCl2). SIRT2-FLAG constructs were immunoprecipitated using anti-FLAG M2 agarose beads (Sigma), washed with IP buffer and TBS (50 mM Tris pH 7.5 and 150mM NaCl), and eluted with 0.15mg/mL 3x FLAG Peptide (Sigma) for 30 minutes at 4◦C. Protein concentration was

determined by coomassie stain. Substrate on beads (HA-ATRIP or CDK9-GFP) were incubated with or without 1 μg of SIRT2-FLAG WT or mutants in 24 μl deacetylation reaction buffer (1μM TSA, 50 mM Tris·HCl, pH 7.5, 150 mM NaCl, 1 mM MgCl2, and 1 mM NAD^+) at 30 ◦C for 3 h. For the dominant negative assay, CDK9-GFP was incubated with 1 ug SIRT2WT or with 0.5 ug SIRT2 WT and 0.5 ug of one of the 4 mutants tested. The reaction was stopped by the addition of 5× SDS loading buffer, and samples were analyzed for acetylation by Western blot with an anti-Ac-ATRIP Lys-32 (custom generated through Epitomics) [67, 71, 87] and Ac-CDK9 Lys-48 (custom generated through Epitomics) [73]. For cellular deacetylation analysis, 293T cells were transiently cotransfected with CDK9-HA and histone acetyltransferase (p300/CBP/pCAF) and SIRT2-FLAG WT or mutants. Cells were cultured with 0.5 μM TSA for 12 h prior to being lysed with IP buffer containing 1 μM TSA, and protein lysates were immunoprecipitated using HA preconjugated beads (Sigma A2095). The immunocaptured protein were analyzed for deacetylation by immunoblotting with anti-Ac-CDK9 Lys-48, anti-HA, alpha-tubulin (Sigma; T6074), and Ac-tubulin Lys-40 (Sigma; T7451). For the Flour de Lys *In vitro* experiments, SIRT2-FLAG WT and mutants were purified from 293T cells and eluted from FLAG-M2 beads (Sigma) as described above. 120 ng SIRT2-FLAG was used following manufacturer's instructions (Enzo life sciences). All deacetylation experiments, both *in vitro* and in cells, were performed at least 4 times.

Cell Viability Assay

HCT116 cells were transfected with 40 nM siRNA using RNAi Max reagent and split, followed by transfection with no SIRT2-FLAG WT or mutants, treated with or without 1.6 mM HU 72 hours post knockdown for 24 hours followed by 24 hours recovery. Viability was measured using Alamar blue (Thermo Fisher) on a Spectra Plus plate reader. A ratio of treated/untreated viability was calculated and normalized to that of nontargeting siRNA [96]. Sequence Alignment. Protein BLAST (blastp) was used through the NCBI website to compare sequence homology between closely and distantly related organisms to human SIRT2 protein sequence obtained from Uniprot and to align protein sequences.

2.5 Results

Cancer-associated SIRT2 mutations are evolutionarily conserved and predicted to be functionally significant.

To determine the functional significance of somatic *SIRT2* mutations in human cancers, we analyzed sequencing data from patient-derived tumor samples reported in The Cancer Genome Atlas through the cBioPortal for Cancer Genomics [85, 97]. The Cancer Genome Atlas currently contains 70 *SIRT2* missense mutations and five *SIRT2* truncation mutations across multiple cancer types, including breast, cervical, colorectal, head and neck, lung, stomach, testicular germ cell, thyroid, and uterine cancer, most of which overlap with the 66 somatic *SIRT2* mutations found in the Catalogue of Somatic Mutations in Cancer (COSMIC) database [86]. We focused our investigation on nine *SIRT2* mutations present in uterine, lung, and colorectal cancers, which were found in both data sets, predicted to be high impact mutations by cBioPortal, and occurred at appreciable frequencies within their study cohort (Fig. 1A). All mutations selected were missense mutations, occurred throughout the length of the protein, and were highly conserved across distantly related species (Fig. 1B). To validate the potential importance of these mutations, we performed *in silico* bioinformatics analyses for functional significance using several conservation and impact prediction platforms, including Grantham, Sorting Intolerant from Tolerant (SIFT), Polymorphism Phenotyping (PolyPhen), and ConSurf (Fig. 1C) [98-106]. Grantham scores predict the evolutionary distance between substituted amino acids and thus the potential for missense mutations to be deleterious or neutral. This analysis was completed using the Align-GVGD program through the Huntsman Cancer Institute at the University of Utah. SIFT and ConSurf

predictions are based on the degree of conservation of amino acid residues in sequence alignments derived from closely related sequences collected through Position-Specific Iterative Basic Local Alignment Search Tool (PSI-BLAST) [107-109]. ConSurf determines the conservation of an amino acid and rates it on a scale of 1–9 with 9 indicating highly conserved. PolyPhen predicts the possible impact of missense mutations on the structure and function of a given human protein by comparing physical and alignment-based comparisons. Consistently, mutations P128L, P140H, R153C, A186V, and F190V were found to be highly conserved and deleterious if mutated, and notably all are located within the SIRT2 deacetylase domain. R42P was also well conserved and predicted to have a high impact on SIRT2 function with its localization within the nuclear export sequence (NES) of SIRT2 [69, 110]. Collectively, these data indicate that cancer-associated *SIRT2* mutations are evolutionarily conserved and are predicted to be functionally significant, suggesting that they are more likely to be driver mutations that benefit cancer progression rather than random carrier mutations.

Cancer-associated mutations impair SIRT2 in vitro deacetylase activity and protein level but not localization.

Each of the cancer-associated *SIRT2* mutations was created by site-directed mutagenesis in a SIRT2-FLAG construct and expressed in 293T cells along with SIRT2 wild type (WT) and H187Y deacetylase-inactive mutant controls. All of the mutants were expressed at comparable levels to SIRT2 WT except for R42P, which showed lack of protein expression similar to an empty vector (Fig. 2A), suggesting that R42P affects either protein stability or mRNA expression. SIRT2 shuttles between the nucleus and

cytoplasm through active nuclear export in a CRM1-dependent manner [69]. To determine whether cancer-associated mutations are important for SIRT2 localization, we examined localization of SIRT2 WT and mutants expressed in U2OS cells before and after treatment with leptomycin B (LMB), which inhibits CRM1-mediated nuclear export, by indirect immunofluorescence. All of the mutants expressed localized predominantly in the cytoplasm and demonstrated nuclear retention following treatment of cells with LMB (Fig. 2B), suggesting that *SIRT2* cancer mutants are capable of proper cytoplasmic and nuclear localization. To determine whether cancer-associated mutations are important for SIRT2 deacetylase activity, we performed *in vitro* measurements using the *Fluor De Lys in vitro* deacetylase assay by Enzo Life Sciences, which uses an acetylated p53 Lys-320 peptide as a substrate. Three of the mutants, SIRT2 P128L, P140H, and A186V, demonstrated significantly decreased deacetylase activity compared with SIRT2 WT with SIRT2 P128L and A186V impairing deacetylase activity similarly to catalytically inactive SIRT2 H187Y (Fig. 2C). All three of these mutations are located within the deacetylase domain of SIRT2 and likely affect NAD^+ cofactor and/or substrate binding or catalytic activity.

Structural analysis of SIRT2 mutations yields insights into their functional significance.

To gain further insight into how cancer-associated mutations might affect SIRT2 biological function, we examined the crystal structure of SIRT2 obtained from the Research Collaboratory for Structural Bioinformatics Protein Data Bank, specifically structure 4RMH [111]. We first focused on four mutants of interest based on their

predicted impact scores, deacetylase activity, and structural location: P128L, P140H, A186V, and F190V. All four were predicted to negatively impact protein function, and three of these demonstrated decreased deacetylase activity *in vitro*. All four were also located in the active site of SIRT2 (Fig. 3A). Pro-128 and Pro-140 make up the ends of an important α helix responsible for composing part of the active site for NAD^+ binding. Mutation of these prolines could therefore alter the orientation of the helix and result in decreased binding of NAD^+ and thus lower deacetylase activity. Pro-140 is also important for the formation of the binding pocket for NAD^+ along with Phe-190; these two amino acids stack on either side of NAD^+ (Fig. 3A, blue molecule). Mutating either of these amino acids therefore would also likely result in decreased binding of NAD^+ and lower deacetylase activity. F190V, however, does not yield a deacetylase-defective phenotype (Fig. 2C), suggesting that this mutation alone is not sufficient to inhibit cofactor binding. Ala-186 lies adjacent to the active site amino acid His-187 and thus could affect its neighboring amino acid's ability to deacetylate substrate (Fig. 3, B and C). In fact, Ala-186 lies in a tight pocket with little space for amino acid structure variation as better illustrated in the space filling model in Fig. 3C. Even the small addition of two methyl groups is likely enough to blow out this pocket and upset the orientation of His-187, thereby inhibiting deacetylation of substrate. Overall, these four amino acids are heavily involved in proper deacetylase activity and/or cofactor binding. The other five mutations for this study lie outside of the active site and binding pocket of SIRT2. Only four of these five amino acids (Glu-203, Arg-153, Leu-341, and Ser-73) have been verified for orientation and structure as the current crystal structures of SIRT2

lack a portion of the N terminus where Arg-42 lies (Fig. 3D). Of these amino acids, three are on the surface of the protein where they potentially interact with other proteins (Glu-203 and Arg-153) and/or perhaps undergo post-translational modification (Ser-73). Therefore, mutation of these amino acids to non-compatible substitutes could upset other aspects of SIRT2 function regulated by protein-protein interaction but that are not necessary for deacetylase activity. The fourth amino acid, Leu-341, is hydrophobic and forms a portion of an α helix. Mutation of this amino acid therefore could lead to a change in structure of the helix and upset the surface structure without affecting SIRT2 deacetylase activity. Fig. 3E shows a close-up of the two types of amino acids discussed, one surface amino acid likely involved in protein-protein interaction (Arg-153) and the other a hydrophobic amino acid serving a more structural purpose (Leu-341). Fig. 3F shows a hypothetical structure and orientation of Arg-42 produced using the PyMOL Molecular Graphics System, version 1.8 (Schrödinger, LLC) that may be involved in protein-protein interaction because it lies on the protein surface and is in a more open portion of the protein. Arg-42 also lies within the NES and may be necessary for proper nuclear export [69, 110].

Cancer-associated mutations impair SIRT2 deacetylation of DDR substrates in vitro and in cells but not interaction with substrate

To determine whether the impairment in deacetylase activity of SIRT2 P128L, P140H, and A186V observed with an acetylated p53 Lys-320 peptide used in the *Fluor De Lys* assay is substrate-specific, we tested for their ability to deacetylate additional SIRT2 substrates involved in the DDR *in vitro*. Consistent with findings using an acetylated p53

Lys-320 peptide, SIRT2-FLAG P128L showed the greatest impairment in *in vitro* deacetylase activity compared with SIRT2-FLAG WT when using acetylated ATRIP Lys-32 and CDK9 Lys-48 as substrates (Fig. 4, A and B). SIRT2-FLAG P140H and A186V failed to show the same degree of impairment in deacetylation of ATRIP Lys-32 and CDK9 Lys-48 (Fig. 4, A and B) compared with p53 Lys-320 (Fig. 2C), suggesting that these mutants are less impactful on SIRT2 deacetylase activity and/or impair deacetylation of specific substrates. To determine whether cancer-associated mutations impair the deacetylation of DDR substrates in cells, we expressed SIRT2-FLAG WT and mutants in 293T cells and determined their ability to deacetylate CDK9-HA and endogenous α-tubulin. Again, SIRT2-FLAG P128L but not P140H demonstrated significant impairment in deacetylation of CDK9 Lys-48 and α-tubulin Lys-40 in cells (Fig. 4, C and E). Interestingly, SIRT2 A186V also demonstrated decreased deacetylase activity against these substrates in cells (Fig. 4, C and E), implying that A186V impairs SIRT2 deacetylase activity for these substrates to a greater degree in cells potentially due to factors present in cells but not *in vitro* conditions. To determine whether the impairment in deacetylation of CDK9 Lys-48 in cells by SIRT2 P128L and A186V may be due to differences in binding with substrate, we analyzed their interaction by co-immunoprecipitation (co-IP). No differences in co-IP of CDK9-HA with SIRT2-FLAG WT and mutants was observed despite impairment in deacetylation of co-immunoprecipitated CDK9-HA by SIRT2-FLAG P128L and A186V (Fig. 4D), providing strong evidence that the impairment in deacetylation of CDK9 Lys-48 by SIRT2-FLAG P128L and A186V mutants is not due to an impairment in binding with substrate. As the majority of cancer-associated *SIRT2* mutations are in a heterozygous state in patients, to

determine whether they exert dominant negative effects on SIRT2 WT deacetylase activity, we performed an *in vitro* deacetylase assay in which acetylated CDK9-GFP was incubated with SIRT2-FLAG WT alone or with equal amounts of both SIRT2-FLAG WT and one of four SIRT2-FLAG mutants. We observed no significant difference in deacetylation of CDK9 Lys-48 by SIRT2-FLAG WT and mutants compared with SIRT2-FLAG WT alone in this *in vitro* deacetylase assay (Fig. 4F), suggesting that SIRT2 mutants do not exert a dominant negative effect on SIRT2 WT activity in this context.

Cancer-associated SIRT2 mutations fail to rescue RSR defects of SIRT2 deficiency.

To determine whether cancer-associated mutations are important for the RSR activities of SIRT2, we analyzed recovery from replication arrest in HCT-116 *SIRT2*-depleted cells complemented with SIRT2-FLAG WT and mutants (Fig. 5A). Ten hours following release from HU-induced replication arrest, *SIRT2*-depleted cells expressing SIRT2-FLAG P128L, P140H, and A186V showed a similar impairment in recovery from replication arrest to *SIRT2*-depleted cells expressing deacetylase inactive H187Y compared with WT (Fig. 5, B and C). *SIRT2*-depleted cells expressing SIRT2-FLAG P128L, P140H, and A186V also showed comparable HU hypersensitivity to H187Y compared with WT (Fig. 5D), suggesting that P128L, P140H, and A186V impair SIRT2's activity in responding to replication stress. Moreover, SIRT2-FLAG P128L and A186V but not P140H failed to alleviate the impairment in HU-induced GFP-ATRIP foci of *SIRT2* deficiency to a similar level as SIRT2-FLAG WT (Fig. 5, E and F), suggesting that these mutants impair the recruitment of ATRIP to stalled replication forks.

Cancer-associated SIRT2 mutations fail to rescue genomic instability of SIRT2 deficiency.

To determine whether cancer-associated mutations contribute to impairment in genome stability, we generated U2OS *SIRT2* knock-out (KO) cells utilizing CRISPR/Cas9 and performed complementation experiments with expression of SIRT2-FLAG WT and mutants (Fig. 6A). U2OS *SIRT2* KO cells demonstrated a significant increase in spontaneous γH2AX foci, a marker for DNA double-strand breaks, which can form from the collapse of stalled replication forks, compared with U2OS SIRT2 WT cells, and this was reduced by expression of exogenous SIRT2-FLAG WT (Fig. 6, B and C). Expression of SIRT2-FLAG P128L, P140H, and A186V all showed impairment in rescue of the spontaneous induction of spontaneous γH2AX foci observed with *SIRT2* deficiency, suggesting that P128L, P140H, and A186V impair SIRT2's ability to maintain genome integrity. As a more direct measure for genomic instability, we analyzed induction of spontaneous micronuclei, a marker for chromosomal breaks, in U2OS SIRT2 KO cells complemented with SIRT2-FLAG WT and mutants. Expression of SIRT2-FLAG P128L, P140H, and A186V also failed to reduce the spontaneous micronuclei of *SIRT2* deficiency to a similar extent as expression of SIRT2-FLAG WT (Fig. 6, D and E). Collectively, these data suggest that P128L, P140H, and A186V impair SIRT2's activity in the DDR, which leads to genomic instability.

A.

Cancer	Mutation Type	Mutation	Patients in Cohort with Mutation	Study
Uterine	P128L	Missense	11 in 549	TCGA COSMIC
Uterine	R153C	Missense	8 of 373	TCGA COSMIC
Uterine	P140H	Missense	8 of 373	TCGA COSMIC
Uterine	A186V	Missense	11 in 548	TCGA COSMIC
Uterine	L341M	Missense	11 in 549	TCGA COSMIC
Uterine	E203G	Missense	11 in 548	TCGA COSMIC
Lung Squamous Cell Carcinoma	S73R	Missense	9 in 504	TCGA COSMIC
Lung Squamous Cell Carcinoma	R42P	Missense	9 in 504	TCGA COSMIC
Colorectal	F190V	Missense	6 in 627	TCGA COSMIC

C.

AA Substitution	Grantham Prediction	SIFT	PolyPhen	ConSurf
R42P	Deleterious	Damaging	Probably Damaging	NA
S73R	Deleterious	Damaging	Benign	3
P128L	Deleterious	Damaging	Probably Damaging	9
P140H	Deleterious	Damaging	Probably Damaging	6
R153C	Deleterious	Damaging	Probably Damaging	9
A186V	Deleterious	Damaging	Probably Damaging	9
F190V	Possibly Deleterious	Damaging	Possibly Damaging	8
E203G	Deleterious	Tolerated	Possibly Damaging	2
L341M	Unlikely Deleterious	Tolerated	Possibly Damaging	8

B.

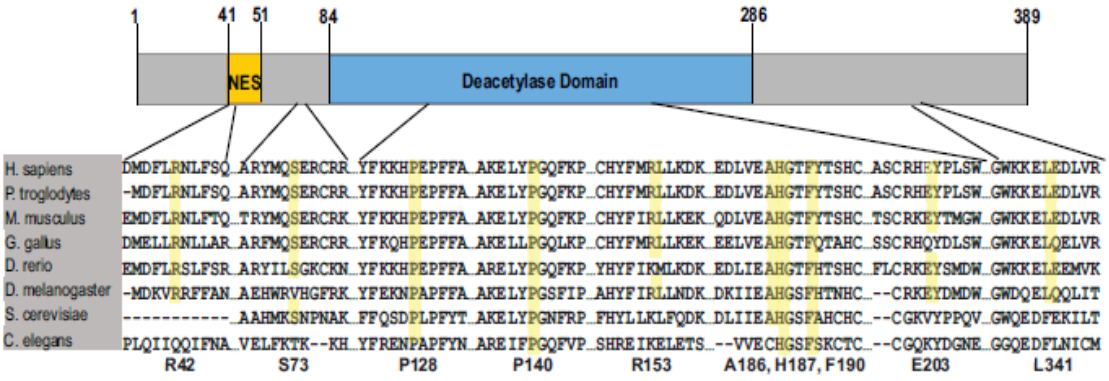

Figure 2.1. Cancer-associated *SIRT2* mutations are evolutionarily conserved and predicted to be functionally significant

A, Table listing cBioPortal data for nine naturally occurring *SIRT2* mutations in human cancer samples along with occurrence in patient cohort, cancer type, and study type. B, Conservation of cancer-associated *SIRT2* mutation amino acids among diverse species, including chimpanzee, mouse, chicken, zebrafish, fruit fly, yeast, and nematode, and their location in the protein structure. The NES is in yellow, and the deacetylase domain is highlighted in blue. C, Impact prediction of cancer mutations by Grantham, SIFT, and PolyPhen, and their conservation scores as calculated by ConSurf. TCGA, The Cancer Genome Atlas; COSMIC, Catalogue of Somatic Mutations in Cancer.

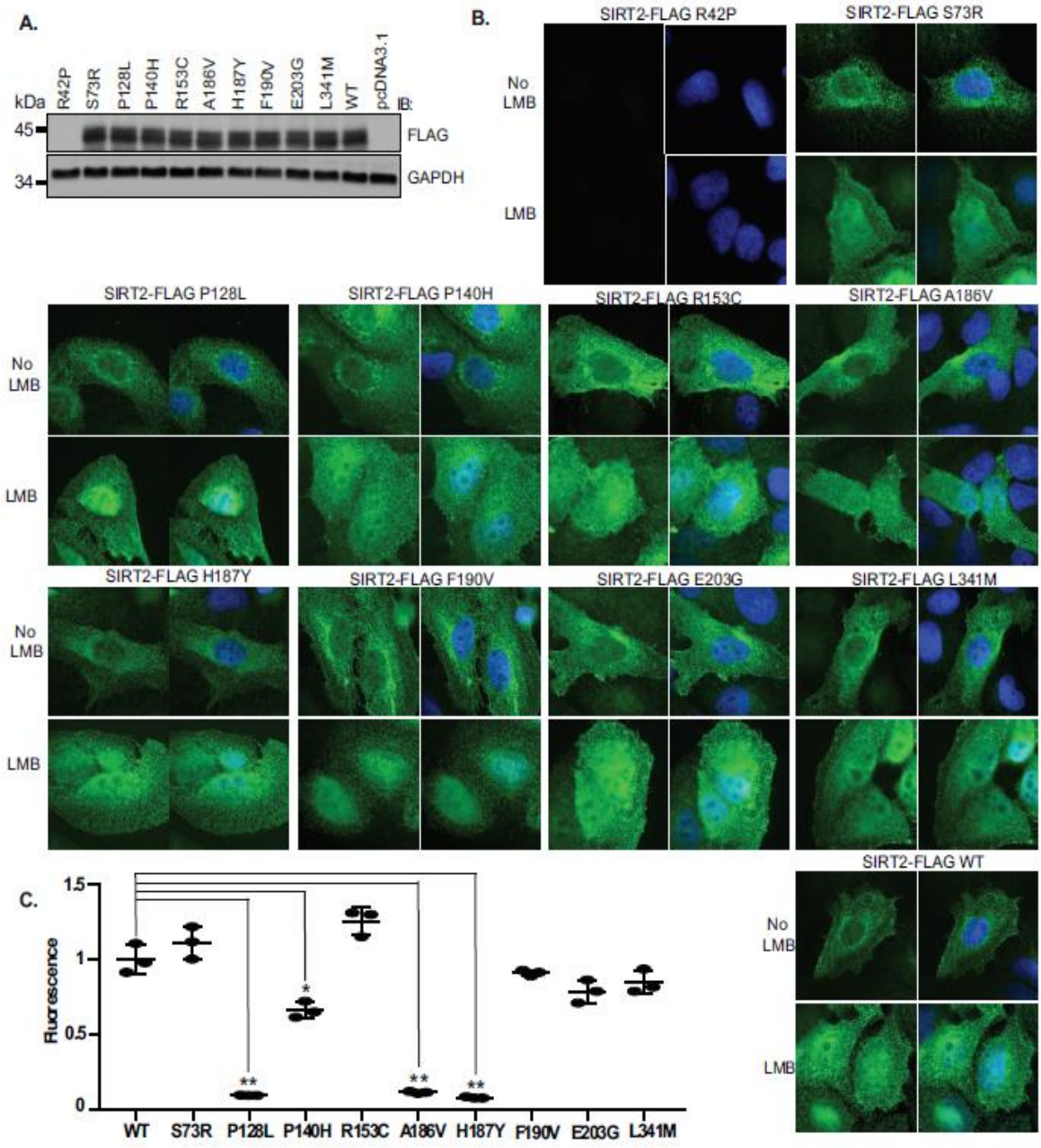
A.
kDa
R42P
S73R
P128L
P140H
R153C
A186V
H187Y
F190V
E203G
L341M
WT
pcDNA3.1
IB:
45
FLAG
34
GAPDH
B.
SIRT2-FLAG R42P
SIRT2-FLAG S73R
No LMB
LMB
SIRT2-FLAG P128L
SIRT2-FLAG P140H
SIRT2-FLAG R153C
SIRT2-FLAG A186V
SIRT2-FLAG H187Y
SIRT2-FLAG F190V
SIRT2-FLAG E203G
SIRT2-FLAG L341M
SIRT2-FLAG WT
C.
Fluorescence
1.5
1
0.5
0
WT
S73R
P128L
P140H
R153C
A186V
H187Y
F190V
E203G
L341M

Figure 2.2. Cancer-associated mutations impair *SIRT2* deacetylase activity and protein level but not localization

A, Western blot analysis demonstrating protein levels of SIRT2-FLAG WT and mutants expressed in U2OS cells. B, U2OS cells were transfected with SIRT2-FLAG WT or mutants. 72 h after transfection, cells were incubated with or without 5 nM LMB for 4 h to inhibit SIRT2 nuclear export, fixed, and processed for indirect immunofluorescence using anti-FLAG antibodies (green) and DAPI staining. Representative images are shown. C, *in vitro* measurements of SIRT2 deacetylase activity using the Fleur de Lys deacetylase assay are shown. SIRT2-FLAG WT and mutants were purified from 293T cells and eluted from FLAG M2 beads. Protein concentration was measured by Coomassie staining with a BSA standard control. 120 ng of SIRT2-FLAG WT and mutants was incubated in a reaction with an acetylated p53 Lys-320 peptide as a substrate. The mean of the relative fluorescence measured from three replicas is shown. Error bars represent S.D. Deacetylase activities of mutants were compared with that of SIRT2-FLAG WT. *,$p<0.05$; **,$p<0.01$. IB, immunoblotting.

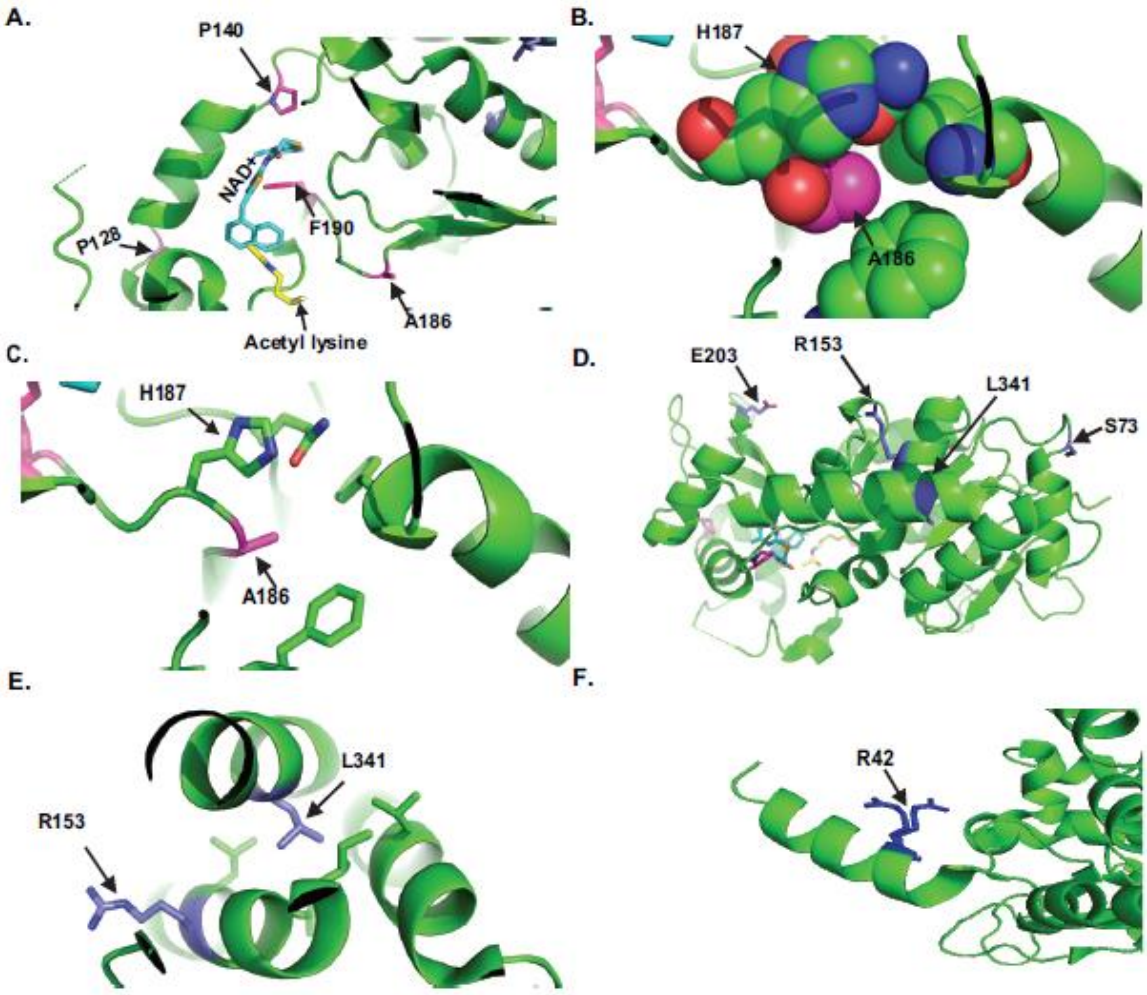
A.
P140
NAD+
F190
P128
A186
Acetyl lysine
B.
H187
A186
C.
H187
A186
D.
E203
R153
L341
S73
E.
L341
R153
F.
R42

Figure 2.3. Structural analysis of SIRT2 mutations yields insights into their functional significance

A, Of the nine mutations selected from cBioPortal, four are found in either the NAD^+-binding pocket or the catalytic domain. Mutations P128L, P140H, and F190V create the NAD^+-binding pocket. NAD^+ can be seen in blue, and the amino acids of interest are in red. Ala-186 lies next to the catalytic amino acid His-187. The protein structure was obtained from the Structural Bioinformatics Protein Data Bank, specifically structure 4RMH [111]. B, A close-up of Ala-186 in a non-space-filling model. C, A close-up of Ala-186 in a space-filling model. D, Of the nine mutations selected from cBioPortal, four are located in non-catalytic domains of the SIRT2 protein structure. These mutations are highlighted in purple. E, A close-up of two of the four mutations from D reveals they are mainly surface or hydrophobic amino acids. F, Hypothetical crystal model of amino acid Arg-42.

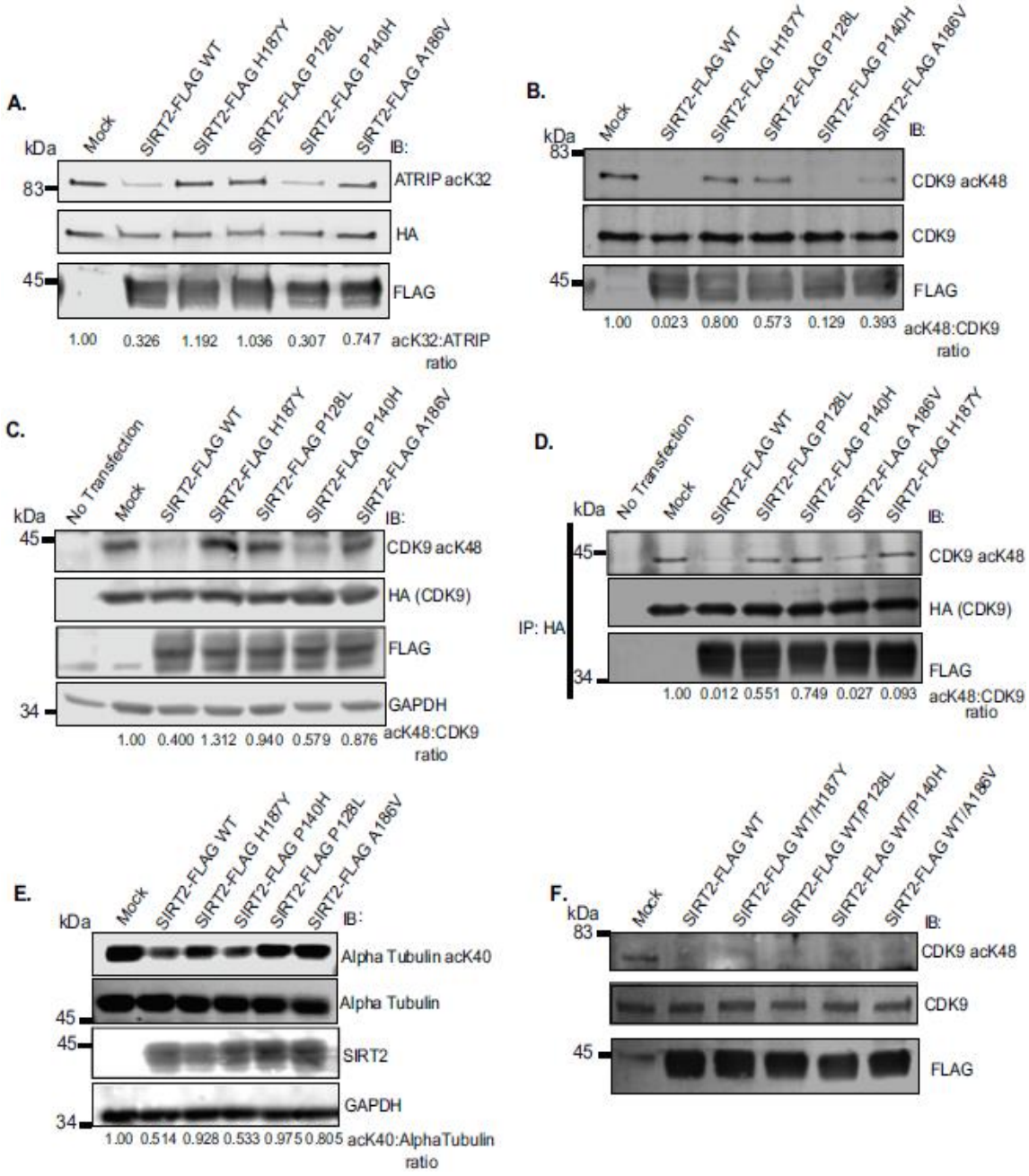
A.
Mock
SIRT2-FLAG WT
SIRT2-FLAG H187Y
SIRT2-FLAG P128L
SIRT2-FLAG P140H
SIRT2-FLAG A186V
kDa
IB:
83
ATRIP acK32
HA
45
FLAG
1.00 0.326 1.192 1.036 0.307 0.747 acK32:ATRIP ratio
B.
Mock
SIRT2-FLAG WT
SIRT2-FLAG H187Y
SIRT2-FLAG P128L
SIRT2-FLAG P140H
SIRT2-FLAG A186V
kDa
IB:
83
CDK9 acK48
CDK9
45
FLAG
1.00 0.023 0.800 0.573 0.129 0.393 acK48:CDK9 ratio
C.
No Transfection
Mock
SIRT2-FLAG WT
SIRT2-FLAG H187Y
SIRT2-FLAG P128L
SIRT2-FLAG P140H
SIRT2-FLAG A186V
kDa
IB:
45
CDK9 acK48
HA (CDK9)
FLAG
34
GAPDH
1.00 0.400 1.312 0.940 0.579 0.876 acK48:CDK9 ratio
D.
No Transfection
Mock
SIRT2-FLAG WT
SIRT2-FLAG P128L
SIRT2-FLAG P140H
SIRT2-FLAG A186V
SIRT2-FLAG H187Y
kDa
IB:
IP: HA
45
CDK9 acK48
HA (CDK9)
FLAG
34
1.00 0.012 0.551 0.749 0.027 0.093 acK48:CDK9 ratio
E.
Mock
SIRT2-FLAG WT
SIRT2-FLAG H187Y
SIRT2-FLAG P140H
SIRT2-FLAG P128L
SIRT2-FLAG A186V
kDa
IB:
Alpha Tubulin acK40
45
Alpha Tubulin
45
SIRT2
GAPDH
34
1.00 0.514 0.928 0.533 0.975 0.805 acK40:AlphaTubulin ratio
F.
Mock
SIRT2-FLAG WT
SIRT2-FLAG WT/H187Y
SIRT2-FLAG WT/P128L
SIRT2-FLAG WT/P140H
SIRT2-FLAG WT/A186V
kDa
IB:
83
CDK9 acK48
CDK9
45
FLAG

Figure 2.4. Cancer-associated mutations impair SIRT2 deacetylation of DDR substrates *in vitro* and in cells but not interaction with substrate

Shown are representative Western blots of several replicas.

A, acetylated ATRIP was isolated from 293T cells transfected with HA-ATRIP and histone acetyltransferases (HATs) pCAF, p300, and CBP and incubated in an *in vitro* deacetylation assay with SIRT2-FLAG WT or mutants isolated from 293T cells and in the presence of TSA with or without NAD^+ and nicotinamide. The reaction mixtures were separated by SDS-PAGE and immunoblotted (IB) with site-specific anti-acetyl ATRIP Lys-32, HA, and FLAG antibodies. B, acetylated CDK9 was isolated from 293T cells transfected with CDK9-GFP and HATs and incubated in an *in vitro* deacetylation assay with SIRT2-FLAG WT or mutants isolated from 293T cells and in the presence of TSA with or without NAD^+ and nicotinamide. The reaction mixtures were separated by SDS-PAGE and immunoblotted with site-specific anti-acetyl CDK9 Lys-48, HA, and FLAG antibodies. C, 293T cells were transfected with CDK9-HA and HATs or were left untransfected. After 24 h, cells were subsequently transfected with SIRT2-FLAG WT or mutants and incubated in the presence of TSA for 24 h. Deacetylation of CDK9-HA was assessed by Western blot analysis using site-specific anti-acetyl CDK9 Lys-48, HA, FLAG, and GAPDH antibodies. D, Immunoprecipitation of samples from Fig. 2C. 293T cells were transfected with CDK9-HA and HATs or were left untransfected. After 24 h, cells were subsequently transfected with SIRT2-FLAG WT or mutants and incubated in the presence of TSA for 24 h. Lysate were immunoprecipitated with an anti-HA antibody, separated by SDS-PAGE, and immunoblotted with site-specific anti-acetyl CDK9 Lys-48, HA, and FLAG antibodies. E, 293T cells were transfected with HATs.

After 24 h, cells were subsequently transfected with SIRT2-FLAG WT or mutants and incubated in the presence of TSA for 24 h. Deacetylation of endogenous α-tubulin was assessed by Western blot analysis using site-specific anti-acetyl-α-tubulin Lys-40, α-tubulin, SIRT2, and GAPDH antibodies. F, acetylated CDK9 was isolated from 293T cells transfected with CDK9-GFP and HATs and incubated in an *in vitro* deacetylation assay without SIRT2 (Mock), with SIRT2-FLAG WT only, or with equal amounts of both SIRT2-FLAG WT and one of four SIRT2-FLAG mutants isolated from 293T cells (SIRT2-FLAG H187Y, P128L, P140H, or A186V) in the presence of TSA with NAD^+. The reaction mixtures were separated by SDS-PAGE and immunoblotted with site-specific anti-acetyl CDK9 Lys-48, CDK9, and FLAG antibodies.

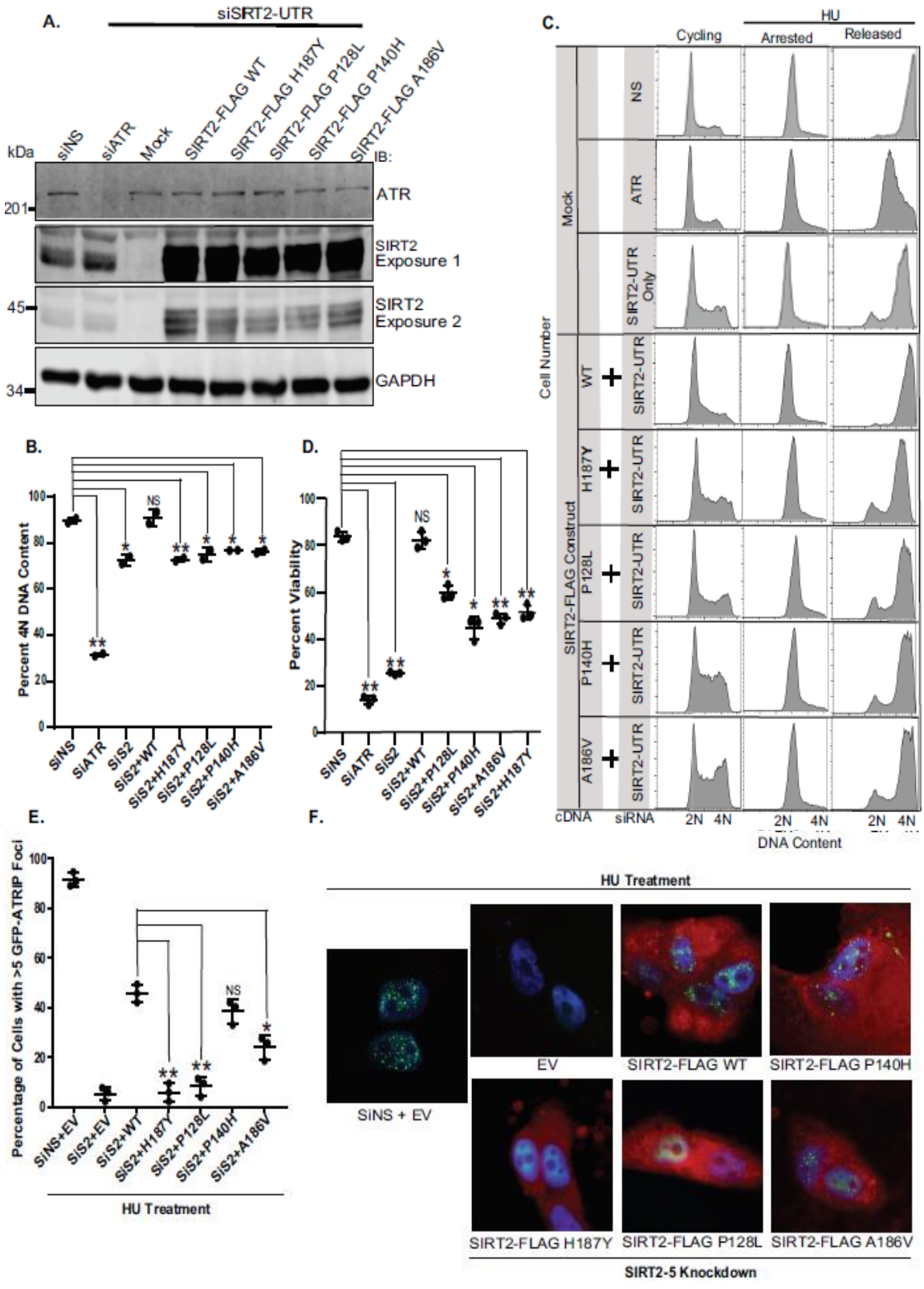
A.
siSIRT2-UTR
siNS
siATR
Mock
SIRT2-FLAG WT
SIRT2-FLAG H187Y
SIRT2-FLAG P128L
SIRT2-FLAG P140H
SIRT2-FLAG A186V
kDa
IB:
201
ATR
SIRT2 Exposure 1
45
SIRT2 Exposure 2
34
GAPDH
B.
Percent 4N DNA Content
NS
SiNS
SiATR
SiS2
SiS2+WT
SiS2+H187Y
SiS2+P128L
SiS2+P140H
SiS2+A186V
D.
Percent Viability
NS
SiNS
SiATR
SiS2
SiS2+WT
SiS2+P128L
SiS2+P140H
SiS2+A186V
SiS2+H187Y
C.
HU
Cycling
Arrested
Released
Cell Number
Mock
NS
ATR
SIRT2-UTR Only
SIRT2-FLAG Construct
WT + SIRT2-UTR
H187Y + SIRT2-UTR
P128L + SIRT2-UTR
P140H + SIRT2-UTR
A186V + SIRT2-UTR
cDNA
siRNA
2N 4N
2N 4N
2N 4N
DNA Content
E.
Percentage of Cells with >5 GFP-ATRIP Foci
NS
SiNS+EV
SiS2+EV
SiS2+WT
SiS2+H187Y
SiS2+P128L
SiS2+P140H
SiS2+A186V
HU Treatment
F.
HU Treatment
SiNS + EV
EV
SIRT2-FLAG WT
SIRT2-FLAG P140H
SIRT2-FLAG H187Y
SIRT2-FLAG P128L
SIRT2-FLAG A186V
SIRT2-5 Knockdown

Figure 2.5. Cancer-associated *SIRT2* mutations fail to rescue RSR defects of *SIRT2* deficiency A, Western blot analysis demonstrating efficiency of SIRT2 and ATR knockdown and expression of SIRT2-FLAG WT and mutants in HCT-116 cells. B, quantitation of cells with 4N DNA content following 10-h release from HU treatment in cells transfected with NS, ATR, or SIRT2-10 UTR siRNA with or without complementation with SIRT2-FLAG WT or mutants. The mean from two replicas is shown, and error bars represent S.D. NS indicates $p<0.05$; *, $p<0.05$; **, $p<0.01$. C, HCT116 cells were transfected with NS, ATR, or SIRT2-10 UTR siRNA, treated with 3 mM HU for 24 h (arrested), and released into nocodazole for 10 h (released). SIRT2–10 UTR knockdown was complemented with SIRT2-FLAG WT and mutants. DNA content was analyzed by flow cytometry. Representative cell cycle profiles are shown. D, HU sensitivity as measured by Alamar Blue cell viability staining of HCT116 cells transfected with NS, siATR, or SIRT2-10 UTR siRNA with or without complementation with SIRT2-FLAG WT or mutants and treated with 1.6mMHUfor 24 h followed by a 24-h release. The mean of HU-treated to untreated viability relative to NS siRNA in triplicate is shown, and error bars represent S.D. E, quantitation of cells with >5 GFP-ATRIP foci following 24-h 3mM HU treatment in a GFP-ATRIP stable U2OS cell line transfected with NS or SIRT2-5 siRNA with or without complementation with EV (pcDNA3.1) or SIRT2-FLAG WT or mutants (SIRT2-FLAG WT constructs contained wobble mutations to protect against knockdown). The mean from three replicas of 100 cells counted in each is shown, and error bars represent S.D. NS indicates $p<0.05$; *, $p<0.05$; **, $p<0.01$. F, representative images of conditions quantified and outlined in E with GFP-ATRIP in green, FLAG in red, and DAPI. IB, immunoblotting.

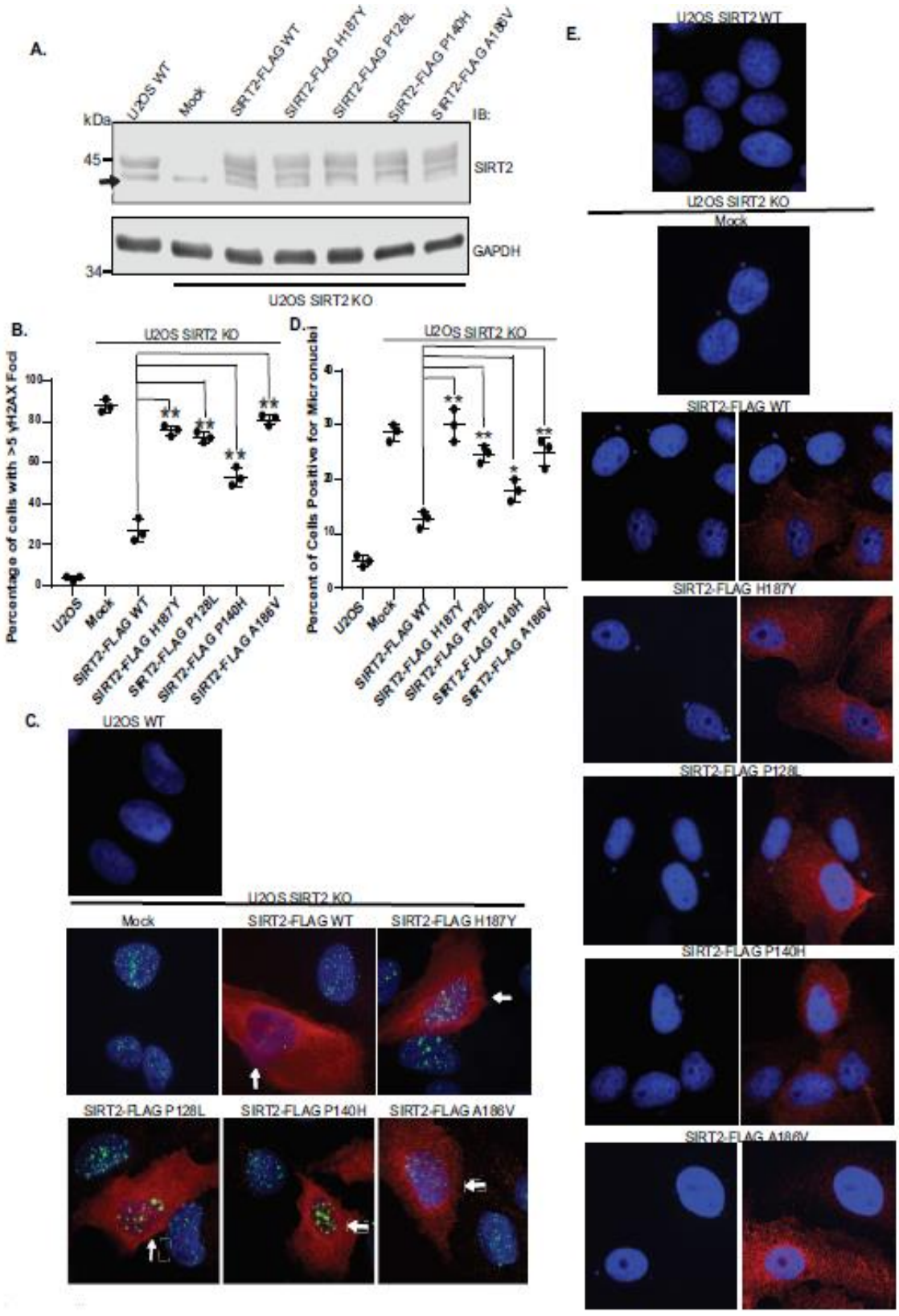
A.
U2OS WT
Mock
SIRT2-FLAG WT
SIRT2-FLAG H187Y
SIRT2-FLAG P128L
SIRT2-FLAG P140H
SIRT2-FLAG A186V
kDa
IB:
45
SIRT2
GAPDH
34
U2OS SIRT2 KO
B.
U2OS SIRT2 KO
Percentage of cells with >5 γH2AX Foci
U2OS
Mock
SIRT2-FLAG WT
SIRT2-FLAG H187Y
SIRT2-FLAG P128L
SIRT2-FLAG P140H
SIRT2-FLAG A186V
D.
U2OS SIRT2 KO
Percent of Cells Positive for Micronuclei
C.
U2OS WT
U2OS SIRT2 KO
Mock
SIRT2-FLAG WT
SIRT2-FLAG H187Y
SIRT2-FLAG P128L
SIRT2-FLAG P140H
SIRT2-FLAG A186V
E.
U2OS SIRT2 WT
U2OS SIRT2 KO
Mock
SIRT2-FLAG WT
SIRT2-FLAG H187Y
SIRT2-FLAG P128L
SIRT2-FLAG P140H
SIRT2-FLAG A186V

Figure 2.6. Cancer-associated *SIRT2* mutations fail to rescue genomic instability of *SIRT2* deficiency.

A, U2OS *SIRT2* KO cells generated by CRISPR/Cas9 were complemented with or without SIRT2-FLAG WT or mutants. Western blot analysis demonstrating efficiency of expression of SIRT2-FLAG WT and mutants in U2OS *SIRT2* KO cells or endogenous SIRT2 in U2OS WT cells is shown. The arrow indicates a nonspecific band beneath the SIRT2 protein band. B, U2OS *SIRT2* KO cells demonstrate increased spontaneous γH2AX foci and were complemented with or without SIRT2-FLAG WT or mutants. The degree of alleviation of spontaneous γH2AXfoci observed was quantified. Quantitation of the percentage of cells with >5 spontaneous γH2AXfoci is shown. The mean was calculated from three replicas of 100 cells for each condition, and error bars represent S.D. *, $p<0.05$; **, $p<0.01$. C, representative images of U2OS *SIRT2* KO cells complemented with or without SIRT2-FLAG WT or mutants and stained for γH2AX foci (green), FLAG (red), and DAPI. U2OS *SIRT2* KO cells with SIRT2 construct expression stain positive for FLAG (red), and examples of this are highlighted by white arrows, whereas cells in the same population that did not express SIRT2 construct do not exhibit red staining in the cytoplasm. D, U2OS *SIRT2* KO cells were transfected with or without SIRT2-FLAG WT or mutants and stained for FLAG in red and DAPI. Induced micronuclei were counted. Quantitation of micronuclei is shown. The mean was calculated from three replicas of 100 cells for each condition, and error bars represent S.D. *, $p<0.05$; **, $p<0.01$. E, representative images of micronuclei conditions from D. IB, immunoblotting.

2.6 Discussion

Using structural insight combined with bioinformatics and functional analyses, we found that naturally occurring cancer associated *SIRT2* mutations at evolutionarily conserved sites disrupt its deacetylation of DDR proteins by impairing its catalytic activity or protein level but not localization or binding with substrate, demonstrating that cancer-associated *SIRT2* mutations are functionally significant. We further found that SIRT2 mutant proteins fail to restore the replication stress sensitivity, impairment in recovery from replication stress, and spontaneous induction of DNA damage of *SIRT2* deficiency in cancer cells, providing evidence that cancer-associated *SIRT2* mutations impair genomic integrity of cancer cells. Thus, somatic *SIRT2* mutations in human tumors contribute to genomic instability by impairing its deacetylase activity or protein level in the DDR, providing a model for the loss of the tumor suppressor function of SIRT2 in human tumors.

Of the original nine *SIRT2* mutations selected, only four demonstrated functional significance by impacting either deacetylase activity or protein level. These four mutations are located within the deacetylase active site, NES, or NAD^+ cofactor-binding site. R42P resulted in decreased protein levels and likely affects either protein stability or expression. P128L, P140H, and A186V resulted in decreased SIRT2 deacetylase activity but had no significant effect on SIRT2 protein levels or localization.

P128L showed the greatest deficit in SIRT2 deacetylase activity against all substrates tested, including ATRIP Lys-32, CDK9 Lys-48, α-tubulin Lys-40, and p53 Lys-320. In

addition, P128L was unable to rescue the replication stress sensitivity, impairment in recovery from replication arrest, impairment in HU induced ATRIP focus accumulation, and spontaneous induction of γH2AX foci and micronuclei of *SIRT2* deficiency. Structural analyses indicate that this lack of activity is due to decreased binding of the SIRT2 cofactor NAD^+. The P128L proline is essential to the proper orientation of the α helix involved in forming the binding pocket for NAD^+ and for the formation of the stacking interaction of Pro-140 with NAD^+. Consequently, its mutation would result in improper orientation/ folding and therefore proper interaction with the essential cofactor for deacetylation reactions.

P140H appears to be partially substrate-specific as it was unable to deacetylate p53 Lys-320 *in vitro* to the same extent as SIRT2 WT but was able to deacetylate other known substrates CDK9 Lys-48, ATRIP Lys-32, and α-tubulin Lys-40 both *in vitro* and in cells. Consistently, P140H rescued the impairment in HU-induced ATRIP focus accumulation of *SIRT2* deficiency to a comparable level as SIRT2 WT. However, P140H was unable to rescue the genome maintenance defects of *SIRT2* deficiency, suggesting that its effect on the DDR activities of SIRT2 may be mediated through p53 or an untested substrate. Interestingly, even in the absence of exogenous damage, *SIRT2*-depleted cells complemented with SIRT2 P140H showed a significant increase in the percentage of cells in S and G_2/M phases even compared with *SIRT2* depletion alone, suggesting a gain of function in impairing cell cycle progression. Structural analyses indicate that this mutation impairs the ability of SIRT2 to bind NAD^+ as it affects the orientation of the same α helix as P128L and is involved in a stacking interaction between Phe-190 and

NAD^+ in the cofactor-binding pocket. It is likely that this mutation is not as impactful as P128L in disrupting the binding of NAD^+ to impair deacetylase activity for the majority of known SIRT2 substrates but may impart a gain of function in impairing cell cycle progression, which leads to increased genomic instability.

A186V also exhibited decreased deacetylase activity for p53 *in vitro* but only displayed decreased deacetylase activity on CDK9 Lys-48 and α-tubulin Lys-40 in cells but not on CDK9 Lys-48 or ATRIP Lys-32 *in vitro*. A186V was unable to rescue the deficiency in ATRIP focus formation in response to replication stress after SIRT2 knockdown to the same extent as SIRT2 WT and P140H likely due to its reduced deacetylase activity of RSR substrates in cells. Additionally, there was an increase in the percentage of cells in S and G_2/M phases as seen with the P140H mutation as well as impairment in SIRT2 DDR phenotypes. Structural analyses reveal that Ala-186 lies adjacent to H187Y, which is an essential catalytic amino acid for deacetylation reactions. Specifically, Ala-186 lies in a narrow pocket that is size-restricting. The addition of methyl groups found in the valine amino acid structure would interfere with the structure of the deacetylation pocket and orientation of His-187, leading to decreased deacetylation of substrate. It is possible that this mutation may be more impactful on certain substrates in cells due to the presence of an unknown regulatory partner, for example CDK9 complexes with several regulatory cyclins in cells.

The other five mutations, S73R, R153C, F190V, E203G, and L341M, did not significantly affect SIRT2 protein levels, localization, or deacetylase activity. S73R and

L341M lie outside of well-defined functional SIRT2 protein domains, and although it is possible that S73R may affect protein function as a site of post-translational modification by phosphorylation, it was predicted to be a benign mutation by PolyPhen and ConSurf based on conservation and structural analyses. Leu-341 is a hydrophobic amino acid likely involved in maintenance of a C-terminal α helical structure and, although highly conserved, was predicted to be a tolerated mutation by SIFT and Grantham prediction. Its higher score on the ConSurf scale is likely due to its functionality in an α helix structure that seems to lack an essential role in SIRT2 deacetylase activity. R153C, F190V, and E203G lie in the SIRT2 deacetylase domain, but only F190V lies in the active site (specifically in the NAD^+-binding pocket). Despite its seemingly essential placement in the stacking interaction with NAD^+ and Pro-140, the mutation of Phe-190 alone was not sufficient to induce a deacetylase-deficient phenotype. R153C and E203G lie on the surface of the protein structure as opposed to inside the active site and are likely involved in protein-protein interactions that are not critical for SIRT2's ability to bind and deacetylate substrate. Interestingly, we found no evidence that cancer-associated *SIRT2* mutants exert a dominant negative effect on the deacetylase activity of SIRT2 WT using an *in vitro* deacetylase assay. However, it is possible that this could differ in a heterozygous state in human cancers *in vivo*.

In summary, our findings support a model for the tumor suppressive function of SIRT2 in which somatic mutations in *SIRT2* contribute to genomic instability by impairing its deacetylase activity or protein level in the DDR and provide a mechanistic basis for understanding the biological and clinical significance of *SIRT2* mutations in genome

maintenance and tumor suppression. In addition, as *SIRT2* depletion in cancer cells results in hypersensitivity to replication stress caused by many types of cancer therapies [71, 73, 87], our findings provide insight into the rationale-driven design of targeted therapies against SIRT2 activity and potential resistance mechanisms in tumors that may be utilized for individualized cancer therapy.

2.7 Acknowledgements

We thank members of the Yu lab for helpful discussion. We kindly thank Eric Verdin for the SIRT2-FLAG plasmid. This work was supported by National Institutes of Health (NIH)/National Cancer Institute (NCI) R01CA178999 and R01CA178999S1, Basser Center for BRCA External Research Grant Program Innovation Award 32356, and Winship Cancer Institute (WCI) Brenda Nease Breast Cancer Research Fund Pilot Award 53237 to D.S.Y.

Chapter 3: SIRT2 Directs DNA-PKcs in the DNA Damage Response

[In Preparation for Publication]

3.1 Author's Contribution

PamelaSara Head and David Yu conceived and coordinated the study, designed the experiments, and wrote the manuscript. PamelaSara Head performed and analyzed the experiments shown in **Figures** 1, 2, 3, 4, 5. Hui Zhang assisted in the experimental design for **Figures** 2, 3, and 4. Anthony Davis assisted in conception and production of **Figures** 2, and 3.

3.2 Abstract

DDR pathways, including cell cycle checkpoints, DNA damage repair pathways, recovery pathways, and apoptotic pathways are critical for maintaining genome integrity and preventing disease. Deficiencies in the DDR result in increased susceptibility to cancer, a leading cause of morbidity and mortality worldwide. However, the mechanisms mediating the activities of the DDR and how their dysregulation leads to genomic instability and tumor permissive phenotypes are not fully understood. SIRT2 is a class III NAD^+ dependent histone deacetylase and a putative human tumor suppressor. SIRT2 is an established regulator of the replication stress response pathway and the G2/M cell cycle checkpoint pathway. Here we demonstrate that SIRT2 is also a regulator of DNA damage repair pathways in that *SIRT2* deletion by CRISPR-Cas9 resulted in increased sensitivity to ionizing radiation and camptothecin treatment and reduced NHEJ efficiency. Additionally, mass spectrometry analysis indicated an interaction between SIRT2 and the nonhomologous end joining kinase, DNA-PKcs. This interaction was confirmed through endogenous immunoprecipitation of DNA-PKcs and SIRT2 in HeLa cells. SIRT2 deacetylates DNA-PKcs in response to DNA damage. This deacetylase activity is important for proper DNA-PKcs DNA damage localization and interaction with Ku. SIRT2 deacetylase activity is also necessary for DNA-PKcs autophosphorylation at serine 2056 and phosphorylation of downstream NHEJ substrates Artemis and XRCC4 in response to IR. Overall, these data demonstrate that SIRT2 regulates DNA-PKcs in response to DNA damage and is therefore a potential novel regulator of nonhomologous end joining.

3.3 Introduction

We are exposed to a multitude of DNA damaging agents on a daily basis such as ionizing radiation (IR), chemical exposures, ultraviolet (UV) light, errors in replication, and byproducts of cellular metabolism leading to an accumulation of DNA lesions in our genome [1]. These lesions activate the DDR which is composed cell cycle checkpoint pathways, DNA repair pathways, recovery pathways and apoptotic pathways. These pathways are critical for maintaining genome integrity and preventing development of genomic instability and tumorigenesis [1-4, 32] The most detrimental of DNA lesions are double-strand breaks (DSBs) which are predominantly repaired via two pathways: homologous recombination repair (HRR) and non-homologous end-joining (NHEJ) [16-18].

HRR is an error-free repair pathway that employs a sister chromatid as a repair template and therefore only takes place during S and G2 phase [16-18]. Throughout the remainder of the cell cycle, NHEJ is used [16-18]. In NHEJ, Ku70 and Ku80 form ring shaped heterodimers that slide onto the ends of the broken DNA strands [17, 18]. Once bound to the DNA on both sides of the DSB, Ku dimers recruit the DNA-dependent protein kinase catalytic subunit (DNA-PKcs) to form a stable complex on the DNA ends [17, 18]. Under specific break conditions, Artemis is recruited to resect damaged DNA to create blunt ends for ligation [17, 18]. Three additional proteins, DNA ligase IV, XRCC4, and XLF, bind and catalyze ligation [17, 18]. During the repair process, DNA-PKcs phosphorylates itself as well as other repair factors in order to self-regulate its activities [17, 18].

DNA-PKcs, like ATM, ATR, and mTOR, is a phosphatidylinositol 3-kinase-related kinase (PIKK) family member [17, 18, 22, 23]. PIKK family members specifically recognize and phosphorylate SQ/TQ (serine or threonine followed by glutamine) motifs [17, 18, 22, 23]. DNA-PKcs is regulated in NHEJ by phosphorylation of its ABCDE and PQR clusters [17, 18, 24, 25]. Phosphorylation of the ABCDE cluster (sites between residues 2609 and 2647) promotes end resection and is regulated by ATM or ATR in response to damage [17, 18, 24, 25]. Autophosphorylation of the PQR cluster (sites between residues 2023 and 2056) promotes end ligation and the release of DNA-PKcs from DNA [17, 18, 24, 25]. DNA-PKcs also phosphorylates a number of other NHEJ proteins including Artemis, XRCC4, Ku, XLF, and DNA Ligase IV [17, 18, 25]. Overall, DNA-PKcs is an important regulator of NHEJ and as a result, it has served as a target for cancer therapy [112]. In fact, the majority of current small molecule drug therapies are directed at DNA damage kinases even though they comprise a small percentage of potential DDR enzyme targets [112]. An emerging therapeutic target is SIRT2, a class III NAD^+-dependent deacetylase involved in the regulation of such cellular functions as cell motility, cell cycling, metabolism, DDR pathways, and aging [44, 46, 47, 71, 89, 90]. *Sirt2* has also been established as a murine tumor suppressor [74, 78, 91]. Indeed, *SIRT2* expression is decreased, or the gene is mutated or deleted in a number of human cancers [71, 78, 80, 81, 83-85].

SIRT2 depletion leads to several genomic instability phenotypes such as hypersensitivity to replication stress, delayed S-phase progression, spontaneous accumulation of RPA damage foci and chromatin, and G2/M DNA damage dependent checkpoint deficits [71,

73, 74, 87]. These phenotypes are the result of dysregulation of DDR pathways that result from the increased ATRIP acetylation at lysine 32 [71] and CDK9 acetylation at lysine 48 [73]. Both of these events are necessary for proper replication stress response (RSR) pathway signaling [71]. These phenotypes are also the result of dysregulation of the G2/M transition and mitotic signaling. SIRT2 normally regulates the G2/M transition and progression through regulation of microtubule networks via deacetylation of α-tubulin at Lys-40 [67, 79], upregulation of APC/C via deacetylation and activation of co-activators CDH1 and CDC20 [92], and regulation of chromatin compaction via histone H4K16 and PR-Set7 deacetylation [74]. We have previously demonstrated the functional significance of naturally-occurring somatic *SIRT2* mutations in cancer [113] and how SIRT2 regulates the RSR [71, 73]. Here we demonstrate a novel role for SIRT2 in its regulation of NHEJ through deacetylation of DNA-PKcs.

3.4 Materials and Methods

Transfections

siRNAs were obtained from Thermo Scientific or Qiagen. Transfections were performed using Lipofectamine 2000 (Invitrogen) or RNAi Max (Invitrogen) following the manufacturer's instructions. Individual siRNAs sequences include:

1. siSIRT2-10 UTR: (TGGGCAGAAGACATTGCTTAT);

2. siSIRT2-5: (GGAGAAAGCTGGCCAGTCG);

4. Nontargeting siRNA: (ATGAACGTGAATTGCTCAATT)

Generation of CRISPR/Cas9 SIRT2 Knockout Cells

U2OS and HCT116 cells were transfected with a plasmid encoding Cas9-GFP construct and a single guide RNA (sgRNA), targeting an *SIRT2* exon 6 (5'-CGGGCTCAAGTTCCGCTTCGGG-3') (Sigma) [113]. Cells were maintained for 72 h post transfection, and then harvested for fluorescence activated cell sorting based on GFP expression [113]. Single cells were assayed in 96 well plates. Resulting cloned cell lines were tested for loss of SIRT2 protein by western blot analysis [113].

Clonogenic assays

For camptothecin sensitivity assays, wildtype or SIRT2 knockout HCT116 cells were transfected with SIRT2-FLAG or SIRT2-FLAG-H187Y expression vectors, or were non-transfected. After 48 h to allow for protein expression, cells were seeded into 6 well plates (400 cells per well). Some groups were treated with DNA-PKcs inhibitors NU7441 or NU7026 as indicated in the figures. Three biological replicates were analyzed for each

experimental group. After 24 h, cells were treated with 0, 50, 100, 200, 400, or 800 nM CPT. Cells were incubated for 10 days with media changed every 3 days. Cells were stained with crystal violet and colonies of ≥50 cells were counted. For IR sensitivity assays, the same experimental design was used. Cells were exposed to 0, 0.5, 1, 2, or 4 Gy of 320 kVp X-rays. A portion of the cells from the 0 Gy groups were reserved for analysis of SIRT2 expression levels by western blotting. Remaining cells were used for clonogenic survival assays.

EJ5 assay

EJ5 U2OS reporter cells [114] were transfected with SIRT2-FLAG-WT, SIRT2-FLAG-H187Y, Empty Vector, or were left untransfected. After 24 h, cells were transfected with non-specific siRNA or SIRT2-10 UTR siRNA. After 48 h, cells were transfected with an I-SceI expression vector. At 72 h post I-SceI transfection, a portion of cells from each group were used for analysis of SIRT2 expression levels by western blotting. The reminder of cells were fixed in 1% PFA/PBS and analyzed for GFP expression via flow cytometry. Each group was performed in 3 biological replicates.

Immunoprecipitation

Harvested cells were lysed for 40 minutes on ice in IP lysis buffer (0.75% CHAPS, 10% (vol/vol) glycerol, 150 mM NaCl, 50mM Tris pH 7.5) freshly supplemented with protease inhibitors. Supernatants were diluted to adjust the CHAPS concentration to 0.375%. Whole cell lysates (3 to 5 mg total protein) were incubated with anti-DNA-PKcs (Thermo Fisher, PIMA513244), anti-SIRT2 (Abcam, ab67299), or anti-GFP antibody

(Abcam; Ab6556). Protein G beads, A agarose beads (Invitrogen), or FLAG conjugated beads (Sigma A2095) were used to immunoprecipitate antibody bound protein. Complexes were washed 4 times with IP washing buffer (0.375% CHAPS, 10% glycerol, 150 mM NaCl, 50 mM Tris pH 7.5) supplemented with protease inhibitors.

Deacetylation Experiments

For analysis of DNA-PKcs deacetylation, HeLa cells were treated with 0.5 μM trichostatin A (TSA) and 20 mM nicotinamide for 12 h. TSA inhibits class I and II HDACs but not class III HDACs [115] while nicotinamide inhibits class III HDACs [116]. Cells were lysed with IP buffer (20 mM Hepes pH 7.4, 180 mM KCl, 0.2 mM EGTA, 1.5 mM MgCl2, 20% glycerol, 1.0% Nonidet P-40) supplemented with 1 μM TSA and fresh protease inhibitors. Acetyl-DNA-PKcs was immunoprecipitated using anti-DNA-PKcs (Thermo Fisher, PIMA513244) and protein G agarose beads (Invitrogen). Samples of immunoprecipitated DNA-PKcs bound to G agarose beads were washed 4 times with IP buffer containing 1μM TSA followed by an additional 2 washes with deacetylation buffer (50 mM Tris pH 7.5, 150mM NaCl, and 1mM MgCl2) to remove nicotinamide. SIRT2-FLAG WT and SIRT2–FLAG H187Y expression vectors were transfected into 293T cells. After 48h to allow for protein expression, SIRT2-FLAG WT and SIRT2-FLAG H187Y proteins were immunoprecipitated using anti-FLAG M2 agarose beads (Sigma) and washed with IP buffer and TBS (50 mM Tris pH 7.5 and 150mM NaCl). SIRT2-FLAG WT and SIRT2-FLAG H187Y proteins were eluted from beads with 0.15mg/mL 3x FLAG Peptide (Sigma) for 30 minutes at 4◦C. SIRT2 protein concentrations were determined by SDS-PAGE with Coomassie stain. Purified acetyl-

DNA-PKcs was incubated with 1 μg of SIRT2-FLAG WT with NAD^+, SIRT2-FLAG WT with nicotinamide and NAD^+, SIRT2-FLAG H187Y and NAD^+, or with no SIRT2-FLAG in deacetylation reaction buffer (1μM TSA, 50 mM Tris·HCl, pH 7.5, 150 mM NaCl, 1 mM MgCl2, and 1 mM NAD^+) at 30 ◦C for 3 h. The reactions were stopped by the addition of 5x SDS loading buffer and were incubated for 5 minutes at 100 ◦C. Samples were analyzed for acetylation by Western blot using an anti-acetyl lysine antibody (Immunechem, ICP0380). For cellular deacetylation analysis, HeLa cells were transiently transfected with SIRT2-FLAG or SIRT2-FLAG-H187Y expression vectors, or were non-transfected. Cells were cultured with 0.5 μM TSA and with or without 20 mM nicotinamide for 12 h prior to being lysed with IP buffer containing 1 μM TSA. Cells were also treated with or without irradiation. Protein lysates were immunoprecipitated using anti-DNA-PKcs (Thermo Fisher, PIMA513244) and protein G agarose beads. The immunocaptured protein was analyzed for deacetylation by immunoblotting with anti-acetyl lysine antibody (Immunechem, ICP0380), anti-DNA-PKcs (Thermo Fisher, PIMA513244), and FLAG (Sigma F4042).

Immunoblot

Harvested cells were lysed for 30 minutes on ice in Nonidet P-40 buffer (200 mM NaCl, 1% Nonidet P-40,50 mM Tris·HCl pH 8.0) or IP lysis buffer (0.75% CHAPS, 10% (vol/vol) glycerol, 150 mM NaCl, 50mM Tris pH 7.5) freshly supplemented with protease inhibitors. Protein samples were resolved by SDS-PAGE and probed with indicated antibodies: anti-SIRT2 (Abcam, ab67299), GAPDH (Santa Cruz sc-25778 or sc-47724), FLAG (Sigma F4042), GFP (Abcam; Ab6556), anti-DNA-PKcs (Thermo

Fisher, PIMA513244), Artemis (Abcam, ab3834), anti-Artemis phospho Ser516 (Genetex, GTX32292), XRCC4 (Thermo Fisher Scientific, MA5-24383) and XRCC4 phospho Ser260 (Thermo Fisher Scientific, PA5-64731). Detection was performed with the Odyssey system.

Laser Microirradiation Assay

For SIRT2 knockdown experiments, U2OS cells stably transfected with DNA-PKcs-GFP were transected transiently with non-specific siRNA or SIRT2 siRNA. After 48 h, cells were plated into 35-mm glass bottom dishes (MatTek Corporation). Laser microirradiation was performed on a Zeiss Observer Z1 microscope equipped with a Micropoint® Laser Illumination and Ablation System (Photonic Instruments). Quantitation of DNA-PKcs localization (signal of DNA-PKcs-GFP at bands of microirradiation) was performed using Image Studio lite software. For each condition, 15 biological replicates were performed. For SIRT2 inhibition experiments, Chinese hamster ovarian DNA-PKcs deficient cells were also used. Cells were plated into 35-mm glass bottom dishes (MatTek Corporation) and after 16 h to allow or cell adhesion, treated with DMSO or SIRT2 specific inhibitor (SirReal2) at 50 uM for 6 h. Laser microirradiation was performed on a Zeiss Observer Z1 microscope equipped with a Micropoint® Laser Illumination and Ablation System (Photonic Instruments). Following 2 min irradiation, samples were fixed in fixed in 4% PFA and stained for ɣH2AX and DAPI. 15 biological replicates were performed for each condition (DMSO or SirReal2).

Immunofluorescence

Wildtype or SIRT2 knockout U2OS cells were transfected with SIRT2-FLAG or SIRT2-FLAG-H187Y expression vectors, or were non-transfected. After 72 h to allow for protein expression, cells were exposed to 0 or 10Gy IR followed by 30 min, 60 min, or 90 min recovery time. Cells were fixed on coverslips with 4% PFA for 10 min, and permeabilized in 0.5% triton X-100 for 10 min. For non-rescue experiments, cells were blocked in 5% BSA and immunostained with anti-γH2AX (Millipore 05-636) and DNA-PKcs phosphoserine 2056 (Abcam, ab18192) followed by Alexa Fluor 555/488 secondary antibodies and DAPI. For rescue experiments, cells were blocked in 5% BSA and immunostained stained with anti-FLAG (Cell Signaling: 2368P) and DNA-PKcs phosphoserine 2056 (Abcam, ab18192) followed by Alexa Fluor 555/488 secondary antibodies and DAPI stain (Southern Biotech). The percentage of cells positive for DNA-PKcs phosphoserine 2056 foci (5 or more foci per nucleus) was counted from 3 biological replicates (100 cells per replica) for each condition.

3.5 Results

SIRT2 is involved in DNA double strand break repair

To determine if SIRT2 deacetylase activity plays a role in DSB repair, HCT116 wildtype or *SIRT2* knockout (KO) cells were transfected with or without SIRT2-FLAG WT or catalytically dead mutant SIRT2-FLAG H187Y, and then seeded for colony formation. Once adhered, cells were treated with or without DNA-PKcs inhibitors NU7026 or NU7441 followed by treatment with 50-800 nM CPT or 0.5-4 Gy IR. Surviving colonies were counted 10 days later. *SIRT2* KO and DNA-PKcs inhibition resulted in increased sensitivity to CPT and IR treatment. However, *SIRT2* KO in combination with DNA-PKcs inhibition did not result in additional sensitivity which indicated SIRT2 and DNA-PKcs act in the same pathway. SIRT2-FLAG WT overexpression but not overexpression of SIRT2-FLAG H187Y in KO cells rescued sensitivity to both CPT and IR treatments. These results indicated that SIRT2 deacetylase activity was important for DSB repair (Figure 3.1A, B, and C).

To determine if SIRT2 functions directly in DSB repair, we examined *SIRT2* depletion in EJ5 U2OS reporter cells. In EJ5 U2OS reporter cells, genomically integrated GFP is separated from its promoter by a puromycin gene. The puromycin gene is flanked by two I-SceI sites. Therefore, expression of the endonuclease I-SceI generates a DSB that can only be repaired by NHEJ [114]. Successful repair of the induced DSB results in genomic loss of the puromycin gene and GFP expression (Figure 3.1D). If NHEJ repair efficiency is reduced due to the loss of an essential regulatory protein, GFP expression remains low following I-SceI expression. *SIRT2* depletion resulted in significantly decreased GFP

expression compared to non-specific siRNA controls. Additionally, overexpression of knockdown resistant SIRT2-FLAG WT but not SIRT2-FLAG H187Y restored GFP expression to control levels. These results indicated that SIRT2 deacetylase activity is necessary for proper NHEJ repair (Figure 3.1E and F).

SIRT2 and DNA-PKcs Interact

To find potential SIRT2 regulatory targets in NHEJ repair, SIRT2-FLAG was immunopurified from HCT116 cells exposed to 0 and 10 Gy IR and subjected to mass spectrometry analysis. The analysis indicated that SIRT2 interacts either directly or indirectly with NHEJ repair kinase DNA-PKcs (data not shown). In order to confirm the interaction, endogenous immunoprecipitations were performed. Endogenous DNA-PKcs or IgG was immunoprecipitated from HeLa whole cell lysate and run on an SDS-PAGE gel. The resulting western blot was immunostained for SIRT2, DNA-PKcs, and GAPDH. Endogenous SIRT2 co-immunoprecipitated with endogenous DNA-PKcs but not IgG (Figure 3.2A). The reciprocal immunoprecipitation reaction was then preformed on SIRT2 or IgG after cells were exposed to 0 or 10Gy IR and in the absence or presence of ethidium bromide (EtBr). Ethidium bromide intercalates with DNA and disrupts protein-DNA binding interactions and can disrupt protein-protein interactions that are dependent on the presence of DNA [117]. Endogenous DNA-PKcs co-immunoprecipitated with SIRT2 with and without damage induction by IR but not IgG. DNA-PKcs also co-immunoprecipitated with SIRT2 in both the absence and presence of EtBr (Figure 3.2B). These results indicated that SIRT2 and DNA-PKcs interact either directly or indirectly and that this interaction is not dependent on DNA damage induction or DNA binding.

SIRT2 Deacetylates DNA-PKcs in Response to DNA Damage

To determine if SIRT2 directly deacetylates DNA-PKcs, we performed an *in vitro* deacetylation assay. Purified pre-acetylated DNA-PKcs was incubated with SIRT2-FLAG WT with NAD^+, SIRT2-FLAG WT with nicotinamide and NAD^+, SIRT2-FLAG H187Y and NAD^+, or with no SIRT2-FLAG in deacetylation reaction buffer. These reactions were run on an SDS-PAGE gel. Incubation with SIRT2-FLAG WT led to loss of acetylation on DNA-PKcs. Incubations with SIRT2-FLAG WT and nicotinamide, SIRT2-FLAG H187Y, or without SIRT2 did not result in loss of DNA-PKcs acetylation. Overall, these results indicated that SIRT2 can deacetylate DNA-PKcs directly *in vitro* (Figure 3.3A).

To determine whether SIRT2 deacetylates DNA-PKcs in cells, HeLa cells were transiently transfected with SIRT2-FLAG or SIRT2-FLAG-H187Y expression vectors, or were non-transfected. Two experimental groups were transfected with SIRT2-FLAG but only one of them was treated with nicotinamide. Non-transfected cells were exposed to 0 or 10 Gy IR. Endogenous DNA-PKcs was purified from each experimental group and run on a SDS-Page gel followed by DNA-PKcs acetylation analysis on the resulting western blot. The SIRT2-FLAG overexpression and the non-transfected, 10 Gy groups exhibited decreased DNA-PKcs acetylation compared to the non-transected, 0 Gy control (Figure 3.3B). However, SIRT2-FLAG overexpression with nicotinamide treatment and SIRT2-FLAG H187Y overexpression groups did not result in decreased DNA-PKcs acetylation compared to the non-transected, 0 Gy control. These results indicated that SIRT2

deacetylates DNA-PKcs in cells and DNA-PKcs is deacetylated in response to DNA damage (Figure 3.3B). Additionally, the amount of SIRT2-FLAG that co-immunoprecipitated with endogenous DNA-PKcs increased in the SIRT2-FLAG overexpression with nicotinamide treatment group compared to the SIRT2-FLAG overexpression group even though the level of SIRT2-FLAG overexpression was the same in both groups in the input western blot (Figure 3.3B). Inhibition of SIRT2 NAD^+ binding by nicotinamide treatment potentially increases the amount of SIRT2 binding to DNA-PKcs, but the exact mechanism for this result is unclear.

To further demonstrate the deacetylation of DNA-PKcs by SIRT2 is damage dependent, we examined DNA-PKcs acetylation after transfection with SIRT2 siRNA or non-specific siRNA and exposure to 0 or 10 Gy IR. DNA-PKcs acetylation decreased in the non-specific siRNA, 10 Gy group compared to the non-specific siRNA, 0 Gy group, but acetylation did not decrease in the SIRT2 siRNA, 10 Gy group. These results further indicated that SIRT2 deacetylates DNA-PKcs in response to DNA damage induced by IR (Figure 3.3C). Overall, SIRT2 is capable of binding and deacetylating DNA-PKcs in and deacetylation is stimulated by DNA damage induction by IR.

SIRT2 Depletion Decreases DNA-PKcs Localization to Microirradiation and Decreased Interaction with Ku

To establish if the interaction between SIRT2 and DNA-PKcs is necessary for DNA-PKcs localization to sites of DNA damage, we performed microirradiation experiments.

U2OS cells stably transfected with DNA-PKcs-GFP were transected transiently with non-specific siRNA or SIRT2 siRNA and exposed to microirradiation. SIRT2 siRNA transfection resulted in decreased DNA-PKcs localization to sites of microirradiation induced DNA damage compared to non-specific siRNA transfection controls (Figure 3.4A-B and 3.4E). To establish if SIRT2 deacetylase activity is necessary for DNA-PKcs localization to sites of DNA damage, we used Chinese hamster ovarian (CHO) DNA-PKcs depleted (V3) cells stably transfected with human DNA-PKcs-GFP in microirradiation experiments. Cells were treated with DMSO or SIRT2 specific inhibitor SirReal2 [111]. SirReal2 inhibitor treatment lead to decreased DNA-PKcs localization to sites of microirradiation induced DNA damage compared to the DMSO treated controls (Figure 3.4C and 3.4F). A sample of cells from both treatment groups were fixed and stained for γH2AX and DAPI. These fixed cells demonstrated that localization of DNA-PKcs localization but not γH2AX deposition is impaired by SIRT2 inhibition (Figure 3.4D).

Previously, it has been established that DNA-PKcs forms a complex with Ku in a DNA-dependent manner at sites of DNA damage [118]. Therefore, to further demonstrate a localization impairment of DNA-PKcs to sites of DNA damage, we transfected wildtype and *SIRT2* KO HCT116 cells with Ku70-GFP or with no transfection and treated cells with 0 or 10 Gy IR. We decided to switch to HCT116 cells over U2OS cells because HCT116 cells have higher transfection efficiency. The amount of DNA-PKcs that co-immunoprecipitated with Ku70-GFP increased following treatment with 10 Gy IR compared to 0 Gy controls in wildtype but not *SIRT2* KO HCT116 cells. These results

indicated that *SIRT2* deficiency leads to decreased localization of DNA-PKcs to sites of DNA damage where it interacts with Ku in a DNA dependent manner (Figure 3.4G). Co-immunoprecipitation of DNA-PKcs with Ku70-GFP in *SIRT2* KO cells in response to IR is rescued by the overexpression of SIRT2-FLAG but not SIRT2-FLAG H187Y. These results indicated that SIRT2 deacetylase activity is important for DNA-PKcs localization and/or interaction with Ku in response to DNA damage (Figure 3.4H).

Deacetylation by SIRT2 Regulates DNA-PKcs Kinase Activity

To determine whether SIRT2 is necessary for DNA-PKcs kinase activity in response to DNA damage, we examined DNA-PKcs autophosphorylation at serine 2056 and DNA-PKcs phosphorylation of NHEJ repair proteins. Wildtype and *SIRT2* KO U2OS cells were treated with 0 and 10 Gy IR and fixed onto coverslips to examine DNA-PKcs autophosphorylation foci. U2OS cells were used because they stain more cleanly in immunofluorescence experiments than HCT116 cells. Cells were fixed at 30, 60, and 90 min post IR and stained with antibodies against γH2AX, DNA-PKcs phosphoserine 2056 (pS2056), and DAPI. The number of cells positive for DNA-PKcs pS2056 foci increased at every time point in wildtype U2OS cells treated with 10 Gy IR compared to wildtype U2OS cells treated with 0 Gy IR. *SIRT2* KO U2OS cells exhibited a significant decrease in the number of cells positive for pS2056 foci following 10 Gy IR treatment at every time point compared to wildtype U2OS 10 Gy IR groups. These results indicated that SIRT2 is needed for activation of DNA-PKcs kinase activity in response to DNA damage induced by IR (Figure 3.5A and 3.5C).

DNA-PKcs autophosphorylation of serine 2056 was rescued in U2OS *SIRT2* KO cells after over-expression of SIRT2-FLAG but not SIRT2-FLAG H187Y (Figures 3.5B and 3.5D-E). In line with these findings, DNA-PKcs autophosphorylation at serine 2056 was also decreased in *SIRT2* KO HCT116 cells exposed to 10 Gy IR compared to wildtype HCT116 cells exposed to 10 Gy IR as seen by western blot analysis (Figure 3.5F). In fact, overexpression of SIRT2-FLAG not only rescued kinase activity in *SIRT2* KO HCT116 cells but also resulted in increased autophosphorylation of DNA-PKcs in the absence of damage induction by IR (Figure 3.5F). SIRT2-FLAG H187Y, however, was unable to rescue kinase activity (Figure 3.5F). Overall, these results demonstrated that SIRT2 deacetylase activity is necessary for DNA-PKcs autophosphorylation at serine 2056 in response to damage induced by IR.

In addition, phosphorylation of downstream DNA-PKcs kinase protein targets Artemis (phosphoserine 516) and XRCC4 (phosphoserine 260) was lost following damage induction by IR in *SIRT2* KO HCT116 cells compared to wildtype HCT116 cells. As seen with DNA-PKcs autophosphorylation at serine 2056, DNA-PKcs phosphorylation of Artemis and XRCC4 is rescued in *SIRT2* KO HCT116 cells with overexpression of SIRT2-FLAG but not SIRT2-FLAG-H187Y. (Figure 3.5G). These results indicated that SIRT2 deacetylation of DNA-PKcs regulates not only autophosphorylation but kinase activity in response to DNA damage induced by IR. Therefore, *SIRT2* loss can lead to dysregulation of DNA-PKcs activity and ultimately dysregulation of NHEJ.

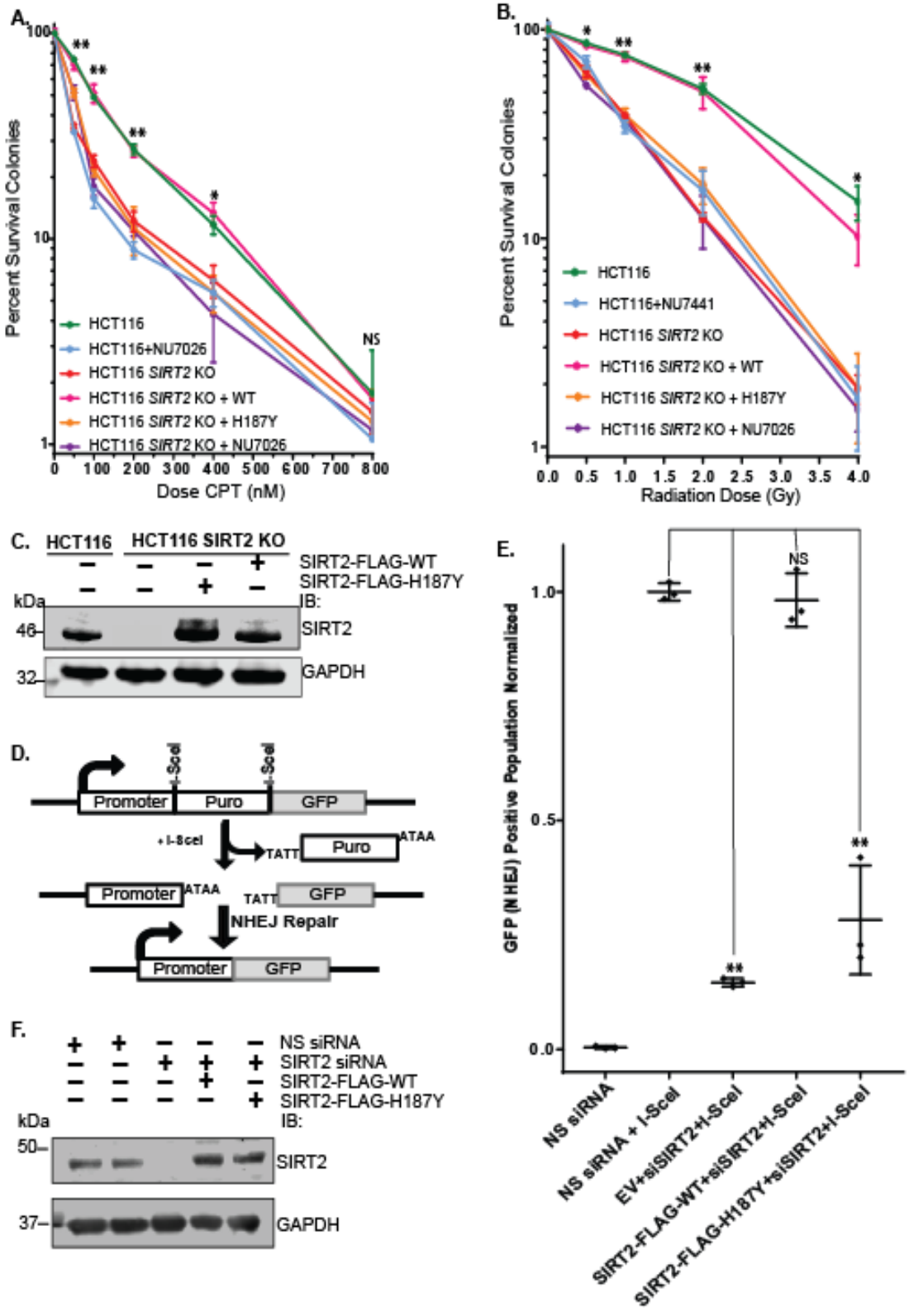
A.
Percent Survival Colonies
Dose CPT (nM)
HCT116
HCT116+NU7026
HCT116 SIRT2 KO
HCT116 SIRT2 KO + WT
HCT116 SIRT2 KO + H187Y
HCT116 SIRT2 KO + NU7026
NS
B.
Percent Survival Colonies
Radiation Dose (Gy)
HCT116
HCT116+NU7441
HCT116 SIRT2 KO
HCT116 SIRT2 KO + WT
HCT116 SIRT2 KO + H187Y
HCT116 SIRT2 KO + NU7026
C.
HCT116
HCT116 SIRT2 KO
SIRT2-FLAG-WT
SIRT2-FLAG-H187Y
kDa
IB:
46
SIRT2
32
GAPDH
D.
Promoter
Puro
GFP
I-SceI
I-SceI
+ I-SceI
TATT
ATAA
NHEJ Repair
E.
GFP (NHEJ) Positive Population Normalized
NS
NS siRNA
NS siRNA + I-SceI
EV+siSIRT2+I-SceI
SIRT2-FLAG-WT+siSIRT2+I-SceI
SIRT2-FLAG-H187Y+siSIRT2+I-SceI
F.
NS siRNA
SIRT2 siRNA
SIRT2-FLAG-WT
SIRT2-FLAG-H187Y
kDa
IB:
50
SIRT2
37
GAPDH

Figure 3.1. SIRT2 is involved in DNA double strand break repair.

A, Wildtype and *SIRT2* KO HCT116 cells were transfected with SIRT2-FLAG-WT, SIRT2-FLAG-H187Y, or with no transfection and treated with NU7026 or with no inhibitor. Cells were then seeded for colony formation. All were treated with indicated doses of CPT and assayed for surviving colonies 10 days later. Total colony number for each condition was normalized to non-damaged controls. Experiments were performed in biological replicates of 3. Error bars represent standard deviation: NS indicates $P \geq 0.05$, *$P < 0.05$, **$P < 0.01$. B, Wildtype and *SIRT2* KO HCT116 cells were transfected with SIRT2-FLAG WT, SIRT2-FLAG H187Y, or with no transfection and treated with NU7441 or with no inhibitor. Cells were then seeded for colony formation. All were treated with indicated doses of IR and assayed for surviving colonies 10 days later. Total colony number for each condition was normalized to non-damaged controls. Experiments were performed in biological replicates of 3. Error bars represent standard deviation: NS indicates $P \geq 0.05$, *$P < 0.05$, **$P < 0.01$. C, Western blot analysis of cells used in clonogenic assays part A and B. D, Diagram of EJ5 assay. E, EJ5 U2OS reporter cells were transfected with SIRT2-FLAG WT, SIRT2-FLAG H187Y, or empty vector (EV). After 24 h, cells were transfected with NS siRNA or SIRT2-10 UTR siRNA (siSIRT2). After 48 h, cells were also transfected with or without I-SceI and later analyzed for GFP expression using flow cytometry. The percentage of GFP positive cells in each sample was normalized to the percentage of GFP positive cells in NS siRNA+ISEC-I control samples. Experiments were performed in biological replicates of 3 and the means were plotted. Error bars represent standard deviation: NS indicates $P \geq 0.05$, *$P < 0.05$, **$P < 0.01$. F, Representative western blot of E.

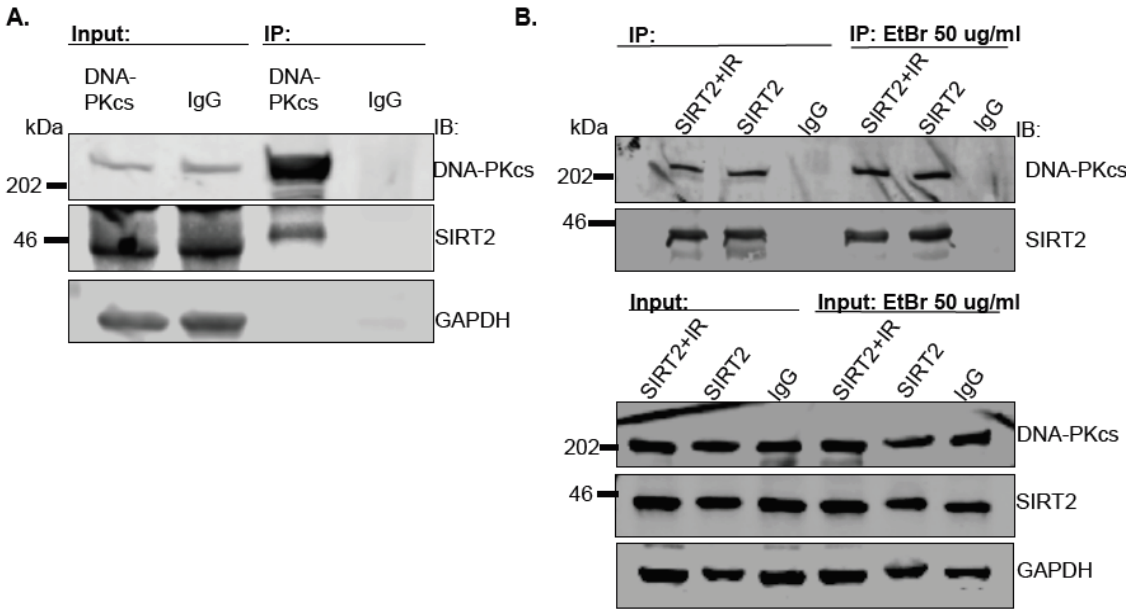

Figure 3.2. SIRT2 and DNA-PKcs Interact

A, Immunoprecipitation of endogenous DNA-PKcs or IgG was carried out on HeLa whole cell lysates, run on SDS-PAGE and immunoblotted (IB) for DNA-PKcs and SIRT2. The adjoining input is seen directly adjacent to the IP. B, Immunoprecipitation of endogenous SIRT2 or IgG was carried out on HeLa whole cell lysates with or without ethidium bromide (EtBr 50 ug/ml) or IR treatment (0 or 10 Gy IR), run on SDS-PAGE and immunoblotted (IB) for DNA-PKcs and SIRT2. The adjoining input is seen directly below the IP.

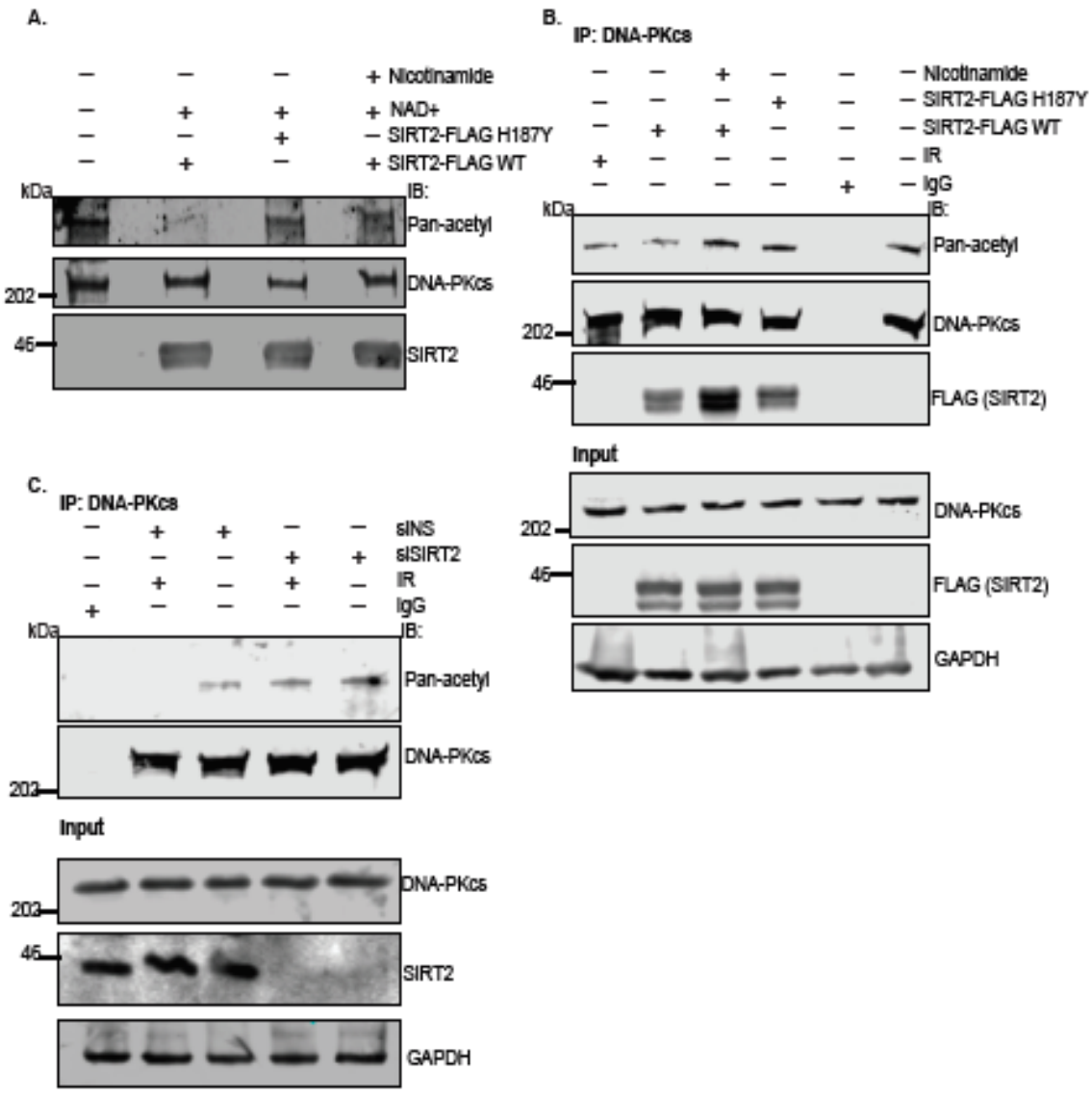
A.
– – – + Nicotinamide
– + + + NAD+
– – + – SIRT2-FLAG H187Y
– + – + SIRT2-FLAG WT
kDa
IB:
Pan-acetyl
DNA-PKcs
202
46
SIRT2
B.
IP: DNA-PKcs
– – + – – – Nicotinamide
– – – + – – SIRT2-FLAG H187Y
– + + – – – SIRT2-FLAG WT
+ – – – – – IR
– – – – + – IgG
kDa
IB:
Pan-acetyl
202
DNA-PKcs
46
FLAG (SIRT2)
Input
202
DNA-PKcs
46
FLAG (SIRT2)
GAPDH
C.
IP: DNA-PKcs
– + + – – siNS
– – – + + siSIRT2
– + – + – IR
+ – – – – IgG
kDa
IB:
Pan-acetyl
203
DNA-PKcs
Input
203
DNA-PKcs
46
SIRT2
GAPDH

Figure 3.3. SIRT2 Deacetylates DNA-PKcs in Response to DNA Damage

A, *In vitro* deacetylation assay of DNA-PKcs by SIRT2. Pre-acetylated endogenous DNA-PKcs was immunopurified from HeLa cells treated overnight with TSA and nicotinamide. SIRT2-FLAG WT and SIRT2-FLAG H187Y proteins were purified from 293T cells and eluted from beads. Acetylated DNA-PKcs was incubated in an *in vitro* deacetylation reaction without SIRT2, with SIRT2-FLAG WT, with SIRT2-FLAG H187Y, or with SIRT2-FLAG WT and nicotinamide. All reactions with SIRT2 received NAD^+. B, Cellular deacetylation assay. HeLa cells were transfected with SIRT2-FLAG WT, SIRT2-FLAG H187Y, or were left untransfected. After 48 h to allow for overexpression, cells received overnight TSA treatment with or without nicotinamide as indicated. Cells were also treated with 0 or 10 Gy IR at 72 h post transfection and allowed 4 h recovery as indicated. Endogenous DNA-PKcs or IgG was immunoprecipitated from whole cell lysate and run on SDS-PAGE gel. The resulting western blots for immunoprecipitation and input were immunoblotted with DNA-PKcs, pan-acetyl, FLAG, and GAPDH antibodies. C, DNA-PKcs acetylation before and after damage and before and after SIRT2 knockdown was assessed through immunoprecipitation of DNA-PKcs from HeLa cells. HeLa cells were transfected with or without NS siRNA or SIRT2 siRNA (SiS2). After 72 h, cells were treated with 0 or 10 Gy IR followed by 4 h recovery. The resulting lysates were immunoprecipitated for endogenous DNA-PKcs or IgG and immunoblotted for pan-acetyl and DNA-PKcs. Input was stained for DNA-PKcs, SIRT2 and GAPDH.

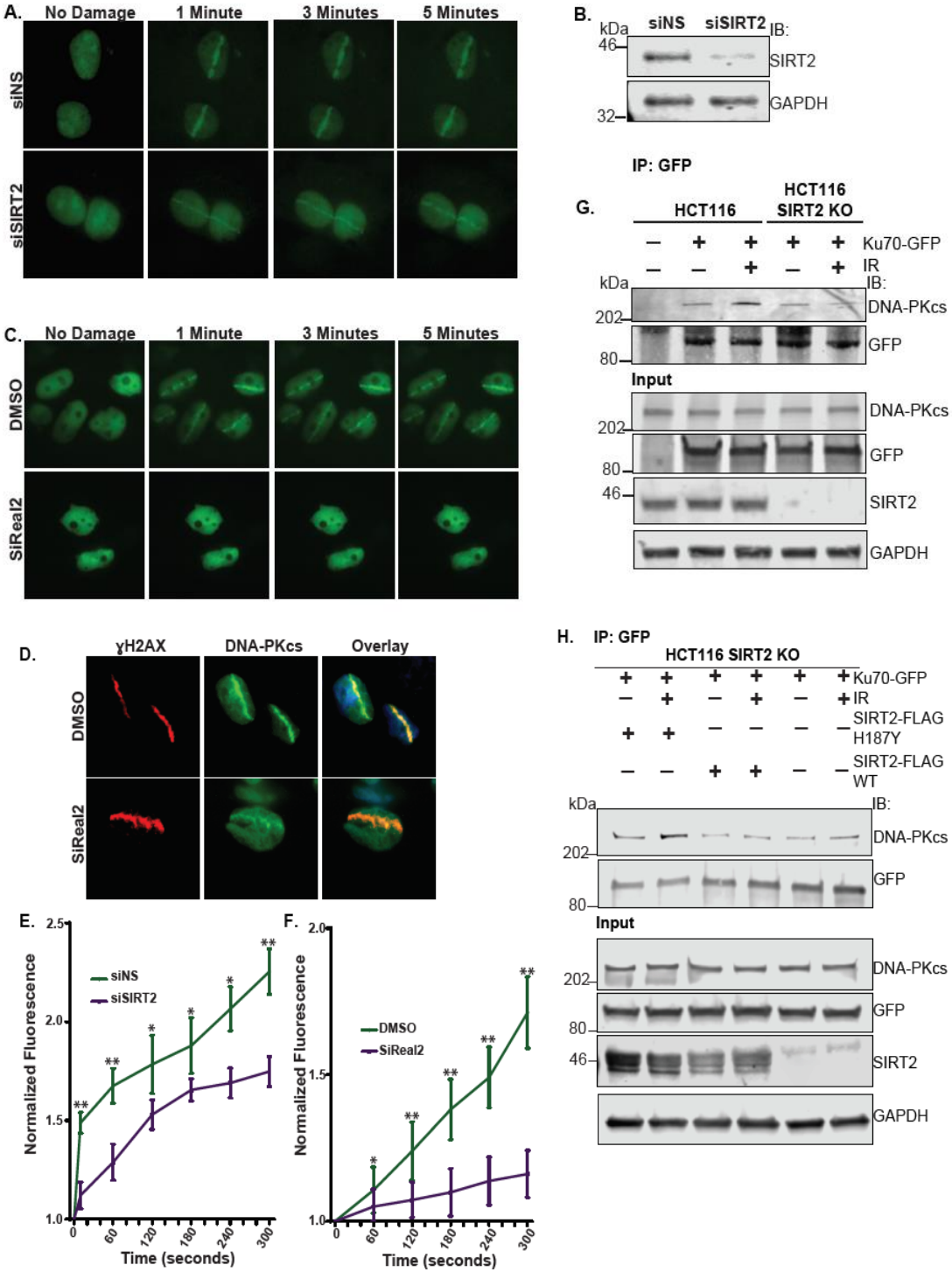
A.
No Damage
1 Minute
3 Minutes
5 Minutes
siNS
siSIRT2
B.
kDa
siNS
siSIRT2
IB:
46
SIRT2
GAPDH
32
IP: GFP
C.
No Damage
1 Minute
3 Minutes
5 Minutes
DMSO
SiReal2
G.
HCT116
HCT116 SIRT2 KO
Ku70-GFP
IR
kDa
IB:
202
DNA-PKcs
GFP
80
Input
202
DNA-PKcs
80
GFP
46
SIRT2
GAPDH
D.
γH2AX
DNA-PKcs
Overlay
DMSO
SiReal2
H.
IP: GFP
HCT116 SIRT2 KO
Ku70-GFP
IR
SIRT2-FLAG H187Y
SIRT2-FLAG WT
kDa
IB:
202
DNA-PKcs
GFP
80
Input
202
DNA-PKcs
80
GFP
46
SIRT2
GAPDH
E.
Normalized Fluorescence
siNS
siSIRT2
Time (seconds)
F.
Normalized Fluorescence
DMSO
SiReal2
Time (seconds)

Figure 3.4. *SIRT2* Depletion Decreases DNA-PKcs Localization to DNA Damage Sites Induced by Laser Microirradiation and Decreases Interaction with Ku

A, DNA-PKcs-GFP stably transfected U2OS cells were subjected to UV (wavelength of 365nm) microirradiation following transfection with SIRT2 siRNA or NS siRNA. Laser microirradiation was performed on a Zeiss Observer Z1 microscope equipped with a Micropoint® Laser Illumination and Ablation System (Photonic Instruments). The laser output was set to 75%, which can reproducibly give focused DNA-PKcs-GFP stripes. Images were taken every minute for 5 minutes following damage. B, Western blot demonstrating SIRT2 knockdown generated from a portion of cells taken from experimental groups used in part A prior to damage induction. C, DNA-PKcs-GFP stably transfected CHO V3 cells were subjected to UV microirradiation with and without SIRT2 inhibition by SirReal 2 (50 uM) or DMSO treatment. Images were taken every minute for 5 minutes following damage. D, CHO V3 cells treated with or without SirReal2 or DMSO were fixed 2 minutes post microirradiation and stained for γH2AX in red, DNA-PKcs-GFP in green, and DAPI stain in the overlay. Laser microirradiation was performed on a Zeiss Observer Z1 microscope equipped with a Micropoint® Laser Illumination and Ablation System (Photonic Instruments). The laser output was set to 75%, which can reproducibly give focused DNA-PKcs-GFP stripes. E, Fluorescence of the GFP stripes were measured, recorded at indicated time points, and analyzed for quantitation using Image Studio Lite Software. There were 15 biological replicates per time point per condition. The average of each time point's replicates was plotted. Error bars represent standard deviation: NS indicates $P \geq 0.05$, *$P < 0.05$, **$P < 0.01$. F, Quantitation of DNA-PKcs-GFP localization to sites of damage was performed for 15 biological replicates per

condition. Fluorescence of the GFP stripes were measured, recorded at indicated time points, and analyzed for quantitation using Image Studio Lite Software. The average of each time point's replicates was plotted. Error bars represent standard deviation. NS indicates $P \geq 0.05$, *$P < 0.05$, **$P < 0.01$. G, Wildtype and SIRT2 KO HCT116 cells were transfected with and without Ku70-GFP, SIRT2-FLAG WT, and SIRT2-FLAG H187Y and treated with 0 or 10 Gy IR. Ku70-GFP was immunoprecipitated and run on SDS-PAGE gels. The resulting western blots were immunoblotted for DNA-PKcs, GFP, SIRT2, and GAPDH.

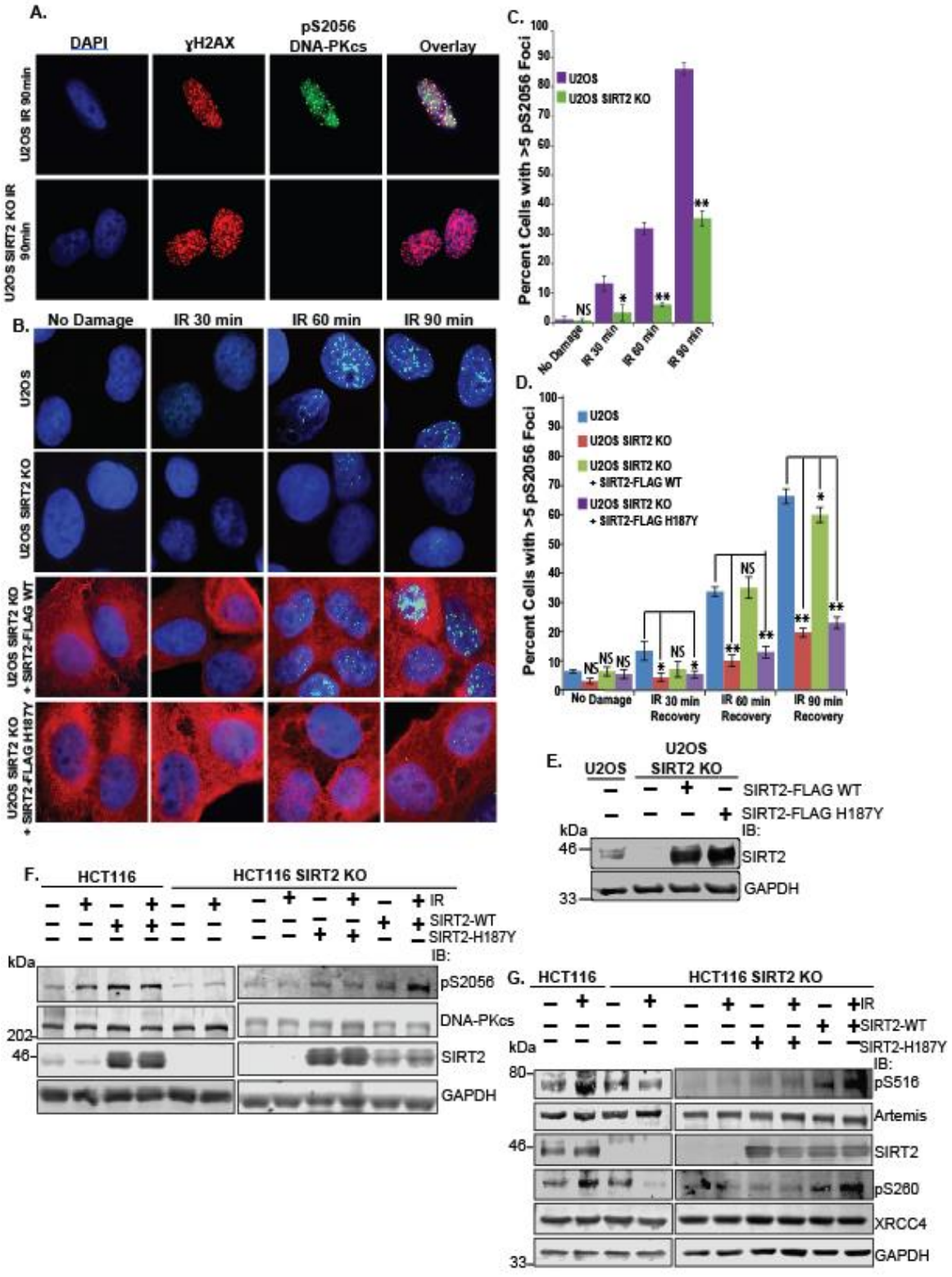
A.
DAPI
γH2AX
pS2056 DNA-PKcs
Overlay
U2OS IR 90min
U2OS SIRT2 KO IR 90min
B.
No Damage
IR 30 min
IR 60 min
IR 90 min
U2OS
U2OS SIRT2 KO
U2OS SIRT2 KO + SIRT2-FLAG WT
U2OS SIRT2 KO + SIRT2-FLAG H187Y
C.
Percent Cells with >5 pS2056 Foci
U2OS
U2OS SIRT2 KO
NS
No Damage
IR 30 min
IR 60 min
IR 90 min
D.
Percent Cells with >5 pS2056 Foci
U2OS
U2OS SIRT2 KO
U2OS SIRT2 KO + SIRT2-FLAG WT
U2OS SIRT2 KO + SIRT2-FLAG H187Y
No Damage
IR 30 min Recovery
IR 60 min Recovery
IR 90 min Recovery
E.
U2OS
U2OS SIRT2 KO
SIRT2-FLAG WT
SIRT2-FLAG H187Y
kDa
IB:
46
SIRT2
GAPDH
33
F.
HCT116
HCT116 SIRT2 KO
IR
SIRT2-WT
SIRT2-H187Y
kDa
IB:
pS2056
DNA-PKcs
202
46
SIRT2
GAPDH
G.
HCT116
HCT116 SIRT2 KO
IR
SIRT2-WT
SIRT2-H187Y
kDa
80
IB:
pS516
Artemis
46
SIRT2
pS260
XRCC4
33
GAPDH

Figure 3.5. Deacetylation by SIRT2 Regulates DNA-PKcs Kinase Activity

A, Wildtype and *SIRT2* KO U2OS cells were treated with 0 or 10 Gy IR. Cells were fixed at 30, 60, or 90 min post IR and stained with anti-γH2AX (red), anti-DNA-PKcs phosphoserine 2056 (green), and DAPI stain (blue). A representative 90 min post IR time point is shown. B, Wildtype and *SIRT2* KO U2OS cells were transfected with SIRT2-FLAG WT, SIRT2-FLAG H187Y, or with no transfection and treated with 0 or 10 Gy IR. Cells were fixed at 30, 60, or 90 min post IR and stained with anti-FLAG (red), anti-DNA-PKcs phosphoserine 2056 (green), and DAPI stain (blue). C, Quantitation of the percentage of cells with >5 DNA-PKcs phosphoserine 2056 foci is shown for A. The mean from each group was calculated from three biological replicates (100 cells per replicate) and error bars represent S.D. *, $p < 0.05$; **, $p < 0.01$. D, Quantitation of the percentage of cells with >5 DNA-PKcs phosphoserine 2056 foci is shown for B. The mean for each group was calculated from three biological replicates (100 cells per replicate) and error bars represent S.D. *, $p < 0.05$; **, $p < 0.01$. E, Western blot analysis for B. F, Western blot analysis of DNA-PKcs autophosphorylation at serine 2056 in response to damage induced by IR in wildtype and *SIRT2* KO HCT116 cells transfected with SIRT2-FLAG WT, SIRT2-FLAG H187Y, or with no transfection. G, Western blot analysis of Artemis and XRCC4 phosphorylation at serine 516 and 260 respectively in response to damage induced by IR in wildtype and *SIRT2* KO HCT116 cells transfected with SIRT2-FLAG WT, SIRT2-FLAG H187Y, or with no transfection.

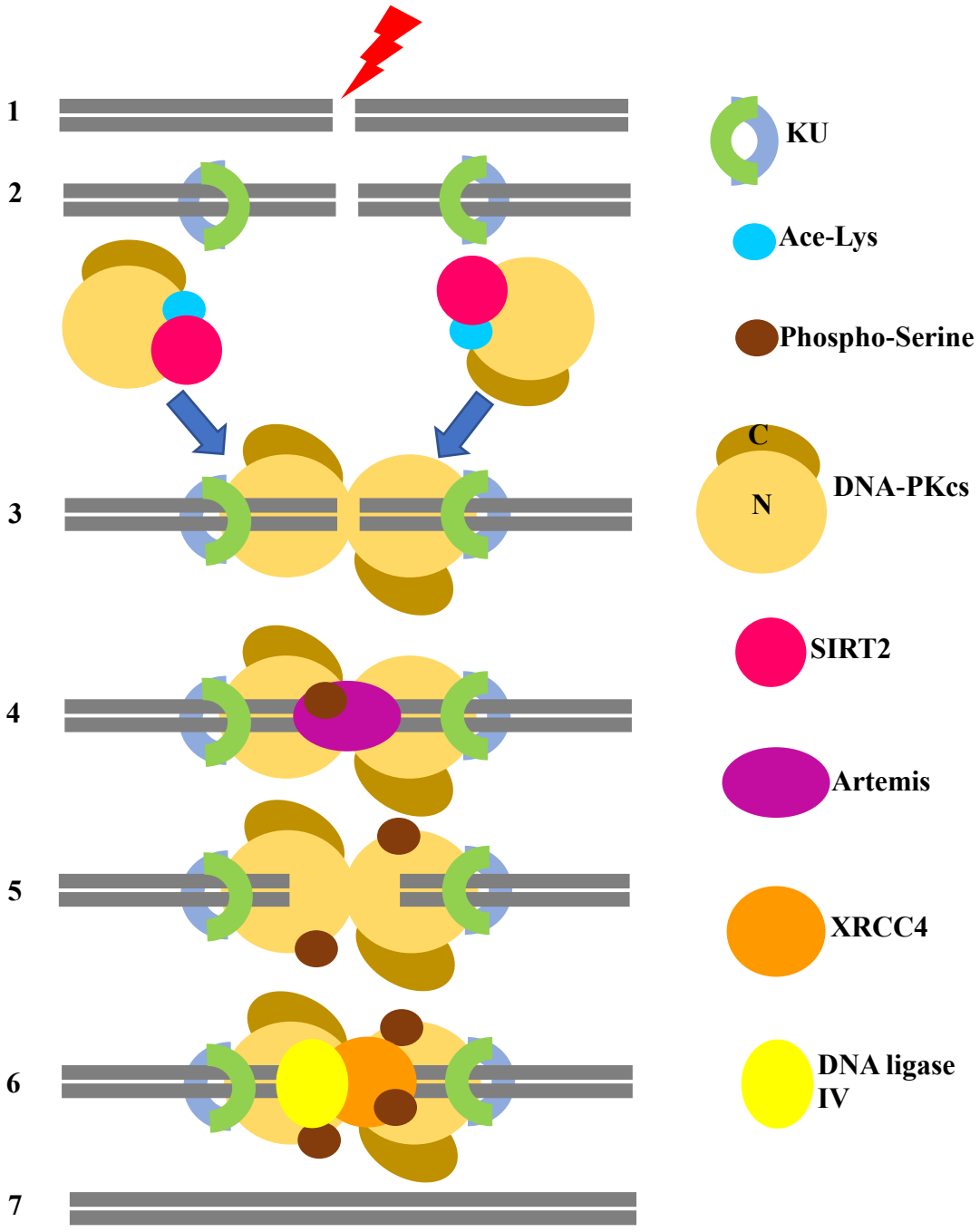
1
2
3
4
5
6
7
KU
Ace-Lys
Phospho-Serine
C
N
DNA-PKcs
SIRT2
Artemis
XRCC4
DNA ligase IV

Figure 3.6. Model of SIRT2 Regulation of DNA-PKcs in NHEJ Repair

DNA damage results in a DSB (1) which leads to the recruitment Ku70 and Ku80 heterodimers to both sides of the DSB (2). SIRT2 deacetylates DNA-PKcs in response to damage on its N terminus (light brown) which is important to DNA-PKcs localization to the sites of DNA damage, its interaction with Ku, and the formation of DNA-PK holoenzyme dimers (3). Once dimerized, DNA-PKcs phosphorylates downstream NHEJ repair factors Artemis and Artemis resects DNA ends (4-5). DNA-PKcs autophosphorylates at serine 2056 (5) and phosphorylates XRCC4 (6). XRCC4 with DNA ligase 4 and DNA-PKcs promotes end ligation (6). DNA-PKcs releases the repaired DNA (7).

3.6 Discussion

We have previously demonstrated that SIRT2 is both a regulator of the RSR, and a potential tumor suppressor in humans [71, 73, 113]. Using a combination of EJ5 assays and clonogenic survival assays, we have now demonstrated that SIRT2 is also a novel regulator of NHEJ repair. *SIRT2* deficiency results increased sensitivity to DNA damaging agents (IR and CPT) and reduced NHEJ repair. Reduced NHEJ repair was determined to be the result of the loss of SIRT2 regulation of DNA-PKcs localization and kinase activity in *SIRT2* depleted cells.

The interaction between SIRT2 and NHEJ repair kinase DNA-PKcs was first discovered via mass spectrometry analysis (data not shown) and was confirmed through immunoprecipitation experiments on endogenous DNA-PKcs and SIRT2. Indeed, SIRT2 co-immunoprecipitated with DNA-PKcs and DNA-PKcs co-immunoprecipitated with SIRT2 before and after damage induction and in the presence of ethidium bromide. These results indicated that this interaction was not dependent on DNA damage induction or on the presence of DNA. Therefore, SIRT2 enzymatic activity is likely regulated by DNA damage induction rather than DNA-PKcs binding.

Indeed, SIRT2 is known to bind acetylated substrate before binding to its co-factor NAD^+ [119] and DNA-PKcs acetylation levels were higher before DNA damage induction by IR than after. In fact, DNA-PKcs acetylation following DNA damage induction by IR is restored through *SIRT2* knockdown and overexpressed SIRT2 was able to deacetylate DNA-PKcs as a direct substrate *in vitro* and in cells. Acetylation of DNA-PKcs, however,

was not impacted by SIRT2 overexpression in the presence of sirtuin inhibitor (nicotinamide) or if SIRT2 deacetylase activity was lost through mutation of its deacetylase domain (SIRT2 H187Y). Additionally, the amount of SIRT2 bound to acetylated DNA-PKcs increased with nicotinamide treatment.

Increased co-immunoprecipitation of SIRT2-FLAG WT with endogenous DNA-PKcs, therefore, was perhaps the result of increased acetylated DNA-PKcs pools caused by inhibition of overexpressed and endogenous SIRT2. Overall, SIRT2 is bound to acetylated DNA-PKcs in a DNA and DNA damage independent manner and SIRT2 deacetylates DNA-PKcs in response to DNA damage induction by IR. However, further testing is necessary to determine the exact mechanism of IR induced SIRT2 activation and of increased SIRT2 DNA-PKcs binding in response to SIRT2 inhibition. Deacetylation by SIRT2 often leads to activation of DDR substrates in terms of substrate localization to damage and/or increased substrate enzymatic activity [71, 73]. Therefore, we determined whether deacetylation by SIRT2 was necessary for DNA-PKcs localization and/or kinase activity in DNA damage repair.

SIRT2 depletion or inhibition lead to decreased localization of DNA-PKcs-GFP to sites microirradiation induced DNA damage and decreased co-immunoprecipitation of endogenous DNA-PKcs with Ku70-GFP in response to IR. Co-immunoprecipitation and therefore localization of DNA-PKcs to Ku at sites of damage was restored by over-expression of SIRT2 WT in *SIRT2* depleted cells but not by overexpression of SIRT2

H187Y. These results indicated that DNA-PKcs localization to sites of DNA damage is promoted by SIRT2 deacetylase activity.

Using immunofluorescence and immunoblotting, we demonstrated that SIRT2 deacetylase activity not only regulated DNA-PKcs localization to damage but also its kinase activity. DNA-PKcs autophosphorylation at serine 2056 in response to IR is decreased in *SIRT2* deficient cells and is only rescued with SIRT2 WT overexpression. Autophosphorylation of serine 2056 occurs after DNA-PKcs localization to sites of DNA damage, therefore, the lack of DNA-PKcs autophosphorylation may be indirectly attributed to lack of localization not kinase activity. However, SIRT2 over-expression wildtype cells increased DNA-PKcs autophosphorylation without induction of DNA damage and therefore SIRT2 regulation of DNA-PKcs kinase activity was independent of localization. In addition, lack of localization and kinase activity of DNA-PKcs in *SIRT2* deficient cells resulted in decreased phosphorylation of downstream DNA-PKcs kinase targets Artemis (serine 516) and XRCC4 (serine 260). These results indicated that *SIRT2* deficiency would lead to NHEJ repair deficiency through loss of DNA-PKcs regulation and subsequent increased chromosomal abnormalities, genomic instability, and ultimately cancer. The site or site or sites of deacetylation on DNA-PKcs regulated by SIRT2 are still unknown, but they likely reside in the N-terminus of DNA-PKcs.

The N-terminus of DNA-PKcs (amino acids 1-2713), which does not contain the kinase activity (PI3K domain), is required for DNA-PKcs localization to DSBs, for the interaction between DNA-PKcs, Ku, and DNA at DSBs, and for the formation of the

DNA-PK holoenzyme dimer [21, 120]. In response to DSBs, DNA bound Ku heterodimers recruit DNA-PKcs to sites of damage by binding DNA-PKcs in its N-terminus [120]. DNA-PKcs also binds DNA at the DSB through its N-terminus and to form a DNA-PKcs-Ku heterotrimer complex [120]. Following complex formation on both sides of the DNA break, the two complexes likely form a dimer across the break through the HEAT repeats in the N-terminus of each DNA-PKcs [21, 120]. Formation of these complexes are required for conformational changes in DNA-PKcs that allow for activation of its kinase domain through signal transduction from the N-terminal HEAT repeats to the C-terminal kinase domain [21].

This dimerization is also thought to promote trans-autophosphorylation of the DNA-PKcs molecules at serine 2056 which is in turn needed for promotion of end ligation and DNA-PKcs release from the DNA [121]. The dimer formation also potentially holds the DNA ends in proximity while providing a platform for downstream DNA-repair enzymes [122]. Therefore, one hypothesis is that SIRT2 deacetylates DNA-PKcs in the N-terminus to promote localization and binding of DNA-PKcs to Ku at sites of DNA damage, to promote formation of DNA-PKcs dimers, and to promote DNA-PKcs kinase activity. However further studies are required to find the sites of deacetylation and determine their functional significance on DNA-PKcs localization and kinase activity in response to damage.

In summary, our findings support a new model for NHEJ repair in which SIRT2 deacetylates DNA-PKcs at one or more sites in its N-terminus in response to damage.

Deacetylation promotes proper DNA-PKcs localization and DNA-PKcs activation of kinase activity (Figure 3.6). Activation of DNA-PKcs is necessary for NHEJ repair and therefore, *SIRT2* depletion leads to loss of NHEJ due to loss of positive regulation of DNA-PKcs. This provides further evidence that SIRT2 acts a tumor suppressor in humans by maintaining genomic stability through positive regulation of the NHEJ repair pathway. Given that *SIRT2* depletion causes IR hypersensitivity and that SIRT2 promotes the repair of DSBs through NHEJ, this work suggests that SIRT2 may be a promising therapeutic target.

3.7 Acknowledgements

We thank members of the Yu lab for helpful discussion. We kindly thank Eric Verdin for the SIRT2-FLAG plasmid. We also thank members of Anthony Davis' lab for DNA-PKcs antibody, DNA-PKcs and Ku70/80 plasmids, and DNA-PKcs-GFP stable cell lines (both U2OS and CHO V3). This work was supported by National Institutes of Health (NIH)/National Cancer Institute (NCI) R01CA178999 and R01CA178999S1, Basser Center for BRCA External Research Grant Program Innovation Award 32356, and Winship Cancer Institute (WCI) Brenda Nease Breast Cancer Research Fund Pilot Award 53237 to D.S.Y.

Chapter 4: General Discussion and Future Directions

4.1 General Discussion

Although great strides have been made in the past few decades in identifying DDR regulatory proteins (e.g. p53, BRCA1, etc.) and in elucidating their roles in maintaining genomic stability, there are still a great number of regulatory proteins whose functions in the DDR are not fully understood. A better understanding might enable us to provide patients with more effective treatments for cancers driven by loss of tumor suppressors or gain of oncogenes. My work presented here expands our current understanding of DDR regulation and genomic stability maintenance. Results support a model of SIRT2 tumor-suppressive function in which somatic mutations in *SIRT2* contribute to genomic instability. These mutations impair SIRT2 deacetylase activity or reduce SIRT2 protein levels in the DDR providing a mechanistic explanation for the role of *SIRT2* mutations in tumorigenesis. Additionally, I have demonstrated that SIRT2 plays an essential role in the NHEJ repair pathway, providing a strong premise for the development of SIRT2 inhibitors for therapeutic applications.

Using structural insights, combined with bioinformatics and functional analyses, we found that naturally-occurring cancer-associated SIRT2 mutations at evolutionarily conserved sites disrupt its deacetylation of DDR proteins by impairing its catalytic activity or reducing its expression level. They do not appear to interfere with localization or with binding substrate. Together results demonstrate that cancer-associated *SIRT2* mutations are functionally significant. I also found that certain *SIRT2* mutants fail to rescue replication stress response phenotypes or spontaneous induction of DNA damage

induced by *SIRT2* deficiency in cancer cells. Thus, somatic SIRT2 mutations in human tumors contribute to genomic instability by impairing its deacetylase activity or protein level in the DDR, demonstrating SIRT2's potential to function as a tumor suppressor in humans. In addition, the inability of mutant proteins to suppress genomic instability indicated they were potentially driver mutations rather than passenger mutations. However, the tumor samples these mutations were discovered in were heterozygous, suggesting they would not have contributed directly to tumorigenesis due to the presence of a functional copy of *SIRT2*. Additionally, these mutations did not show dominant-negative phenotypes *in vitro,* but it is possible that SIRT2 mutants demonstrate haploinsufficiency in patients especially in the presence of activated oncogenes and loss of other tumor suppressors. Future experiments should investigate haploinsufficiency and potential dominant negative effects that may arise in cells through the generation of knock-in mutants. For example, CRISPR-Cas9 could be implemented to generate lines that have a heterozygous genotype for each of these *SIRT2* mutants and endogenous expression levels of both WT and mutant genes to examine genomic instability phenotypes.

Furthermore, our results describe a novel mechanism for the regulation of NHEJ repair whereby DNA-PKcs deacetylation by SIRT2 activates DNA-PKcs localization to sites of damage, kinase activity, and downstream signaling in DSB repair. We found that SIRT2 binds and deacetylates DNA-PKcs in response to IR, and that this deacetylation is necessary for DNA-PKcs localization to sites of microirradiation and for interaction with Ku. SIRT2 deacetylation of DNA-PKcs prior to and/or after its localization to DSBs,

regulates DNA-PKcs kinase activity. SIRT2 directed deacetylation is necessary for DNA-PKcs autophosphorylation as well as phosphorylation of downstream DNA-PKcs NHEJ substrates. Therefore, deficiencies in *SIRT2* result in deficiencies in NHEJ repair which in turn could lead to increased genomic instability, providing further evidence of SIRT2's role in tumor suppression. However, future studies will be required to determine the exact acetylation sites on DNA-PKcs that SIRT2 acts on and how this deacetylation alters DNA-PKcs localization to DNA damage and kinase activity.

Characterization of truncation mutations could help establish the region in DNA-PKcs that SIRT2 binds to before and after damage induction. First, tagged DNA-PKcs fragments would be overexpressed followed by immunoprecipitation of the tag and run on an SDS-PAGE gel. The resulting western blot could be stained for endogenous SIRT2 co-immunoprecipitation. The fragment or fragments that co-immunoprecipitates SIRT2 are likely the regions of interaction. Mass Spectrometry analysis of these fragments with and without DNA damage induction and or SIRT2 overexpression will also allow for the identification of specific acetylation sites on DNA-PKcs. Additionally, generation of DNA-PKcs acetylation mimics (mutations of lysine to glutamine) and deacetylation mimics (mutations of lysine to arginine) should be generated and tested for proper localization to damage and kinase activity. SIRT2 has now been established to maintain genomic integrity through suppression of tumorigenesis via regulation of mitotic checkpoints [78], replications stress [71, 73], and now NHEJ, and therefore could play other potential roles in other DDR pathways.

Our data indicate that *SIRT2* deficiency results in reduced colony formation in response to IR and CPT treatment. Although both damaging agents result in DSBs, IR treatment results in a range of DNA lesions while CPT treatment primarily results in DSBs during S/G_2 suggesting a role for SIRT2 in HR. Therefore, it would prove beneficial to continue expanding the search for SIRT2 targets in the DDR and determine if there is crosstalk between these pathways. In addition, it is essential for future studies to also examine the upstream regulation of SIRT2 to determine the mechanisms by which SIRT2 is activated to promote its function in the DDR.

4.2 Crosstalk: Additional Roles for SIRT2 in DNA Damage Repair

DDR pathways do not exist in a vacuum, in that they are not completely independent of each other. Proteins involved in one pathway often have additional roles in others. The pathways themselves can influence the activation or suppression of others in response to DNA damage through pathway crosstalk. In fact, many tumor suppressor proteins regulate multiple DDR pathways, which is why mutagenic deletion or inactivation can result in genomic instability and tumor development. The best examples of pathway crosstalk in the DDR can be seen in the regulation of the DNA damage repair pathways.

SIRT2 is a prime example of a DNA damage repair protein that influences multiple DNA damage repair pathways [26]. Specifically, SIRT2 regulates a network of proteins involved in upstream cell cycle checkpoint signaling pathways (RSR, G2/M), downstream DNA damage repair pathways (DSB repair and potentially SSBR, NER, and BER), and under extreme oxidative stress, apoptotic pathways (Figure 4.1). For example,

in the RSR, SIRT2 regulates cell cycle checkpoint signaling through deacetylation of ATRIP. ATRIP localization and accumulation at sites of stalled replication forks is lost when SIRT2 deacetylase activity is impaired as seen in chapter 2.

ATRIP is essential for ATR localization and activation at stalled forks [72]. Therefore ATRIP is necessary for the potentiation of downstream signaling required for cell cycle checkpoint activation and fork stabilization [72]. For example, *SIRT2* mutation induced dysregulation of ATRIP would upset downstream phosphorylation of CHK1, which is necessary for checkpoint activation and for recruitment of other fork stabilizing proteins like CDK9 [71]. These conditions would lead to delayed activation of cell cycle arrest (and subsequent DNA damage repair pathway activation) and prolonged unstable replication fork stalling [71]. This dysregulation would increase the incidence of fork collapse into DNA strand breaks [71]. Therefore, upstream signaling coordinated by SIRT2 deacetylase activity during initial RSR activation influences the ability of the cell to repair more minor lesions (i.e. mismatches, bulky and non-bulky lesions) before development of more devastating SSB and DSBs from fork collapse. In this scenario, *SIRT2* loss leads to direct dysregulation of the checkpoint induced by replication stress which indirectly affects the activation of DNA damage repair pathways, but my work has demonstrated more direct roles for SIRT2 regulation of DNA damage repair as well.

In chapter 3, I demonstrated SIRT2 deacetylates DNA-PKcs and that SIRT2 deacetylase activity is necessary for DNA-PKcs localization to DNA damage sites, its interaction with Ku, and its kinase activity. DNA-PKcs is an essential upstream DNA damage kinase

in NHEJ repair which helps to maintain the DNA damage ends in proximity during repair, to recruit and load NHEJ repair factors to DNA damage ends, to promote end resection by Artemis, and to promote end ligation by XRCC4 and DNA ligase IV. *SIRT2* loss led to impaired NHEJ efficiency as measure by EJ5 reporter cell assays [17, 18, 21, 25]. Therefore, *SIRT2* deletion or mutation, or SIRT2 inhibition would not only result in increased genomic instability through dysregulation of cell cycle checkpoints but also through loss of NHEJ repair. NHEJ repair is activated in response to DSB during G0 and G1 and without it, alt-NHEJ is activated instead leading to increased genomic incorporation of insertions and deletion mutations [123]. In addition, I also demonstrated that *SIRT2* loss leads to IR and CPT sensitivity suggesting that SIRT2 may regulate other DNA damage repair pathways in addition to NHEJ.

Future experiments should endeavor to establish what roles SIRT2 may play in other DNA damage repair pathways. Further establishment of potential SIRT2 DNA damage repair crosstalk will help to warrant the development and implementation of SIRT2 inhibitors for cancer treatment and to allow us to better predict the outcome of SIRT2 inhibitor use under different cancer physiologies. In the experiments presented in Chapters 2 and 3, several types of DNA damaging agents were used to induce phenotype including microirradiation (UV radiation), gamma irradiation (IR), HU drug treatment, and/or CPT drug treatment to induce replication stress or DSB, but these agents cause a variety of DNA damage.

In Chapter 3, *SIRT2* depletion lead to a deficiency in NHEJ repair as measured by an EJ5 assay which specifically measures the ability of the cell to repair DSBs in the absence of a repair template. Results demonstrated the importance of SIRT2 to proper NHEJ [114]. However, UV radiation treatment induces DSBs and bulky base damage (NER recognized damage), gamma irradiation treatment induces DSBs, SSBs, and non-bulky base damage (BER recognized damage), HU treatment induces replication stress and prolonged treatment can induce SSB and DSBs, and CPT treatment induces SSBs and DSBs in S phase of the cell cycle through inhibition of TOPOI. Therefore, the increase sensitivity to these damaging agents seen with *SIRT2* deficiency in Chapters 2 and 3 could be due to additional regulatory roles for SIRT2 in the other DNA damage induced pathways (SIRT2 crosstalk) such as alt-NHEJ, SSB repair, BER, NER, and HRR. Future experiments are required to tease out these other potential functions.

An EJ2 reporter cell assay could be employed to look into alt-NHEJ repair [124]. EJ2 cells are U2OS cells have been stably transfected with GFP separated from an N-terminal tag with an I-SceI site followed by a stop codon (only the N-terminal tag is expressed by the promoter) [124]. On both sides of the I-SceI and stop codon are natural microhomologies that occur in the tag gene [124]. Overexpression of I-SceI leads to repair by alt-NHEJ and only alt-NHEJ will lead to functional GFP expression [124]. If *SIRT2* depletion leads to significantly less GFP expression compared to non-specific knockdown controls, SIRT2 may also play a role in alt-NHEJ repair.

A comet assay (single-cell gel electrophoresis) would also provide insight into the functional significance of SIRT2 in BER, NER, or SSB repair and DSB repair pathways. Cells are embedded into an agarose gel following DNA damage induction on a microscope slide and then lysed with detergent under high salt conditions [125]. Electrophoresis is performed at a high pH and nucleoids containing supercoiled loops of DNA linked to a nuclear matrix from the lysed cells move along the gradient [124]. The DNA is stained by ethidium bromide and visualized using fluorescent microscopy [124]. The structure of the nucleoids resemble comets and the higher the intensity of the comet tail structures compared to the head, the greater the unrepaired DNA damage [124]. The type of damage induced can be adjusted depending on the agents used allowing one to test for deficiencies specifically in BER, NER, DSB repair, or SSB repair [124]. If *SIRT2* depletion leads to more intense tails compared to controls, SIRT2 is involved more specifically with the repair pathway induced.

Other members of our lab (Dr. Hui Zhang, Dr. Chunyang Li, and Elizabeth Minten) have demonstrated an additional role for SIRT2 in HRR through the deacetylation and regulation of BRCA1 both *in vitro* and in cells (data not shown). SIRT2 deacetylation of BRCA1 increased in response to damage (data not shown). Using a Direct-Repeat-GFP (DR-GFP) reporter assay SIRT2 was shown to be essential to proper HRR. In a DR-GFP assay, U2OS cells have been stably transfected with both a nonfunctional SceGFP gene (containing an in frame premature stop codon and an I-SceI site) under a promoter followed and a functional GFP gene downstream of the SceGFP gene without a promoter [124]. Overexpression of I-SceI leads to a DSB in the SceGFP gene which is repaired by

HRR using the functional GFP gene copy downstream [124]. This repair leads to the removal of the stop codon and thus functional GFP expression [124]. If HRR is efficiency is maintained following knockdown of a gene of interest compared to non-specific knockdown controls (both cell populations express the same amount of GFP), then the protein of interest is not essential to HRR [124]. *SIRT2* depletion lead to significantly decreased GFP expression that was only restored by SIRT2-FLAG WT but not deacetylase dead SIRT2-FLAG H187Y indicating SIRT2 deactylase activity is also essential to HRR (data not shown). Since SIRT2 is necessary for both HRR and NHEJ and because SIRT2 deacetylates upstream repair proteins (BRCA1 and DNA-PKcs) in these pathways, SIRT2 deacetylation activity may help in pathway choice, another mechanism of crosstalk.

BRCA1 is inhibited during G1 by 53BP1 and BRCA1 expression is lowest during G0, G1 and mitosis which promotes NHEJ over HRR pathway activation [126]. However during S and G2, BRCA1 expression is high and it inhibits 53BP1 through suppression of its effector protein Rap1-interacting factor 1 (RIF1) to promote HRR over NHEJ [126]. During pathway choice, SIRT2 may deacetylate and upregulate BRCA1 activity when BRCA1 is elevated in S and G2 leading to upregulation of HRR. However, during G0 and G1 when BRCA1 levels are low and BRCA1 is inhibited, SIRT2 could preferentially deacetylate DNA-PKcs to upregulate NHEJ. Future experiments are needed to examine the functional significance of SIRT2 deacetylation of BRCA1 and HRR regulation; however, it is clear that *SIRT2* loss leads to deficiencies in both NHEJ repair and HRR. SIRT2 may also have potential roles in SSBR, NER, and BER. Therefore, *SIRT2* loss

would lead to the dysregulation of multiple DDR pathways which could be exploited in future cancer therapies similar to PARP1 inhibition has benefited treatment of various breast and ovarian cancers (Figure 4.1).

For example, loss of function mutations in tumor suppressor BRCA1 and BRCA2 genes leads to an increased susceptibility to breast and ovarian cancers due to loss of HRR mechanisms [127]. Loss of the HRR pathway shifts the burden of DSB repair onto other repair pathways in the cell such as NHEJ and alt-NHEJ [127]. Because these pathways are more error prone, the amount of genomic incorporation of mutation and genomic instability is higher. Because PARP1 is the primary DNA damage sensor and regulator of so many DNA damage repair pathways (SSB, alt-NHEJ, BER, NER, and HRR) inhibition leads to an intolerable deficiency in DNA damage repair mechanisms and sensitize cancer cells previously resistant to chemo- and/or radiotherapies [127]. Therefore, targeting proteins that exhibit a high amount of crosstalk between repair pathways such as SIRT2 can increase the effectiveness of current therapeutics (Figure 4.1). Uncovering other pathways under SIRT2 regulation will broaden our knowledge of the DDR and help up to identify more novel downstream SIRT2 targets, however, it is equally important to determine how SIRT2 is regulated upstream in response to DNA damage induction.

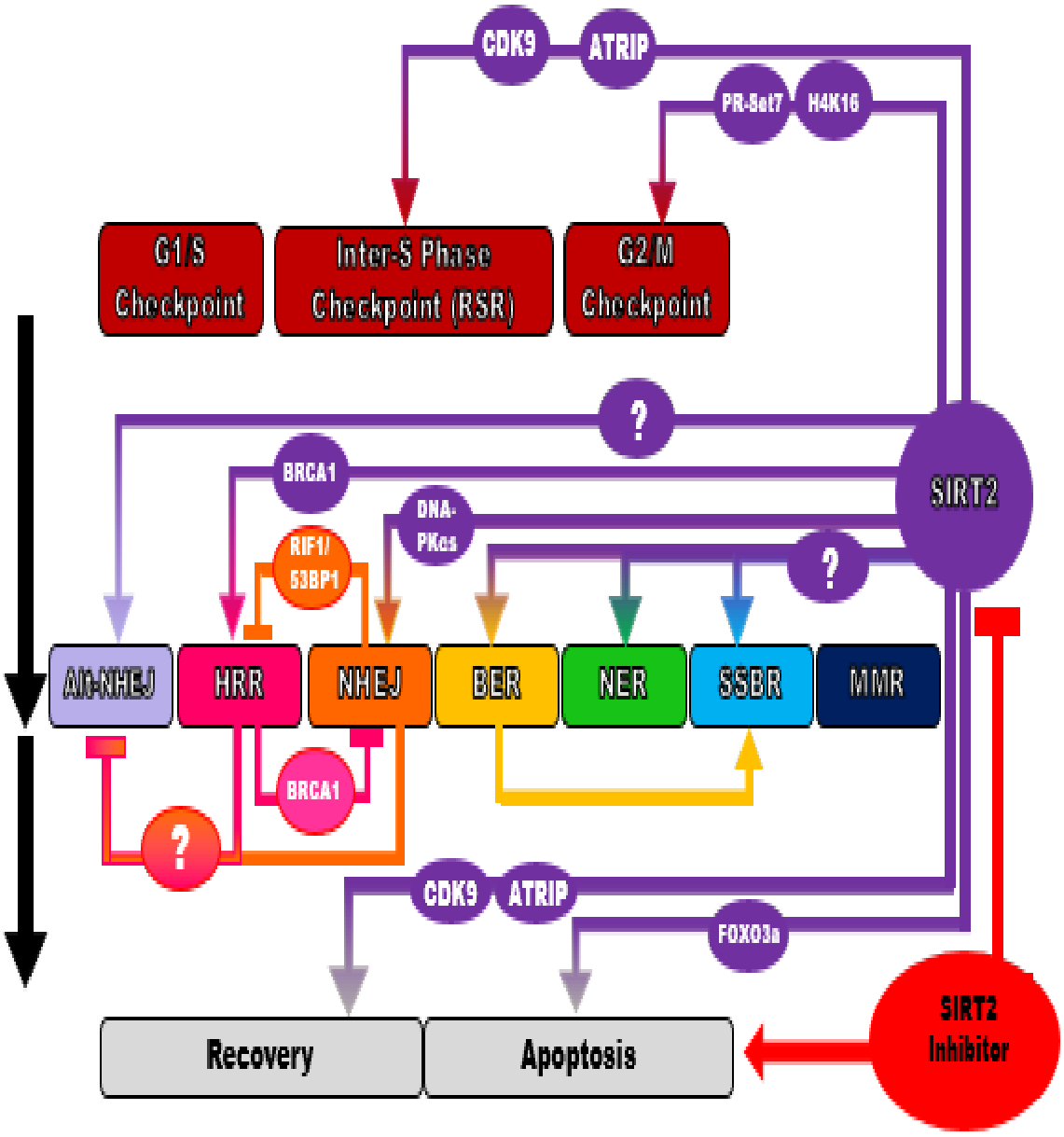

Figure 4.1 SIRT2 Crosstalk Diagram. SIRT2 regulates a multitude of proteins in various levels of the DDR with more substrates still being discovered. Therefore, SIRT2 inhibition could potentially lead to increased sensitivity of cancer cells to current therapies.

4.3 SIRT2: Regulation of Localization and Activity

Many questions remain regarding SIRT2 upstream regulation in the DDR. Specifically, how is SIRT2 imported into the nucleus, and how is its enzymatic activity regulated during the DDR? SIRT2 nuclear import has been investigated in multiple studies, but the mechanism has not yet been elucidated. To gain access to the nucleus, a protein must cross the nuclear envelope by traversing through a nuclear pore complex [128-131]. Proteins smaller than ~40 kDa and small molecules can passively diffuse through the pore into the nucleus, but the majority of proteins require assistance from nuclear transport proteins called importins [128-131]. In the classical import pathway, a specific pattern of basic acid residues defined as the classical nuclear localization signal or cNLS on the cargo protein [128-131]. The cNLS is recognized by an importin-α adaptor protein in the cytoplasm to form a heterotrimer complex with an importin-β receptor protein [128-131].

The complex moves through the nuclear pore to the nucleus where the importins release the cargo after binding Ran-GTP [128-131]. However, there are over 20 transport proteins in mammals, and of which do not require an adaptor protein for transport and can recognize non-classical NLS sequences [131]. Additionally, there are importin-independent import pathways such as calmodulin-mediated transport, and some proteins possess similar structures to transport proteins such as HEAT repeats and Armadillo repeats that allow them to interact directly with nucleoporin proteins and transport themselves into the nucleus [130]. SIRT2 itself likely contains a non-classical NLS that is recognized by one or more importin-β receptor proteins.

SIRT1, SIRT6, and SIRT7 all contain one or more NLSs which vary greatly in sequence from one another [45, 132]. SIRT1 has both a classical NLS in its N-terminus (PLRKRPRR) and a non-classical NLS which is devoid of any basic amino acid residues (IVINILSE) [45]. SIRT6 has one classical NLS in its C-terminus (PKRVKAK) and SIRT7 has one non-classical NLS in its N-terminus (RRREGLKRR) [45, 132]. SIRT2 only has a documented nuclear export signal (NES) shown to be recognized by Exportin 1, also known as CRM1 [67, 69]. Yet, SIRT2 localizes to the nucleus during the G_2/M transition, many SIRT2 DDR substrates exhibit nuclear localization, and SIRT2 can be trapped in the nucleus through leptomycin B (LMB) treatment, indicating there is likely a non-classical NLS in its sequence [67, 69].

As SIRT2 lacks stretches of basic amino acids, its NLS may be similar to the second NLS on SIRT1 and/or rely more on structure than sequence for recognition by importins [131]. It is also worth mentioning that such an NLS is more likely to reside in the C-terminal portion of the protein rather than the N-terminal. LMB-trapping assays revealed that N-terminally tagged GFP-SIRT2 but not C-terminally tagged SIRT2-GFP, can move into the nucleus of 293T and HeLa cell lines (data not shown), indicating that the GFP tag may block a potential NLS on the C-terminus. Future experiments should therefore include generating truncation fragments and/or mutations of the C-terminus followed by localization assays with LMB to tease out the NLS, as localization likely plays a significant role in SIRT2 regulation in the DDR. Additionally, one could perform sequential knockout experiments on known importin proteins followed by LMB

treatment to determine if the loss of one or more importins leads to loss of SIRT2 localization and subsequent trapping in the nucleus. Localization has great potential to regulate SIRT2 activity as compartmentalization could prevent SIRT2 interaction with substrate. Oligomerization of SIRT2 could help prevent SIRT2 interaction with importins and thus sequester to the cytoplasm and keep it inactive under favorable cellular conditions (Figure 4.2A).

SIRT1 has been established to be regulated at least in part by oligomerization [133, 134]. Phosphorylation of SIRT1 at threonine 522 promotes activation in response to cellular stress and prevents the formation of the less active oligomer form [133, 134]. In fact, SIRT1 T522E (phosphomimetic mutant) localizes to the nucleus as a monomer while SIRT1 T522A oligomerizes and is localized to the nuclear periphery and exhibits less enzymatic activity [133, 134]. SIRT2 also exists as an oligomer (homotrimer) or monomer in the cytoplasm of cell [75]. The oligomer does not localize or interact with substrate (α-tubulin) like the monomer indicating SIRT2 oligomerization, like SIRT1 oligomerization, suppresses deacetylase activity and substrate binding [75, 134].

It is therefore possible that SIRT2 localization and enzymatic activity is regulated at least in part by oligomerization and/or PTM like SIRT1 (Figure 4.2A). Experiments by North et. al. indicated that SIRT2 is actively exported from the nucleus rather than actively transported in under normal cellular conditions [69]. Since the majority of SIRT2 is found in the cytoplasm, the rate of export is higher than that of import and/or the amount of SIRT2 shuttling in is low. One hypothesis is that SIRT2 oligomerization prevents

interaction with importin proteins helping to sequester SIRT2 to the cytoplasm (Figure 4.2A). Therefore, activation of SIRT2 (conversion to the monomer form) by PTM or other mechanism allows for it to interact with importins and shuttle into the nucleus (Figure 4.2A). However, SIRT2 is normally quickly shuttled out of the nucleus but DNA damage signaling and/or interaction with nuclear proteins may prevent active export (Figure 4.2B). Further testing is required to determine how the oligomerization of SIRT2 is regulated and how it may regulate SIRT2 import. The homotrimer for the yeast version of SIRT2, Hst2p, has been crystalized and it indicates that key residues in the N- and C-terminal regions are necessary for the formation of the homotrimer [135].

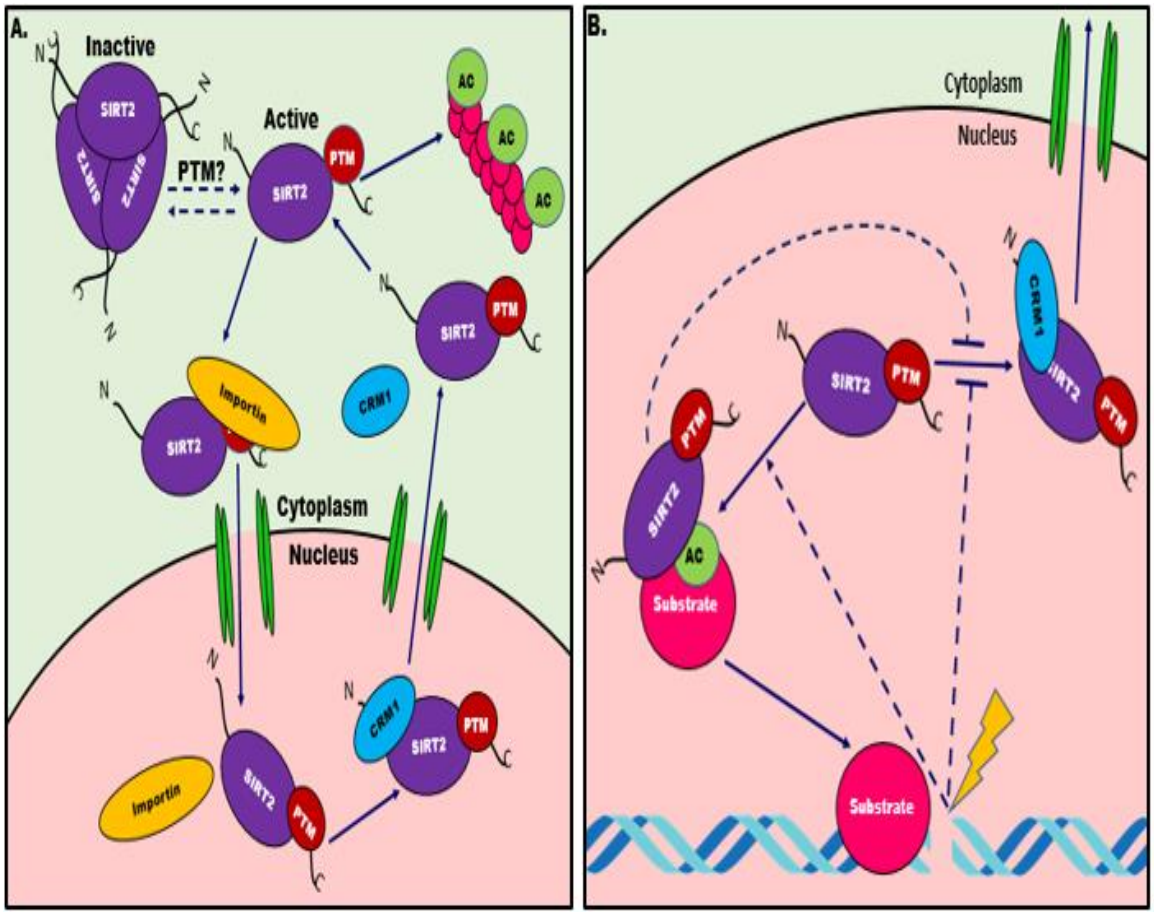

Figure 4.2 Hypothetical Regulation of SIRT2 Activity. A, The majority of SIRT2 exists as an inactive homotrimer in cell cytoplasm until activation and deoligomerization possibly by PTM. Monomer SIRT2 actively deacetylates α-tubulin and other cytoplasmic substrates and can interact with importin through its C-terminus to localize into the nucleus. However, SIRT2 is actively transported out by CRM1 shortly after import to keep nuclear levels low and cytoplasmic levels high. B, SIRT2 nuclear export is inhibited by unknown mechanisms activated by the DDR and/or by binding to nuclear substrates (DNA-PKcs, ATRIP, CDK9, etc.) involved in the DDR.

These residues and tertiary structures are highly conserved in human SIRT2 (Figure 4.3) [135]. Future studies could examine mutation and/or PTM of residues in these regions and determine if they are important to SIRT2 oligomerization, enzymatic activity and/or localization in the DDR. Further PTM in addition to any PTM involved in transition from oligomer to monomer and vice versa may prevent normal export from the nucleus as well and thus contribute to SIRT2 regulation during the DDR. However, SIRT2 deacetylase activity but not localization was shown to be regulated by phosphorylation and acetylation during various phases of the cell cycle by CDKs.

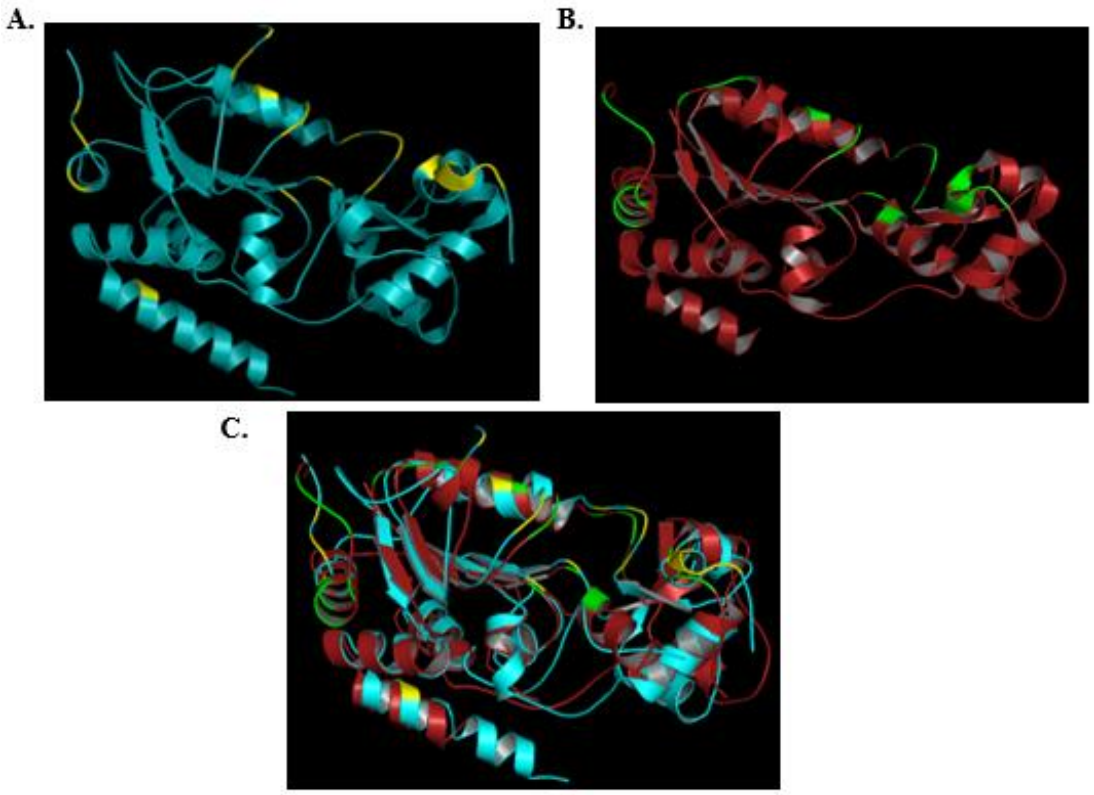

Figure 4.3 Conservation of Structure Between Yeast Hst2p and Human SIRT2 and the Potential for Human SIRT2 to be Regulated by Oligomerization. A, Human SIRT2 crystal structure obtained from the RCSB Protein Data Bank (SIRT2 structure 4RMH) in blue with yellow highlights on amino acids corresponding to yeast Hst2p amino acids used in trimer interactions. B. Yeast Hst2p crystal structure from the RCSB Protein Data Bank (Hst2 structure 1Q14) in red with green highlights on amino acids involved in trimer formation [135]. C. Overlay of structures from 4.3A and B. Images generated using Pymol.

SIRT2 deacetylase activity has been demonstrated to be regulated by phosphorylation and acetylation. The Cyclin E-CDK2 and Cyclin B-CDK1 complex phosphorylates SIRT2 at Serine 368 and 372 which leads to the inhibition of its catalytic activity [76].

Hyperphosphorylation of these sites occurs in the G2/M transition and in mitosis to suppress checkpoint activation [76]. Phosphorylation does not alter subcellular localization of SIRT2, protein stability, or the ability of SIRT2 to bind substrate [76] [136]. However, phosphorylation does lead to decreased deacetylation of histone targets and α-tubulin as well as decreased SIRT2 activity involved in chromatin condensation and suppression of cell motility [76]. These sites are dephosphorylated by CDC14A and CDC14B [70]. Overall phosphorylation of SIRT2 by CDKs is cell cycle dependent event that suppresses SIRT2 activity [70]. Acetylation, like phosphorylation, has also been demonstrated to suppress SIRT2 deacetylase activity. Histone acetyltransferase p300 acetylates SIRT2 resulting in decreased SIRT2 deacetylase activity [137]. Acetylation reduces SIRT2 activity on α-tubulin and reduces SIRT2 transcriptional suppression of p53 [137]. Additionally, SIRT2 activity regulation is dependent on the availability of NAD^+.

4.4 SIRT2: Activity and NAD^+ Pools

Nicotinamide Adenine Dinucleotide (NAD^+) is a vital cofactor for Sirtuin and PARP protein function and as a result NAD^+ production and availability is tightly linked to cellular stresses [26]. For instance, energy deprivation induced stress as a result of caloric restriction, glucose deprivation, fasting, and exercise leads to an increase in NAD^+ production [26]. This is accomplished by regulation of the AMPK/PGC-1α axis in which low ATP levels resulting from energy deprivation lead to increased production of NAD^+ [49]. NAD^+ is synthesized through de novo synthesis or the Preiss-Handler pathways in the mitochondria or through the NAD^+ Salvage pathway in various compartments of the

cell leading to increased cellular levels of NAD^+ [26]. NAD^+ in turn is used in the tricarboxylic acid cycle (TAC) to generate ATP as well as to activate SIRT1 upregulation of PGC-1α and HIF-1α which are needed to increase production of GLUT receptors for glucose uptake by the cell [49].

During oxidative stress, NAD^+ production is necessary for the reduction of ROS produced during ATP generation (reduction of oxygen in the electron transport chains) through various Sirtuin activation to suppress glucose uptake, increase energy production from fatty acids, and upregulate proteins pathways that reduce ROS levels directly (SOD2) [65]. Additionally, NAD^+ is necessary for the proper function of Sirtuin and PARP proteins during the DDR in response to stress induced by DNA damage and/or replication fork stalling. In all of these stress response pathways, NAD^+ is needed across various cell compartments such as the mitochondria to produce ATP in the TAC or the nucleus to activate Sirtuin or PARP activity, but only NAD^+ precursors can cross cellular membranes indicating that NAD^+ pools must be produced and maintained in a compartment specific manner [26].

The production of NAD^+, therefore, is accomplished through the NAD^+ salvage pathway outside of the mitochondria [26]. This pathway is maintained by nicotinamide phosphoribosyltransferase (NAMPT) and one of three isoforms of the NMN adenylyltransferase (NMNAT) protein [26]. NAMPT converts the deacetylation or ADP-ribosylation reaction/deacetylation byproduct nicotinamide (NAM) into nicotinamide mononucleotide (NMN) which is converted to NAD^+ by NMNAT [26]. The rate limiting

step of this pathway is the initial conversion of NAM to NMN and both steps are dependent on ATP [26]. Cytoplasmic pools of NAD^+ are generally higher than nuclear pools and maintenance of the nuclear pool by NAMPT and NMNAT isoform 1 (NMNAT1) is necessary for regulation of the DDR [26]. Members of the PARP protein family use NAD^+ to catalyze the polymerization of ADP-ribose units onto target proteins and creating NAM as a byproduct and are heavily involved in DNA damage repair [26, 123]. Therefore, SIRT2 protein regulation during the DDR is also dependent on its ability to compete with PARP and other nuclear sirtuins for the co-factor NAD^+.

SIRT1, SIRT6, SIRT7, PARP1 and PARP2 are involved in many DDR pathways and as a result, nuclear NAD^+ levels are depleted in response to damage [43-47, 49, 51-54, 59, 61, 62]. It is possible that increased PARP1 activity at sites of damage leads to the inhibition of SIRT2 not only through depletion of local NAD^+ levels but also through the increased local levels of NAM at sites of damage produced by both proteins' enzymatic activities. PARP1, therefore, may regulate SIRT2 activity on DDR substrate indirectly by controlling the local amount of available co-factor and inhibitor at sites of damage. However, SIRT2 may be able to circumvent nuclear NAD^+ pool depletion through generation of a local NAD^+ pool for function at sites of DNA damage.

Previously, both SIRT1 and PARP1 were shown to interact with nuclear NMNAT1 at target gene promoters in the nucleus and thus would have access to a local pool of NAD^+ through NMNAT1 production of NAD^+ from NMN [26, 116, 138]. In a mass spectrometry analysis in which I purified SIRT2-FLAG from HCT116 cells exposed to

either HU or IR, I saw a potential interaction between SIRT2 and NAMPT and this interaction appeared to increase in response to damaging agents when compared to non-damage controls (data not shown). Therefore, one hypothesis is that SIRT2 like SIRT1 and PARP1 associates with components of the NAD^+ salvage pathway to create a local pool of nuclear NAD^+ to maintain deacetylase activity on DDR pathway protein targets (Figure 4.4A). Furthermore, SIRT2 does not appear localize to sites of DNA damage induced by microirradiation like its substrate DNA-PKcs or to accumulate at sites of damage foci like its substrate ATRIP (data not shown). Therefore, SIRT2 may be able to compete for NAD^+ by pre-binding substrate in advance of damage induction in a DNA independent manner as seen for DNA-PKcs. This pre-binding may allow for faster binding of available co-factor and subsequent activation or deactivation of DDR substrates before NAD^+ depletion occurs (Figure 4.4A). This may be necessary to promote NHEJ over alt-NHEJ which is promoted by PARP1.

Alternatively, rather than SIRT2 shuttling into the nucleus to act on DDR substrates, the substrates themselves may shuttle out into the cytoplasm where a separate generally greater pool of NAD^+ is maintained to be deacetylated by SIRT2 before shuttling back into the nucleus where they function in the DDR (Figure 4.4B) [26]. Therefore, it is possible that SIRT2 deacetylates substrate in the cytoplasm or at least not directly at the sites of damage DNA in the nucleus where local levels of NAD^+ are depleted and local NAM levels are elevated. Future experiments are needed to confirm the interaction of SIRT2 with NAD^+ Salvage pathway proteins as well as to examine SIRT2-substrate localization through cell and chromatin fractionation experiments during the DDR.

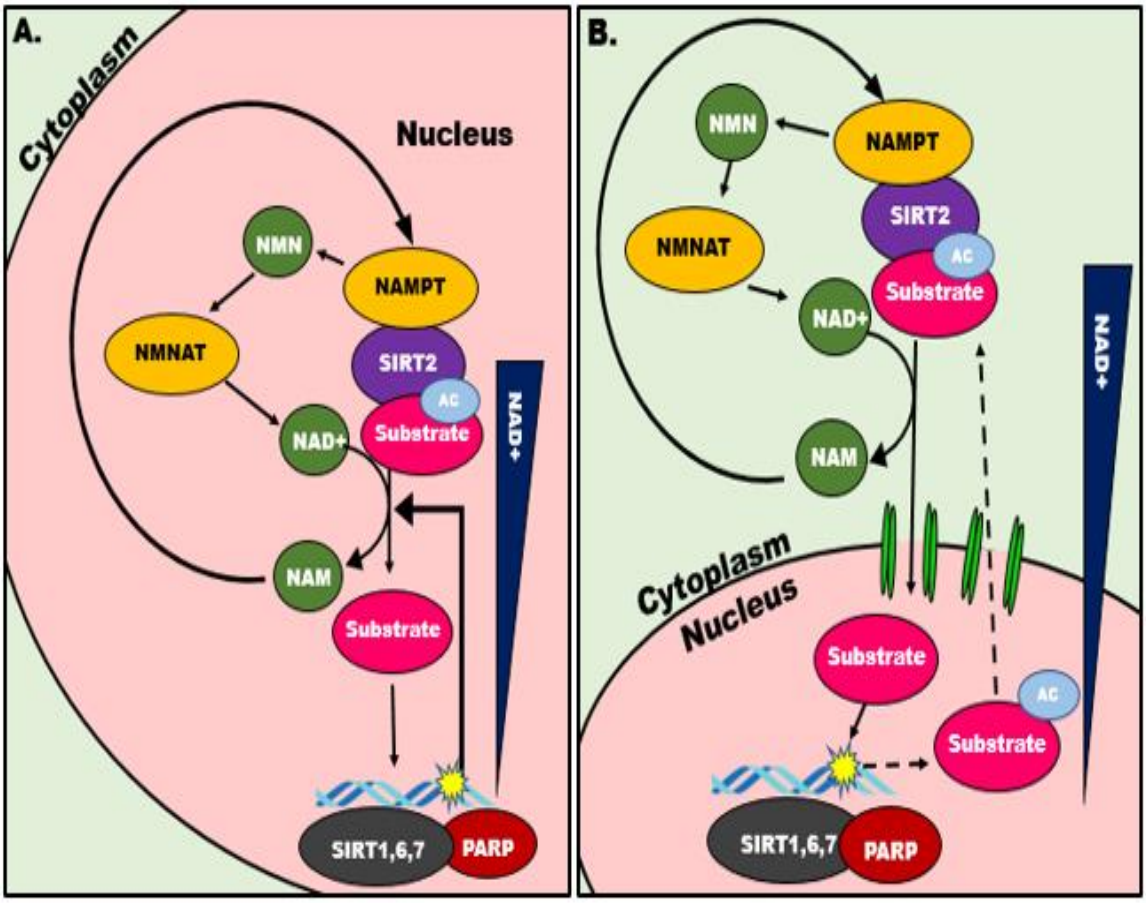

Figure 4.4 Hypothetical Model of SIRT2 Deacetylase Activity Under NAD^+ Depletion. A, SIRT2 may overcome depleted NAD^+ caused by activation of other Sirtuins and PARP proteins by complexing with proteins from the NAD^+ Salvage pathway, by deacetylating substrate away from DNA damage sites, and/or by pre-binding substrate before damage to increase the rate of deacetylation following activation of deacetylase activity during the DDR. Following deacetylation, SIRT2 DDR substrates localizes to sites of damage. B, Alternative model in which SIRT2 DDR substrate relocates to the cytoplasm (where NAD^+ levels are generally higher than the nucleus) in response to DNA damage for SIRT2 deacetylation. Deacetylated SIRT2 DDR substrate is imported into the nucleus where it localizes to the DNA damage sites.

In summary, SIRT2 is a human tumor suppressor which functions to regulate mitotic checkpoints, the RSR, and NHEJ, but may also function as a regulator of other DNA damage repair pathways such as alt-NHEJ, HRR, SSB, NER, and BER. Current cancer therapeutic targets are limited in that the majority are targeted at DDR kinases, however, kinases only compose roughly 4% of all DDR proteins [112]. Therefore, there is strong need to expand our current repertoire of enzyme targets. My research provides strong evidence to support the development of SIRT2 inhibitors for future therapeutic application and to support the use of SIRT2 as a future cancer biomarker (Figure 4.5). Further research is needed, however, to establish how else SIRT2 may regulate other forms of DNA damage through assays that more precisely examine the efficiency of individual repair pathways. Furthermore, future endeavors should examine how SIRT2 is regulated in response to damage. To accomplish this, assays that examine PTM and oligomerization of SIRT2 and that examine SIRT2 and substrate localization during the DNA damage response should be performed. The potential interaction between SIRT2 and NAD^+ salvage proteins should be validated as well.

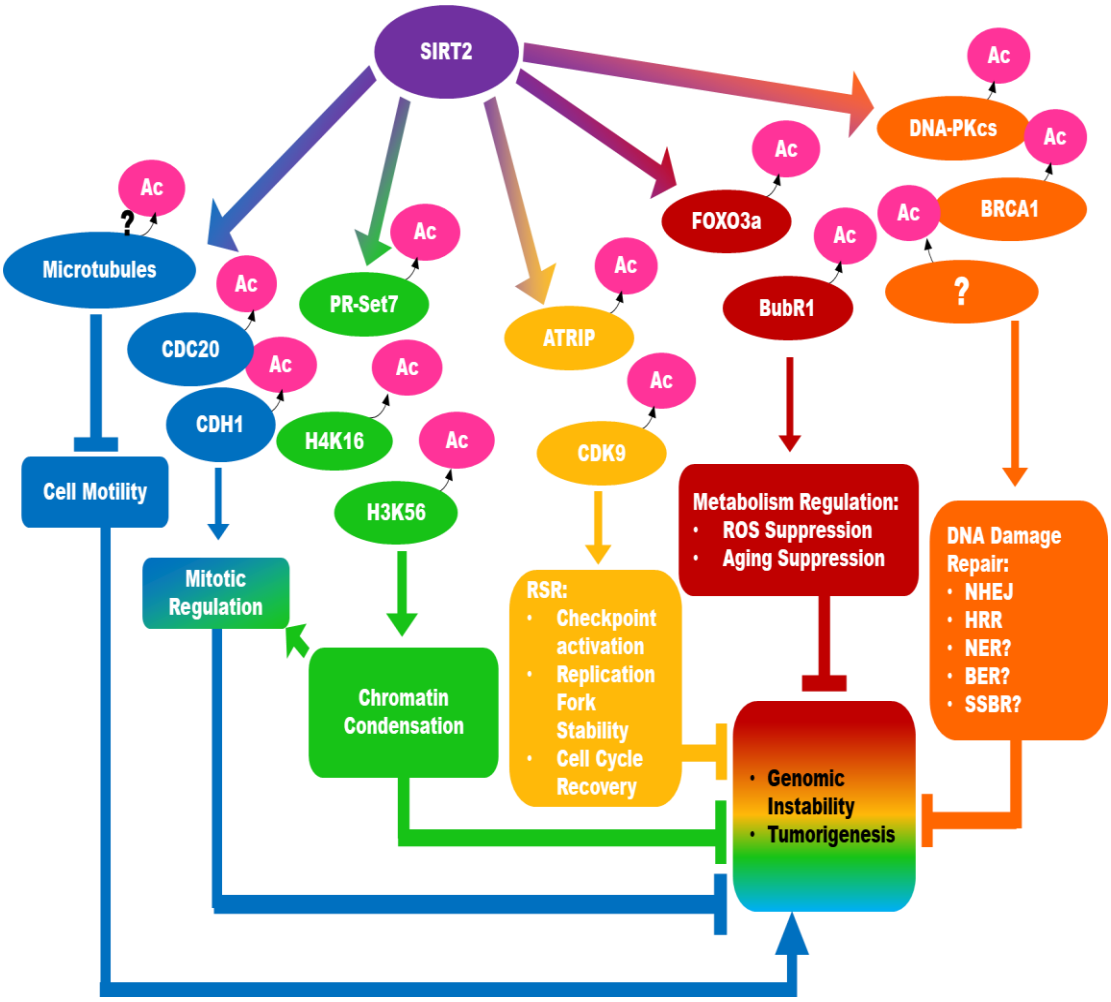

Figure 4.5 SIRT2 Pathway Regulation Schematic Updated. SIRT2 regulates a network of DDR proteins such as APCCDH1/CDC20, microtubules, H3K56, H4K16, PR-Set7, CDK9, BubR1, FOXO3a, DNA-PKcs, BRCA1, ATRIP, and potentially more to prevent genomic instability and tumorigenesis. The upstream regulation of SIRT2 activity, however, is still not clear. Due to SIRT2's genomic instability suppressive functions across a wide net of protein pathways, SIRT2 may prove to be an informative biomarker and an effective cancer therapeutic target.

Chapter 5: REFERENCES

1. Sirbu, B.M. and D. Cortez, *DNA damage response: three levels of DNA repair regulation.* Cold Spring Harb Perspect Biol, 2013. **5**(8): p. a012724.
2. Bennetzen, M.V., et al., *Acetylation dynamics of human nuclear proteins during the ionizing radiation-induced DNA damage response.* Cell Cycle, 2013. **12**(11): p. 1688-95.
3. Polo, S.E. and S.P. Jackson, *Dynamics of DNA damage response proteins at DNA breaks: a focus on protein modifications.* Genes Dev, 2011. **25**(5): p. 409-33.
4. Giglia-Mari, G., A. Zotter, and W. Vermeulen, *DNA damage response.* Cold Spring Harb Perspect Biol, 2011. **3**(1): p. a000745.
5. Bartek, J., J. Bartkova, and J. Lukas, *DNA damage signalling guards against activated oncogenes and tumour progression.* Oncogene, 2007. **26**(56): p. 7773-9.
6. Gong, F. and K.M. Miller, *Mammalian DNA repair: HATs and HDACs make their mark through histone acetylation.* Mutat Res, 2013. **750**(1-2): p. 23-30.
7. Sancar, A., et al., *Molecular mechanisms of mammalian DNA repair and the DNA damage checkpoints.* Annu Rev Biochem, 2004. **73**: p. 39-85.
8. Ishikawa, K., H. Ishii, and T. Saito, *DNA damage-dependent cell cycle checkpoints and genomic stability.* DNA Cell Biol, 2006. **25**(7): p. 406-11.
9. Shaltiel, I.A., et al., *The same, only different - DNA damage checkpoints and their reversal throughout the cell cycle.* J Cell Sci, 2015. **128**(4): p. 607-20.
10. Fishel, R., *Mismatch repair.* J Biol Chem, 2015. **290**(44): p. 26395-403.
11. Hsieh, P. and K. Yamane, *DNA mismatch repair: molecular mechanism, cancer, and ageing.* Mech Ageing Dev, 2008. **129**(7-8): p. 391-407.

12. Li, G.M., *New insights and challenges in mismatch repair: getting over the chromatin hurdle.* DNA Repair (Amst), 2014. **19**: p. 48-54.

13. Spivak, G., *Nucleotide excision repair in humans.* DNA Repair (Amst), 2015. **36**: p. 13-8.

14. Krokan, H.E. and M. Bjoras, *Base excision repair.* Cold Spring Harb Perspect Biol, 2013. **5**(4): p. a012583.

15. Caldecott, K.W., *Single-strand break repair and genetic disease.* Nat Rev Genet, 2008. **9**(8): p. 619-31.

16. Daddacha, W., et al., *SAMHD1 Promotes DNA End Resection to Facilitate DNA Repair by Homologous Recombination.* Cell Reports. **20**(8): p. 1921-1935.

17. Davis, A.J. and D.J. Chen, *DNA double strand break repair via non-homologous end-joining.* Transl Cancer Res, 2013. **2**(3): p. 130-143.

18. Dobbs, T.A., J.A. Tainer, and S.P. Lees-Miller, *A structural model for regulation of NHEJ by DNA-PKcs autophosphorylation.* DNA Repair (Amst), 2010. **9**(12): p. 1307-14.

19. Jasin, M. and R. Rothstein, *Repair of strand breaks by homologous recombination.* Cold Spring Harb Perspect Biol, 2013. **5**(11): p. a012740.

20. Sharif, H., et al., *Cryo-EM structure of the DNA-PK holoenzyme.* Proc Natl Acad Sci U S A, 2017. **114**(28): p. 7367-7372.

21. Yin, X., et al., *Cryo-EM structure of human DNA-PK holoenzyme.* Cell Res, 2017. **27**(11): p. 1341-1350.

22. Sun, Y., et al., *A role for the Tip60 histone acetyltransferase in the acetylation and activation of ATM.* Proc Natl Acad Sci U S A, 2005. **102**(37): p. 13182-7.

23. Jiang, X., et al., *The FATC domains of PIKK proteins are functionally equivalent and participate in the Tip60-dependent activation of DNA-PKcs and ATM.* J Biol Chem, 2006. **281**(23): p. 15741-6.

24. Jiang, W., et al., *Differential phosphorylation of DNA-PKcs regulates the interplay between end-processing and end-ligation during nonhomologous end-joining.* Mol Cell, 2015. **58**(1): p. 172-85.

25. Goodarzi, A.A., et al., *DNA-PK autophosphorylation facilitates Artemis endonuclease activity.* EMBO J, 2006. **25**(16): p. 3880-9.

26. Canto, C., K.J. Menzies, and J. Auwerx, *NAD(+) Metabolism and the Control of Energy Homeostasis: A Balancing Act between Mitochondria and the Nucleus.* Cell Metab, 2015. **22**(1): p. 31-53.

27. Donehower, L.A., *Phosphatases reverse p53-mediated cell cycle checkpoints.* Proc Natl Acad Sci U S A, 2014. **111**(20): p. 7172-3.

28. Petermann, E. and T. Helleday, *Pathways of mammalian replication fork restart.* Nat Rev Mol Cell Biol, 2010. **11**(10): p. 683-7.

29. Urban, V., J. Dobrovolna, and P. Janscak, *Distinct functions of human RecQ helicases during DNA replication.* Biophys Chem, 2017. **225**: p. 20-26.

30. Evan, G.I. and K.H. Vousden, *Proliferation, cell cycle and apoptosis in cancer.* Nature, 2001. **411**(6835): p. 342-8.

31. Haupt, S., et al., *Apoptosis - the p53 network.* J Cell Sci, 2003. **116**(Pt 20): p. 4077-85.

32. Hoeijmakers, J.H., *DNA damage, aging, and cancer.* N Engl J Med, 2009. **361**(15): p. 1475-85.

33. Negrini, S., V.G. Gorgoulis, and T.D. Halazonetis, *Genomic instability--an evolving hallmark of cancer.* Nat Rev Mol Cell Biol, 2010. **11**(3): p. 220-8.

34. Shortt, J. and R.W. Johnstone, *Oncogenes in cell survival and cell death.* Cold Spring Harb Perspect Biol, 2012. **4**(12).

35. Bretones, G., M.D. Delgado, and J. Leon, *Myc and cell cycle control.* Biochim Biophys Acta, 2015. **1849**(5): p. 506-16.

36. Bozic, I., et al., *Accumulation of driver and passenger mutations during tumor progression.* Proc Natl Acad Sci U S A, 2010. **107**(43): p. 18545-50.

37. Larsson, L.G., *Oncogene- and tumor suppressor gene-mediated suppression of cellular senescence.* Semin Cancer Biol, 2011. **21**(6): p. 367-76.

38. Berger, A.H., A.G. Knudson, and P.P. Pandolfi, *A continuum model for tumour suppression.* Nature, 2011. **476**(7359): p. 163-9.

39. Osborne, C., P. Wilson, and D. Tripathy, *Oncogenes and tumor suppressor genes in breast cancer: potential diagnostic and therapeutic applications.* Oncologist, 2004. **9**(4): p. 361-77.

40. Nalejska, E., E. Maczynska, and M.A. Lewandowska, *Prognostic and predictive biomarkers: tools in personalized oncology.* Mol Diagn Ther, 2014. **18**(3): p. 273-84.

41. Morris, L.G. and T.A. Chan, *Therapeutic targeting of tumor suppressor genes.* Cancer, 2015. **121**(9): p. 1357-68.

42. Willers, H., et al., *Basic mechanisms of therapeutic resistance to radiation and chemotherapy in lung cancer.* Cancer J, 2013. **19**(3): p. 200-7.

43. Chang, H.C. and L. Guarente, *SIRT1 and other sirtuins in metabolism.* Trends Endocrinol Metab, 2014. **25**(3): p. 138-45.

44. Choi, J.E. and R. Mostoslavsky, *Sirtuins, metabolism, and DNA repair.* Curr Opin Genet Dev, 2014. **26**: p. 24-32.

45. Flick, F. and B. Luscher, *Regulation of sirtuin function by posttranslational modifications.* Front Pharmacol, 2012. **3**: p. 29.

46. Finkel, T., C.X. Deng, and R. Mostoslavsky, *Recent progress in the biology and physiology of sirtuins.* Nature, 2009. **460**(7255): p. 587-91.

47. Guarente, L., *Franklin H. Epstein Lecture: Sirtuins, aging, and medicine.* N Engl J Med, 2011. **364**(23): p. 2235-44.

48. Yuan, H., L. Su, and W.Y. Chen, *The emerging and diverse roles of sirtuins in cancer: a clinical perspective.* Onco Targets Ther, 2013. **6**: p. 1399-416.

49. Canto, C., et al., *AMPK regulates energy expenditure by modulating NAD+ metabolism and SIRT1 activity.* Nature, 2009. **458**(7241): p. 1056-60.

50. Bordone, L., et al., *SIRT1 transgenic mice show phenotypes resembling calorie restriction.* Aging Cell, 2007. **6**(6): p. 759-67.

51. Yuan, Y., et al., *Regulation of SIRT1 in aging: Roles in mitochondrial function and biogenesis.* Mech Ageing Dev, 2016. **155**: p. 10-21.

52. Li, K., et al., *Regulation of WRN protein cellular localization and enzymatic activities by SIRT1-mediated deacetylation.* J Biol Chem, 2008. **283**(12): p. 7590-8.

53. Kugel, S. and R. Mostoslavsky, *Chromatin and beyond: the multitasking roles for SIRT6.* Trends Biochem Sci, 2014. **39**(2): p. 72-81.

54. Chen, W., et al., *Sirt6 Promotes DNA End Joining in iPSCs Derived from Old Mice.* Cell Rep, 2017. **18**(12): p. 2880-2892.

55. Kaidi, A., et al., *Human SIRT6 promotes DNA end resection through CtIP deacetylation.* Science, 2010. **329**(5997): p. 1348-53.

56. Mao, Z., et al., *SIRT6 promotes DNA repair under stress by activating PARP1.* Science, 2011. **332**(6036): p. 1443-6.

57. Xu, Z., et al., *SIRT6 rescues the age related decline in base excision repair in a PARP1-dependent manner.* Cell Cycle, 2015. **14**(2): p. 269-76.

58. Toiber, D., et al., *SIRT6 recruits SNF2H to DNA break sites, preventing genomic instability through chromatin remodeling.* Mol Cell, 2013. **51**(4): p. 454-68.

59. Blank, M.F. and I. Grummt, *The seven faces of SIRT7.* Transcription, 2017. **8**(2): p. 67-74.

60. Kiran, S., et al., *Sirtuin 7 in cell proliferation, stress and disease: Rise of the Seventh Sirtuin!* Cell Signal, 2015. **27**(3): p. 673-82.

61. Vazquez, B.N., et al., *SIRT7 promotes genome integrity and modulates non-homologous end joining DNA repair.* EMBO J, 2016. **35**(14): p. 1488-503.

62. Vazquez, B.N., J.K. Thackray, and L. Serrano, *Sirtuins and DNA damage repair: SIRT7 comes to play.* Nucleus, 2017. **8**(2): p. 107-115.

63. Lombard, D.B. and B.M. Zwaans, *SIRT3: as simple as it seems?* Gerontology, 2014. **60**(1): p. 56-64.

64. McDonnell, E., et al., *SIRT3 regulates progression and development of diseases of aging.* Trends Endocrinol Metab, 2015. **26**(9): p. 486-492.

65. Hirschey, M.D., et al., *SIRT3 regulates mitochondrial protein acetylation and intermediary metabolism.* Cold Spring Harb Symp Quant Biol, 2011. **76**: p. 267-77.

66. Osborne, B., et al., *The role of mitochondrial sirtuins in health and disease.* Free Radic Biol Med, 2016. **100**: p. 164-174.

67. North, B.J., Marshall, B. L., Borra, M. T., Denu, J. M., Verdin, E., *The human Sir2 ortholog, SIRT2, is an NAD+-dependent tubulin deacetylase.* Mol Cell, 2003. **11**(2): p. 437-44.

68. North, B.J., et al., *SIRT2 induces the checkpoint kinase BubR1 to increase lifespan.* EMBO J, 2014. **33**(13): p. 1438-53.

69. North, B.J. and E. Verdin, *Interphase nucleo-cytoplasmic shuttling and localization of SIRT2 during mitosis.* PLoS One, 2007. **2**(8): p. e784.

70. North, B.J. and E. Verdin, *Mitotic regulation of SIRT2 by cyclin-dependent kinase 1-dependent phosphorylation.* J Biol Chem, 2007. **282**(27): p. 19546-55.

71. Zhang, H., et al., *ATRIP Deacetylation by SIRT2 Drives ATR Checkpoint Activation by Promoting Binding to RPA-ssDNA.* Cell Rep, 2016. **14**(6): p. 1435-47.

72. Zhang, H., P.E. Head, and D.S. Yu, *SIRT2 orchestrates the DNA damage response.* Cell Cycle, 2016. **15**(16): p. 2089-2090.

73. Zhang, H., et al., *SIRT2 directs the replication stress response through CDK9 deacetylation.* Proc Natl Acad Sci U S A, 2013. **110**(33): p. 13546-51.

74. Serrano, L., et al., *The tumor suppressor SirT2 regulates cell cycle progression and genome stability by modulating the mitotic deposition of H4K20 methylation.* Genes Dev, 2013. **27**(6): p. 639-53.

75. Alejandro Vaquero, M.B.S., Dong Hoon Lee, Ann Sutton, Hwei-Ling Cheng, Frederick W. Alt, Lourdes Serrano, Rolf Sternglanz, and Danny Reinberg, *SirT2 is a histone deacetylase with preference for histone H4 Lys 16 during mitosis.* GENES & DEVELOPMENT, 2006(20): p. 1256–1261.

76. Pandithage, R., et al., *The regulation of SIRT2 function by cyclin-dependent kinases affects cell motility.* J Cell Biol, 2008. **180**(5): p. 915-29.

77. Wang, F., et al., *SIRT2 deacetylates FOXO3a in response to oxidative stress and caloric restriction.* Aging Cell, 2007. **6**(4): p. 505-14.

78. Kim, H.S., et al., *SIRT2 maintains genome integrity and suppresses tumorigenesis through regulating APC/C activity.* Cancer Cell, 2011. **20**(4): p. 487-99.

79. Inoue, T., et al., *SIRT2, a tubulin deacetylase, acts to block the entry to chromosome condensation in response to mitotic stress.* Oncogene, 2007. **26**(7): p. 945-57.

80. Hiratsuka, M., et al., *Proteomics-based identification of differentially expressed genes in human gliomas: down-regulation of SIRT2 gene.* Biochem Biophys Res Commun, 2003. **309**(3): p. 558-66.

81. Temel, M., et al., *The expression levels of the sirtuins in patients with BCC.* Tumour Biol, 2016. **37**(5): p. 6429-35.

82. Li, Z., et al., *SIRT2 inhibits non-small cell lung cancer cell growth through impairing Skp2-mediated p27 degradation.* Oncotarget, 2016. **7**(14): p. 18927-39.

83. Bartosch, C., et al., *Assessing sirtuin expression in endometrial carcinoma and non-neoplastic endometrium.* Oncotarget, 2016. **7**(2): p. 1144-54.

84. Li, Z., et al., *Regulation of SIRT2 levels for human non-small cell lung cancer therapy.* Lung Cancer, 2013. **82**(1): p. 9-15.

85. Weinstein, J.N., et al., *The Cancer Genome Atlas Pan-Cancer analysis project.* Nat Genet, 2013. **45**(10): p. 1113-20.

86. Forbes, S.A., et al., *COSMIC: exploring the world's knowledge of somatic mutations in human cancer.* Nucleic Acids Res, 2015. **43**(Database issue): p. D805-11.

87. Matsushita, N., et al., *Role of NAD-dependent deacetylases SIRT1 and SIRT2 in radiation and cisplatin-induced cell death in vertebrate cells.* Genes Cells, 2005. **10**(4): p. 321-32.

88. Robertson, G.P., H.J. Huang, and W.K. Cavenee, *Identification and validation of tumor suppressor genes.* Mol Cell Biol Res Commun, 1999. **2**(1): p. 1-10.

89. Saunders, L.R. and E. Verdin, *Sirtuins: critical regulators at the crossroads between cancer and aging.* Oncogene, 2007. **26**(37): p. 5489-504.

90. Donmez, G. and T.F. Outeiro, *SIRT1 and SIRT2: emerging targets in neurodegeneration.* EMBO Mol Med, 2013. **5**(3): p. 344-52.

91. Song, H.Y., et al., *SIRT2 deletion enhances KRAS-induced tumorigenesis in vivo by regulating K147 acetylation status.* Oncotarget, 2016.

92. Suematsu, T., et al., *Deacetylation of the mitotic checkpoint protein BubR1 at lysine 250 by SIRT2 and subsequent effects on BubR1 degradation during the*

prometaphase/anaphase transition. Biochem Biophys Res Commun, 2014. **453**(3): p. 588-94.

93. Cerami, E., et al., *The cBio cancer genomics portal: an open platform for exploring multidimensional cancer genomics data.* Cancer Discov, 2012. **2**(5): p. 401-4.

94. Smith, S.C., et al., *A gemcitabine sensitivity screen identifies a role for NEK9 in the replication stress response.* Nucleic Acids Res, 2014. **42**(18): p. 11517-27.

95. Hall, W.A., et al., *Low CHD5 expression activates the DNA damage response and predicts poor outcome in patients undergoing adjuvant therapy for resected pancreatic cancer.* Oncogene, 2014. **33**(47): p. 5450-6.

96. Colbert, L.E., et al., *CHD7 expression predicts survival outcomes in patients with resected pancreatic cancer.* Cancer Res, 2014. **74**(10): p. 2677-87.

97. Gao, J., et al., *Integrative analysis of complex cancer genomics and clinical profiles using the cBioPortal.* Sci Signal, 2013. **6**(269): p. pl1.

98. Tavtigian, S.V., et al., *Comprehensive statistical study of 452 BRCA1 missense substitutions with classification of eight recurrent substitutions as neutral.* J Med Genet, 2006. **43**(4): p. 295-305.

99. Kumar, P., S. Henikoff, and P.C. Ng, *Predicting the effects of coding non-synonymous variants on protein function using the SIFT algorithm.* Nat Protoc, 2009. **4**(7): p. 1073-81.

100. Ng, P.C. and S. Henikoff, *Predicting the effects of amino acid substitutions on protein function.* Annu Rev Genomics Hum Genet, 2006. **7**: p. 61-80.

101. Ng, P.C. and S. Henikoff, *SIFT: Predicting amino acid changes that affect protein function.* Nucleic Acids Res, 2003. **31**(13): p. 3812-4.

102. Ng, P.C. and S. Henikoff, *Accounting for human polymorphisms predicted to affect protein function.* Genome Res, 2002. **12**(3): p. 436-46.

103. Ng, P.C. and S. Henikoff, *Predicting deleterious amino acid substitutions.* Genome Res, 2001. **11**(5): p. 863-74.

104. Adzhubei, I.A., et al., *A method and server for predicting damaging missense mutations.* Nat Methods, 2010. **7**(4): p. 248-9.

105. Celniker, G., Nimrod, G., Ashkenazy, H., Glaser, F., Martz, E., Mayrose, I., Pupko, T., and Ben-Tal, N. , *ConSurf: Using Evolutionary Data to Raise Testable Hypotheses about Protein Function.* Isr. J. Chem, 2013. **53**(3-4): p. 199–206.

106. Ashkenazy, H., et al., *ConSurf 2010: calculating evolutionary conservation in sequence and structure of proteins and nucleic acids.* Nucleic Acids Res, 2010. **38**(Web Server issue): p. W529-33.

107. Altschul, S.F., et al., *Basic local alignment search tool.* J Mol Biol, 1990. **215**(3): p. 403-10.

108. Altschul, S.F., et al., *Gapped BLAST and PSI-BLAST: a new generation of protein database search programs.* Nucleic Acids Res, 1997. **25**(17): p. 3389-402.

109. Gish, W. and D.J. States, *Identification of protein coding regions by database similarity search.* Nat Genet, 1993. **3**(3): p. 266-72.

110. Consortium, U., *UniProt: a hub for protein information.* Nucleic Acids Res, 2015. **43**(Database issue): p. D204-12.

111. Rumpf, T., et al., *Selective Sirt2 inhibition by ligand-induced rearrangement of the active site.* Nat Commun, 2015. **6**: p. 6263.

112. Pearl, L.H., et al., *Therapeutic opportunities within the DNA damage response.* Nat Rev Cancer, 2015. **15**(3): p. 166-80.

113. Head, P.E., et al., *Sirtuin 2 mutations in human cancers impair its function in genome maintenance.* J Biol Chem, 2017. **292**(24): p. 9919-9931.

114. Gunn, A. and J.M. Stark, *I-SceI-based assays to examine distinct repair outcomes of mammalian chromosomal double strand breaks.* Methods Mol Biol, 2012. **920**: p. 379-91.

115. Kim, H.J. and S.C. Bae, *Histone deacetylase inhibitors: molecular mechanisms of action and clinical trials as anti-cancer drugs.* Am J Transl Res, 2011. **3**(2): p. 166-79.

116. Zhang, T., et al., *Enzymes in the NAD+ salvage pathway regulate SIRT1 activity at target gene promoters.* J Biol Chem, 2009. **284**(30): p. 20408-17.

117. Nick McElhinny, S.A., et al., *Ku recruits the XRCC4-ligase IV complex to DNA ends.* Mol Cell Biol, 2000. **20**(9): p. 2996-3003.

118. Yano, K., et al., *Functional significance of the interaction with Ku in DNA double-strand break recognition of XLF.* FEBS Lett, 2011. **585**(6): p. 841-6.

119. Feldman, J.L., K.E. Dittenhafer-Reed, and J.M. Denu, *Sirtuin catalysis and regulation.* J Biol Chem, 2012. **287**(51): p. 42419-27.

120. Davis, A.J., K.J. Lee, and D.J. Chen, *The N-terminal region of the DNA-dependent protein kinase catalytic subunit is required for its DNA double-stranded break-mediated activation.* J Biol Chem, 2013. **288**(10): p. 7037-46.

121. Hammel, M., et al., *Ku and DNA-dependent protein kinase dynamic conformations and assembly regulate DNA binding and the initial non-homologous end joining complex.* J Biol Chem, 2010. **285**(2): p. 1414-23.

122. Spagnolo, L., et al., *Three-dimensional structure of the human DNA-PKcs/Ku70/Ku80 complex assembled on DNA and its implications for DNA DSB repair.* Mol Cell, 2006. **22**(4): p. 511-9.

123. Ray Chaudhuri, A. and A. Nussenzweig, *The multifaceted roles of PARP1 in DNA repair and chromatin remodelling.* Nat Rev Mol Cell Biol, 2017. **18**(10): p. 610-621.

124. Schumacher, A.J., et al., *The HSV-1 exonuclease, UL12, stimulates recombination by a single strand annealing mechanism.* PLoS Pathog, 2012. **8**(8): p. e1002862.

125. Collins, A.R., *The comet assay for DNA damage and repair: principles, applications, and limitations.* Mol Biotechnol, 2004. **26**(3): p. 249-61.

126. Chen, Y., et al., *BRCA1 is a 220-kDa nuclear phosphoprotein that is expressed and phosphorylated in a cell cycle-dependent manner.* Cancer Res, 1996. **56**(14): p. 3168-72.

127. Morgan, R.D., et al., *PARP inhibitors in platinum-sensitive high-grade serous ovarian cancer.* Cancer Chemother Pharmacol, 2018. **81**(4): p. 647-658.

128. Pemberton, L.F. and B.M. Paschal, *Mechanisms of receptor-mediated nuclear import and nuclear export.* Traffic, 2005. **6**(3): p. 187-98.

129. Freitas, N. and C. Cunha, *Mechanisms and signals for the nuclear import of proteins.* Curr Genomics, 2009. **10**(8): p. 550-7.

130. Wagstaff, K.M. and D.A. Jans, *Importins and beyond: non-conventional nuclear transport mechanisms.* Traffic, 2009. **10**(9): p. 1188-98.

131. Tran, E.J., M.C. King, and A.H. Corbett, *Macromolecular transport between the nucleus and the cytoplasm: Advances in mechanism and emerging links to disease.* Biochimica Et Biophysica Acta-Molecular Cell Research, 2014. **1843**(11): p. 2784-2795.

132. Kiran, S., et al., *Intracellular distribution of human SIRT7 and mapping of the nuclear/nucleolar localization signal.* FEBS J, 2013. **280**(14): p. 3451-66.

133. Guo, X., et al., *The NAD(+)-dependent protein deacetylase activity of SIRT1 is regulated by its oligomeric status.* Sci Rep, 2012. **2**: p. 640.

134. Vaquero, A., et al., *Human SirT1 interacts with histone H1 and promotes formation of facultative heterochromatin.* Mol Cell, 2004. **16**(1): p. 93-105.

135. Zhao, K., et al., *Structure and autoregulation of the yeast Hst2 homolog of Sir2.* Nat Struct Biol, 2003. **10**(10): p. 864-71.

136. Nahhas, F., et al., *Mutations in SIRT2 deacetylase which regulate enzymatic activity but not its interaction with HDAC6 and tubulin.* Mol Cell Biochem, 2007. **303**(1-2): p. 221-30.

137. Han, Y., et al., *Acetylation of Sirt2 by p300 attenuates its deacetylase activity.* Biochem Biophys Res Commun, 2008. **375**(4): p. 576-80.

138. Zhang, T., et al., *Regulation of poly(ADP-ribose) polymerase-1-dependent gene expression through promoter-directed recruitment of a nuclear NAD+ synthase.* J Biol Chem, 2012. **287**(15): p. 12405-16.